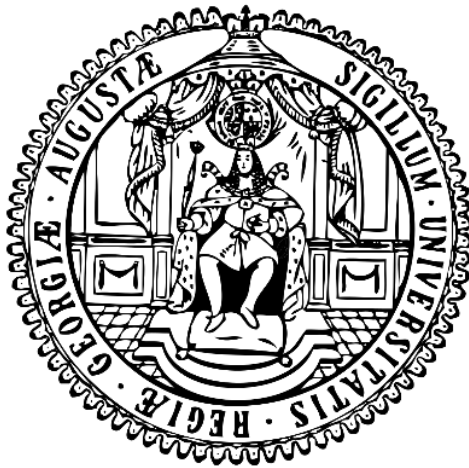


# Validation of novel protein-protein interactions in *Bacillus subtilis*

**Dissertation**

for the award of the degree

“Doctor rerum naturalium”



Division of Mathematics and Natural Sciences  
of the Georg-August-Universität Göttingen  
within the doctoral program “Microbiology & Biochemistry”  
of the Georg-August University School of Science (GAUSS)  
submitted by

**Rica Bremenkamp**

From Uslar

Göttingen 2022



## **Examination board**

### **Thesis advisory committee**

Prof. Dr. Jörg Stülke

Institute of Microbiology and Genetics, Department for General Microbiology, University of Göttingen

Prof. Dr. Ralf Ficner

Institute of Microbiology and Genetics, Department of Molecular Structural Biology, University of Göttingen

Prof. Dr. Ivo Feussner

Albrecht von Haller Institute, Department of Plant Biochemistry, University of Göttingen

### **Members of the examination board**

Prof. Dr. Stefanie Pöggeler

Institute of Microbiology and Genetics; Department of Genetics of Eukaryotic Microorganisms, University of Göttingen

Prof. Dr. Kai Heimel

Institute of Microbiology and Genetics, Department of Molecular Microbiology and Genetics, University of Göttingen

Prof. Dr. Rolf Daniel

Institute of Microbiology and Genetics; Department of Genomic and Applied Microbiology, University of Göttingen

Date of oral examination: 08.12.2022



## Statement of authorship

I hereby declare that the doctoral thesis entitled “Validation of novel protein-protein interactions in *Bacillus subtilis*” has been written independently and with no other sources and aids than quoted.

Rica Bremenkamp

Göttingen, the 14<sup>th</sup> of October 2022

## Danksagung

Zuallererst möchte ich mich natürlich bei Jörg bedanken. Du hast es mir nicht nur ermöglicht hier in der Abteilung meine Doktorarbeit anzufertigen, sondern schon durch das Angebot und die Betreuung unseres iGEM Team im Master einen wichtigen Grundstein für meinen wissenschaftlichen also auch privaten Werdegang hier in Göttingen gelegt. Dafür bin ich dir sehr dankbar! Auch deine offene-Tür-Politik hat es mir immer besonders leicht gemacht, mit dir über alle Schwierigkeiten zu reden.

Des Weiteren möchte ich mich bei Prof. Dr. Ficner und Prof. Dr. Feußner bedanken, dass Sie Teil meines Thesis Advisory Committees sind und trotz der etwas komplizierten Lagen wegen Corona immer Zeit und Möglichkeiten für Treffen gefunden haben. Außerdem danke ich Prof. Dr. Heimel, Prof. Dr. Pöggeler und Prof. Dr. Daniel, dass Sie Teil meiner Prüfungskommission sind.

Ich kann nicht häufig genug betonen wie dankbar ich für die Kollaboration mit dem Rappsilber Labor von der TU Berlin bin. Vor allem Francis, aber auch Andrea, Christian und Juri haben mir viel weitergeholfen und ich habe mich immer willkommen in eurer Runde gefühlt. Ich habe so viel gelernt durch unsere enge Zusammenarbeit und nur durch euch ist diese Arbeit zu dem geworden was sie heute ist.

Natürlich darf ich aber auch die AG Stülke und die AG Rismondo nicht vergessen. Ich würde gerne jeden namentlich nennen aber ich glaube das würde den Rahmen hier ein wenig sprängen. Ich danke allen die Teil meiner Reise waren. Vor allem auch meinen Studenten Lily, Kallisto, Anna und Lomi (Lorenz). Ich hoffe ihr habt die gemeinsame Zeit genauso genossen wie ich und ich konnte euch ein bisschen was über das Leben innerhalb und außerhalb des Labors beibringen. Vielen Dank für eure Mithilfe an diesem Projekt!

In unserem anfänglichen reinem Mädels Labor mit euch, Christina und Larissa, hat auf jeden Fall immer gute Stimmung geherrscht und auch eure Begeisterung für die Wissenschaft hat mich noch mal ganz neu mitgerissen. Ihr seid beide absolute Laborgöttinnen und ich werde euch wahrscheinlich für den Rest meines Lebens ein bisschen versuchen nachzueifern. Mein kurzer Umzug ins alte Zuhause, das S2 Labor zu Lisa und Neil, hat mich noch mal an meine Masterzeit erinnert und ich habe mich wieder pudelwohl gefühlt. Aber ich glaube ich muss mich bei euch für meinen Gesang und meine Playlists die doch von eurem Musikgeschmack abweichen entschuldigen. Danke das ihr euch immer meine ganzen Geschichten angehört habt und meiner nie müßig geworden seid! Ich möchte mich auch bei Silvia bedanken, dass du durch deine wertvolle Arbeit immer gewährleistest, dass wir im Labor alles haben um uns komplett austoben zu können.

Langsam ist auch mir klar, dass Janek, Robert, Dennis und ich nicht nur Arbeitskollegen, sondern so ziemlich beste Freunde sind. Ich fühle mich extrem privilegiert fast jeden Tag der letzten drei Jahre mit euch an meiner Seite verbracht zu haben. Das und euch werde ich schrecklich vermissen

sobald meine Zeit hier im Labor zu Ende ist. In guten wie in schlechten Zeiten wart ihr immer für mich da! Das gilt natürlich auch für Marie und Tim sowie Jonas und Linda. Ich bin sehr froh bei euch Vieren immer das professionelle dritte Rad sein zu dürfen. Natürlich darf auch der Rest der Göttinger Bande bei dieser Aufzählung nicht fehlen. Natalie, Nora, mögen noch viele weitere Wein-Abende, Picknicks im Park und Festivals folgen! Jasper und Lina, ich bin allzeit bereit für die Ski Piste.

Auch meinen längsten Freund(inn)en, Tina, Malou, Max und Valerie möchte ich danken, dass ihr mich schon so lange begleitet und ich euch jeder Zeit anrufen kann.

Ich danke auch dem Hochschulsport Göttingen, vor allem für ihr FIZ und die Beachvolleyballplätze. Sie haben immer für meine geistige und körperliche Gesundheit gesorgt! Dazu beigetragen haben natürlich auch all meine Volleyballer.

Zu guter Letzt gebührt glaube ich meiner Familie der größte Dank. Danke Mama, Papa und Meike, ohne euch wäre ich nichts. Ihr habt mir immer alles ermöglicht und ich versuche jeden Tag euch stolz zu machen. Danke Philipp, du bist mein Anker.

## List of publications

O'Reilly, F. J., Graziadei, A., Forbrig, C., **Bremenkamp, R.**, Charles, K., Lenz, S., Elfmann, C., Fischer, L., Stülke, J., Rappsilber, J., 2022. Protein complexes in *Bacillus subtilis* by AI-assisted structural proteomics. BioRxiv, 2022.07.26.501605 doi: <https://doi.org/10.1101/2022.07.26.501605>



---

## Table of contents

Table of contents .....	I
List of abbreviations .....	IV
Abstract .....	VII
<b>1. Introduction .....</b>	<b>1</b>
<b>1.1 The ribosome .....</b>	<b>2</b>
<b>1.2 Carbon metabolism in <i>B. subtilis</i>.....</b>	<b>5</b>
1.2.1 Glycolysis / Gluconeogenesis .....	5
1.2.2 The tricarboxylic acid cycle.....	8
1.2.3 The pyruvate dehydrogenase.....	10
<b>1.3 Iron metabolism .....</b>	<b>13</b>
1.3.1 The regulator family Fur .....	13
1.3.2 Fur.....	14
<b>1.4 Novel protein-protein interactions .....</b>	<b>16</b>
<b>1.5 Objective of this thesis.....</b>	<b>17</b>
<b>2. Material and Methods .....</b>	<b>19</b>
<b>2.1 Material.....</b>	<b>19</b>
2.1.1 Bacterial strains and plasmids .....	19
2.1.2 Growth media.....	19
2.1.3 Antibiotics.....	21
<b>2.2 Methods .....</b>	<b>22</b>
2.2.1 Standard methods .....	22
2.2.2 Cultivation and storage of bacteria .....	22
2.2.3 Preparation of competent <i>E. coli</i> and transformation .....	22
2.2.4 Preparation of competent <i>B. subtilis</i> cells and transformation .....	23
2.2.5 Working with DNA.....	24
2.2.6 Phenotypic characterizations of <i>B. subtilis</i> strains .....	31

---

2.2.7 Working with proteins.....	34
<b>3. Results .....</b>	<b>47</b>
<b>3.1 YabR, YugI and the ribosome .....</b>	<b>47</b>
3.1.1 Phenotypic characterization.....	47
3.1.2 Searching for potential interaction partners.....	54
3.1.3 Validation of binding of YabR and YugI to the ribosome .....	56
<b>3.2 YneR as a novel interactor of the pyruvate dehydrogenase .....</b>	<b>58</b>
<b>3.3 Regulation of iron homeostasis .....</b>	<b>60</b>
3.3.1 Deletion of YlaN and suppressor screen .....	61
3.3.2 The role of YlaN in regulating Fur-DNA binding .....	63
<b>3.4 Interactions of binary complexes .....</b>	<b>66</b>
<b>4. Discussion .....</b>	<b>71</b>
<b>4.1 Regulation of protein complexes .....</b>	<b>71</b>
4.1.1 A novel inhibitor of the pyruvate dehydrogenase .....	71
4.1.2 Regulation of the transcription regulator Fur by YlaN .....	75
<b>4.2 Proteins still in the search for a function .....</b>	<b>77</b>
4.2.1 Novel interactions at the ribosome.....	77
4.2.2 The potential role of YugI.....	79
4.2.3 YabR – the protein, the mystery.....	82
<b>4.3 Challenges in protein interaction studies .....</b>	<b>83</b>
<b>4.4 Outlook .....</b>	<b>84</b>
<b>5. References .....</b>	<b>87</b>
<b>6. Appendix.....</b>	<b>105</b>
<b>6.1 Supplementary information .....</b>	<b>105</b>
<b>6.2 Materials .....</b>	<b>105</b>
6.2.1 Chemicals.....	105
6.2.2 Enzymes.....	106
6.2.3 Commercial systems.....	106

6.2.4 Instruments / Equipment .....	107
6.2.5 Materials.....	108
6.2.6 Software and webpages .....	109
<b>6.3 Bacterial strains .....</b>	<b>109</b>
6.3.1 <i>E. coli</i> strains.....	109
6.3.2 <i>B. subtilis</i> strains.....	110
6.2.3 Strains constructed in this work.....	110
<b>6.4 Plasmids .....</b>	<b>111</b>
6.4.1 Plasmids used in this work .....	111
6.4.2 Plasmids constructed in this work.....	113
<b>6.5 Oligonucleotides .....</b>	<b>116</b>
6.5.1 Oligonucleotides designed for this work.....	116
6.5.2 Additional oligonucleotides used in this work .....	126
<b>6.6 Curriculum vitae.....</b>	<b>130</b>

---

## List of abbreviations

---

### General abbreviations

---

3-HP	3-hydroxypropionic acid
3-HPA	3-hydroxypropionaldehyde
% (v/v)	% (volume/volume)
% (w/v)	% (weight/ volume)
ADP	Adenosine diphosphate
APS	Ammonium persulfate
ATP	Adenosine triphosphate
BSA	Bovine serum albumin
bp	Base pair
CAA	Casamino acids
CAF	Ammonium iron citrate
c-di-AMP	Bis-(3'-5')-cyclic dimeric adenosine monophosphate
CE	Crude extract
CLMS	Crosslinking mass-spectrometry
CoFrac-MS	Co-fractionation mass spectrometry
DHAP	Dihydroxyacetone phosphate
DMSO	Dimethyl sulfoxide
dNTP	Deoxyribonucleic triphosphate
DTT	Dithiothreitol
EDTA	Ethylendiaminetetra acetic acid
<i>et al.</i> ,	Et alii
EV	Empty vector
Fig.	Figure
GABA	$\gamma$ -aminobutyric acid
IPTG	Isopropyl- $\beta$ -D-thiogalactopyranoside
iPTM	predicted interface TM-score
LB	Lysogeny broth (medium)
LC-MS	Liquid-chromatography mass-spectrometry
LFH	Long flanking homology
MSSM	Modified Sodium Spizizen Minimal (medium)
NADH/NAD <sup>+</sup>	Nicotinamide adenine dinucleotide

---

List of abbreviations

---

NADPH/NADP <sup>+</sup>	Nicotinamide adenine dinucleotide phosphate
Ni <sup>2+</sup> -NTA	Nickel-nitrilotri acid
OD	Optical density
ONPG	o-Nitrophenol-β-D-galactopyranosid
PAGE	Polyacrylamide gel electrophoresis
PAP	SDS loading dye
PCR	Polymerase chain reaction
PFA	Para-formaldehyde
PLP	Page Buffer
pTM	predicted TM-score
(p)ppGpp	Guanosin-3',5'-bispyrophosphat
Psi	Pound per square inch
rpm	Rounds per minute
RT	Room temperature
SDS	Sodium dodecyl sulphate
SP	Sporulation medium
SPINE	Strep-protein interaction experiment
TCA	Tricarboxylic acid
TEMED	N,N,N',N'-tetramethylethyldiamine
T <sub>m</sub>	Melting temperature
TRIS	Tris-(hydroxymethyl)-aminomethane
WT	Wild type
x-gal	5-bromo-4-chloro-3-indolyl-β-D-galactopyranoside
<i>Δgene</i>	Deletion of the gene

---



## Abstract

Protein-protein interactions are the basis for many biological processes in the cell. Understanding these interactions is crucial for the general analysis of how the cell functions and the potential identification of novel therapeutical targets. Over the years, many different techniques have been developed to study these protein interactions, among them high throughput approaches such as crosslinking mass spectrometry and co-fractionation mass spectrometry. The combination of these approaches with the artificial intelligence-based protein conformation prediction tool AlphaFold allowed the identification of many novel protein complexes in *B. subtilis*, including complexes that involved proteins of unknown function. The aim of this work was to validate these novel protein interactions and to prove the functionality of this workflow. An additional objective was assigning functions to some of the so far understudied proteins that were identified in these complexes. The complexes between the pyruvate dehydrogenase and YneR, the iron sensor Fur and the essential protein of unknown function YlaN as well as the interaction of the paralogous protein YabR and Yugl with the ribosome were studied intensively. YneR was identified as the first known inhibitor of the pyruvate dehydrogenase activity in *B. subtilis*, and therefore renamed to PdhI. This was achieved through growth experiments. Electrophoretic mobility shift assays showed that YlaN inhibits Fur-DNA binding activity. AlphaFold Multimer prediction revealed a potentially strong change in the conformation of the Fur dimer upon binding of YlaN. Furthermore, we showed that *ylaN* can be deleted, if *fur* had been deleted before. Together, these findings demonstrate that the essentiality of YlaN is due to the regulation of the DNA binding activity of Fur. The paralogous proteins YabR and Yugl bind to the 30S subunit of the ribosome. This was validated *via* Western blot analysis of purified ribosomes and bacterial two-hybrid assays. Deletion of *yabR* affected growth on minimal medium and Yugl seems to play a role in tetracycline susceptibility. It was suspected that both proteins perform the same essential function in the cell and can replace each other. This hypothesis could be refuted by the creation of a double deletion strain. To summarize, this work illustrates that the combination of the complementary techniques crosslinking mass spectrometry and co-fractionation mass spectrometry allows the accurate prediction of protein complexes in *B. subtilis* without the need for genetic manipulation of the organism. The validation of this concept led to the identification of the function of multiple proteins and the discovery of so far unknown regulatory mechanisms.





### 1. Introduction

Microorganisms can be found in every corner of this planet and were the first form of life that developed. There are a couple of principle enzymatic reactions that are needed to sustain life and are present throughout all domains of life. Therefore, to understand life and potentially discover new drugs, it is important to study and understand these central pathways and reactions in great detail. Here, model organisms like *Bacillus subtilis* come into play. *B. subtilis* is easily genetically modifiable and extensively used as an industrial workhorse (Cui *et al.*, 2018). This organism is harmless but closely related to human pathogens such as *Listeria monocytogenes* or *B. anthracis*. Information gathered in *B. subtilis* could potentially lead to the development of novel antibiotics against its pathogenic relatives.

Since the beginning of life, interactions have started to evolve. These interactions range from social interactions between different species or individuals down to interactions that take place within a single cell. Interactions within the cell most often involve two or more proteins but can also be dependent on nucleic acids or other molecules. Protein-protein interactions can fulfil a multitude of functions in the cell, as they can function as regulation switches or lead to a new or additional function of the proteins involved. Proteins with interaction partners can either form permanent complexes or interact only transiently under specific conditions. The formation of the complex depends on the affinity of the two proteins towards each other, as well as their localization and general concentration in the cell (Nooren, 2003). Some proteins are only found involved in complexes since they are not stable on their own. These complexes are called obligate complexes. In contrast to that, non-obligate complexes contain proteins that can also exist separate from each other. These complexes often have a regulatory function since their interaction only occurs under specific conditions (Nooren, 2003). Protein-protein interactions can additionally be divided into interactions between identical or heterologous proteins (homo-oligomers), or unrelated proteins (hetero-oligomers). To understand how the cell functions, it is crucial to understand how proteins function. Interestingly, even though *B. subtilis* is a very well characterised model organism, 25 % of its proteins have no function assigned to them or remain poorly investigated (Michna *et al.*, 2016). A helpful tool to identify the function of a protein is the analysis of its interaction partners, which ideally are of known function (Deng *et al.*, 2003).

### 1.1 The ribosome

One protein complex that has been extensively studied in the past is the ribosome. The ribosome is a complex machinery that fulfills the essential function of protein synthesis in every living organism. It consists of two subunits that are each made up of ribosomal proteins (r-proteins) and ribosomal RNA (rRNA). The prokaryotic ribosome is referred to as 70S ribosome and consists of the small 30S and the large 50S subunit. The 30S subunit of *B. subtilis* contains the 16S rRNA and over 20 proteins while the 50S subunit contains the 5S and 23S rRNA as well as over 30 proteins. In total, *B. subtilis* encodes 57 ribosomal proteins (Akanuma *et al.*, 2012). Overall, the rRNA makes up about two thirds of the ribosome while the highly conserved r-proteins constitute one third of the mass (Lauber *et al.*, 2009). The mature 70S ribosome contains three binding sites; the aminoacyl (A) site where the incoming aminoacyl-tRNA enters the ribosome, the peptidyl (P) site where the tRNA is fused to the growing polypeptide chain and the exit (E) site, where unloaded tRNA exits the ribosome. Once the mature ribosome is assembled, amino acids are gradually added to a growing peptide chain.

While it was first assumed that the r-proteins are the major players in ribosome function, it was later discovered that in fact the rRNA contains the catalytic properties of the ribosome, technically making the ribosome a ribozyme (Nissen *et al.*, 2000). It is challenging to pinpoint a specific function to each r-protein, since most of them are rather small in size and work in a highly cooperative manner with the rRNA and other r-proteins. It is generally agreed upon that the main function of the r-proteins is scaffolding of the rRNA and stabilization of the complex. Interestingly, 22 of the 57 genes that encode ribosomal proteins in *B. subtilis* are non-essential and can be deleted individually without leading to a complete growth arrest (Akanuma *et al.*, 2012). *B. subtilis* seems to lack the S1 protein. In *E. coli*, S1 is the largest ribosomal protein and one of the few, where a specific function could be assigned. It is located on the small subunit of the ribosome and contains an RNA binding domain. The protein is involved in guiding, folding and general movement of the mRNA (Loveland & Korostelev, 2018; Sengupta *et al.*, 2001; Subramanian, 1983). The lack of the S1 protein is not the only difference in the ribosome between *B. subtilis* and *E. coli*. There is also a divergence in the essentiality of conserved ribosomal proteins. While the proteins L22 (RplV), L23 (RplW), and L28 (RpmB) can be deleted in *B. subtilis*, they are essential for growth of *E. coli* (Akanuma *et al.*, 2012; Shoji *et al.*, 2011). In *B. subtilis*, the deletion of L22 has a strong negative effect on growth and sporulation, but assembly of the ribosome is not affected. Therefore, it is assumed that the protein is not involved in maturation of the ribosome. It has been concluded that the protein is involved in folding of the 23S rRNA. It has additionally been observed that L22 facilitates binding of L32 (RpmF) to the ribosome (Akanuma *et al.*, 2012; Ban *et al.*, 2000). In contrast to L22, L2 (RplB) is essential for cell proliferation in *B. subtilis*. Yet,

a mutation in this protein has been identified that led to a temperature sensitive strain. Here, growth and ribosome assembly were impaired (Suzuki *et al.*, 2014). The reduction of ribosome assembly has been attributed to a weaker interaction with the 23S RNA (Harada *et al.*, 1998). The mutation also leads to a reduction of not only the amount of L2 in the ribosome, but also goes hand in hand with a reduction of L16 (RplP) (Suzuki *et al.*, 2014). These two examples already illustrate quite accurately that protein-protein interactions are very important for ribosome assembly and function, Furthermore, they show that ribosomal proteins not only interact with the rRNA but are also strongly linked to each other. Interestingly, some ribosomal proteins are also only associated to the ribosome under specific growth conditions. This is the case for L25 (Ctc). This protein was first known as a general stress protein, but was later revealed to bind the ribosome under stress conditions to ensure accurate translation (Schmalisch *et al.*, 2002).

The activity of the ribosome does not only depend on the correct assembly of the ribosome but also on its template. Ribosomes do not translate every mRNA with the same efficiency and sometimes even complete stalling of the complex can be observed. This happens due to several reasons. The first one is the secondary structure the mRNA might adapt and the time it takes the ribosome to unwind the nucleic acid (Wen *et al.*, 2008). Secondly, specific peptide chains can interact with components of the exit tunnel while passing through it. This then leads a lower translation speed or complete stalling of the ribosomal complex (Lu & Deutsch, 2008). In *B. subtilis*, the most prominent example for such a regulation is the MifM leader peptide which regulates the expression of YidC2 (Sohmen *et al.*, 2015). Stalling of the ribosome complex is achieved by an interaction of the MifM nascent chain with the ribosomal protein L22 (RplV) which leads to a blocking of the incoming aminoacyl-tRNA (Sohmen *et al.*, 2015). Yet, ribosome stalling can also be induced in a non-controlled manner in bacteria. This can have dire consequences for the cells if not resolved. The cause of this stalling can be damaged or truncated mRNA. There are two main forms of ribosome stalling, namely the no-go complex and the no-stop complex. In case of no-go stalling, the ribosome gets stuck on the mRNA and cannot proceed translation due to for example translational misreading (Müller *et al.*, 2021). In case of no-stop stalling, the ribosome gets stuck on the 3' end of a mRNA due to a lack of a stop codon. This prohibits recruitment of the release factors (RFs) and therefore termination of translation (Keiler *et al.*, 1996). Independent of the cause of ribosome stalling, these complexes need to be resolved before the concentration of active ribosome reaches a critical low level that affects cellular function. One of the major mechanisms for releasing stalled ribosomes caused by no-stop mRNA is *trans*-translation. Here, transfer-messenger RNA (tmRNA) plays an important role. It can act as tRNA<sup>ala</sup> while it also has mRNA properties. To release the ribosome, the tmRNA enters the complex and adds an alanine to the polypeptide chain which leads to a continuation of translation and

replacement of the faulty mRNA with the tmRNA. The mRNA part of the tmRNA encodes a degradation signal and a stop codon, which enables termination of translation. The ribosome is then recycled and the resulting peptide chain degraded (Keiler *et al.*, 1996). In *B. subtilis*, the tmRNA is encoded by *ssmR* and requires the binding of the small protein B (SmpB) for proper function (Karzai *et al.*, 2000). This mechanism is highly conserved in Eubacteria and was first described for *E. coli* (Ray & Apirion, 1979). An alternative mechanism to release non-stop stalled ribosomes involves RF (release factor) recruitment independent of the stop codon. In *E. coli* this is done by ArfA, which recruits RF2 to the stalled complex. This then leads to hydrolysis of the peptidyl-tRNA that is located at the P-site (Chadani *et al.*, 2012). A distinct but similar mechanism has been identified in *B. subtilis*. Here, binding of the protein BrfA subsequently leads to the recruitment of the RF2. BrfA is capable of monitoring the state of the mRNA channel of the ribosome and only engages if it is vacant, thus only binding to the ribosome if it is stalled (Shimokawa-Chiba *et al.*, 2019). A mechanism to rescue ribosomes that stalled within an ORF and not on the 3' end of the mRNA is based on the ribosome-associated protein quality-control (RQC) pathway. Independent on the position where ribosomes stall, following ribosomes often collided with the stalled ribosome. Recently, a sensor for this event has been identified in *B. subtilis*, namely the ATPase RqcU (Cerullo *et al.*, 2022). Next to sensing the collision, the ATPase also induces ribosome splitting. Then, downstream systems of the RQC pathway are recruited. This entails the two proteins RqcH and RqcP. Once the ribosome is split into its subunits, a polyalanine tail is added to the unfinished peptide chain. While RqcP stabilizes the P-site tRNA conformation, RqcH is responsible for adding the alanine tail to the peptide chain. The ribosomal protein L11 (RplK) has been shown to interact with RqcH and facilitate recruitment of the RQC factor to the 50S subunit (Takada *et al.*, 2021).

All the above-mentioned examples of protein interactions that take place at the ribosome impressively illustrate the complexity of the process that is translation. There is no such thing as a fixed and rigid composition of the ribosome and even nowadays, new proteins interacting with the ribosome are being discovered. It is therefore highly likely, that there is a multitude of proteins interacting with the ribosome still unknown and waiting to be discovered.

The speed in which bacteria can grow depends strongly on the speed of protein synthesis. Proteins make up most of each cell. The whole system that is needed for protein synthesis, including the ribosome, DNA, mRNA, tRNA as well as the RNA polymerase and other related factors make up over 60 % of the dry mass in exponentially growing cells (Bremer & Dennis, 2008). Protein synthesis is also an expensive process. It consumes a lot of energy and the cells need to be able to provide the amino acids. Therefore, the main function of metabolism in bacteria is to provide energy and precursors for protein synthesis.

## 1.2 Carbon metabolism in *B. subtilis*

The life of most organisms depends on the production of energy through carbon metabolism and the resulting catabolic intermediates. Most of the metabolic pathways present in living organism are connected to the central carbon metabolism at some point. This central carbon metabolism can be divided into three main pathways (I) the glycolysis, (II) the pentose phosphate pathway and (III) the TCA cycle. An illustration of glycolysis and the TCA cycle is depicted in figure 1.1.

### 1.2.1 Glycolysis / Gluconeogenesis

Glycolysis is the first pathway in the central carbon metabolism and converts glucose to pyruvate which leads to the production of energy in form of ATP. It can be divided into two main parts; the first part consumes energy and is also referred to as the preparatory phase. The second part, in which energy is generated is referred to as pay-off phase. Interestingly, the enzymes that are involved in the pay-off phase are highly conserved in most living organisms while some organisms do not possess the enzymes for the preparatory phase (e. g. some Archaea) or have alternative pathways to bypass this phase, such as the Entner-Doudoroff or the pentose phosphate pathway (Conway, 1992; Dandekar *et al.*, 1999). *B. subtilis* does not contain the enzymes to perform the Entner-Doudoroff pathway (Stülke & Hillen, 2000). An overview over glycolysis in *B. subtilis* is depicted in Fig 1.1. The reverse pathway of glycolysis is called gluconeogenesis. This pathway takes place to produce glucose in case of growth on an alternative carbon source. For this purpose, all enzymes involved in glycolysis can either also catalyse the reverse reaction or have a counterpart that is able to do so.

Interestingly, some enzymes of glycolysis are moonlighting proteins, meaning that they fulfil an additional function in the cell. The phosphofruktokinase (PfkA), the glyceraldehyde 3-phosphate dehydrogenase (GapA) and the enolase (Eno) have been identified to interact with enzymes that are involved in mRNA processing (Commichau *et al.*, 2009; UI Haq *et al.*, 2021). The interaction of Eno and PfkA with the RNase Y in complex with RNase J1, RNase J2 and polynucleotide phosphorylase suggests the existence of an RNA degradosome similar to the one described for *E. coli* (Carpousis, 2007; Commichau *et al.*, 2009). It has recently been described that the small protein SR7P supports the interaction of Eno with RNase Y. The interaction between Eno, SR7P and RNase Y increases RNA degradation by the RNase compared to the binary interaction between Eno and RNase Y (UI Haq *et al.*, 2021). GapA is able to bind RNase Y as well as RNase J1 and additionally interacts with the small protein SR1P. This interaction promotes the binding of GapA to RNase J1, which subsequently leads to an

increased activity of the RNase (Gimpel & Brantl, 2016). Again, this interaction might affect the RNA degradosome in *B. subtilis*.

The regulation of glycolysis is performed mostly on a transcriptional level. The important transcriptional regulator of glycolysis is the central glycolytic genes regulator CggR which was discovered during the investigation of the expression of *gapA* (Fillinger *et al.*, 2000). *B. subtilis* encodes two glyceraldehyde-3-phosphate dehydrogenases, namely GapA and GapB. The two proteins catalyse the interconversion of glyceraldehyde 3-phosphate and 1,3-bisphosphoglycerate. While GapA is NAD<sup>+</sup>-dependent and involved in glycolysis, GapB is NADP<sup>+</sup>-dependent and needed for gluconeogenesis. It was discovered that the expression of *gapA* is repressed by CggR which is encoded in the same operon as *gapA*. Intriguingly, CggR can bind fructose 1,6-bisphosphate, which decreases DNA binding activity of the regulator. It can therefore be stated that the presence of a precursor of glyceraldehyde 3-phosphate leads to the expression of *gapA* (Folly *et al.*, 2018).

The genes of gluconeogenesis are regulated by the transcriptional regulator CcpN. It was first discovered during the analysis of the expression of *gapB* and *pckA*, which both play important roles during gluconeogenesis. Disruption of *ccpA* lead to carbon catabolite repression independent expression of the two genes (Servant *et al.*, 2005). The appropriate control of these genes is important due to the fact that GapB catalyses the reaction back from 1,3-bisphosphoglycerate to glyceraldehyde 3-phosphate which cannot be achieved by GapA. Furthermore, PckA connects the TCA cycle to gluconeogenesis by catalysing the reaction of oxaloacetate to phosphoenolpyruvate. CcpN has additionally been shown to be involved in the regulation of the expression of a small non-coding RNA SR1, which suppresses genes of the arginine biosynthesis (Licht *et al.*, 2005). Next to gluconeogenesis, it could be shown that CcpN also interacts with DivIVA and moonlights in the control of cell elongation (Sharma *et al.*, 2020).

Next to the transcriptional regulation of glycolysis, protein interactions also play a role in modulating the activity of this pathway. It could be shown, that the glycolytic proteins phosphofructokinase, the phosphoglycerate mutase and the enolase interact and form what is termed the glycosome in various organisms (Commichau *et al.*, 2009; Michels *et al.*, 2006). The protein complex is presumed to enable substrate channelling and increase metabolic flux during glycolysis, but the beneficial effect on substrate channelling has been a subject of discussions in the past (Cornish-Bowden & Cardenas, 1993).

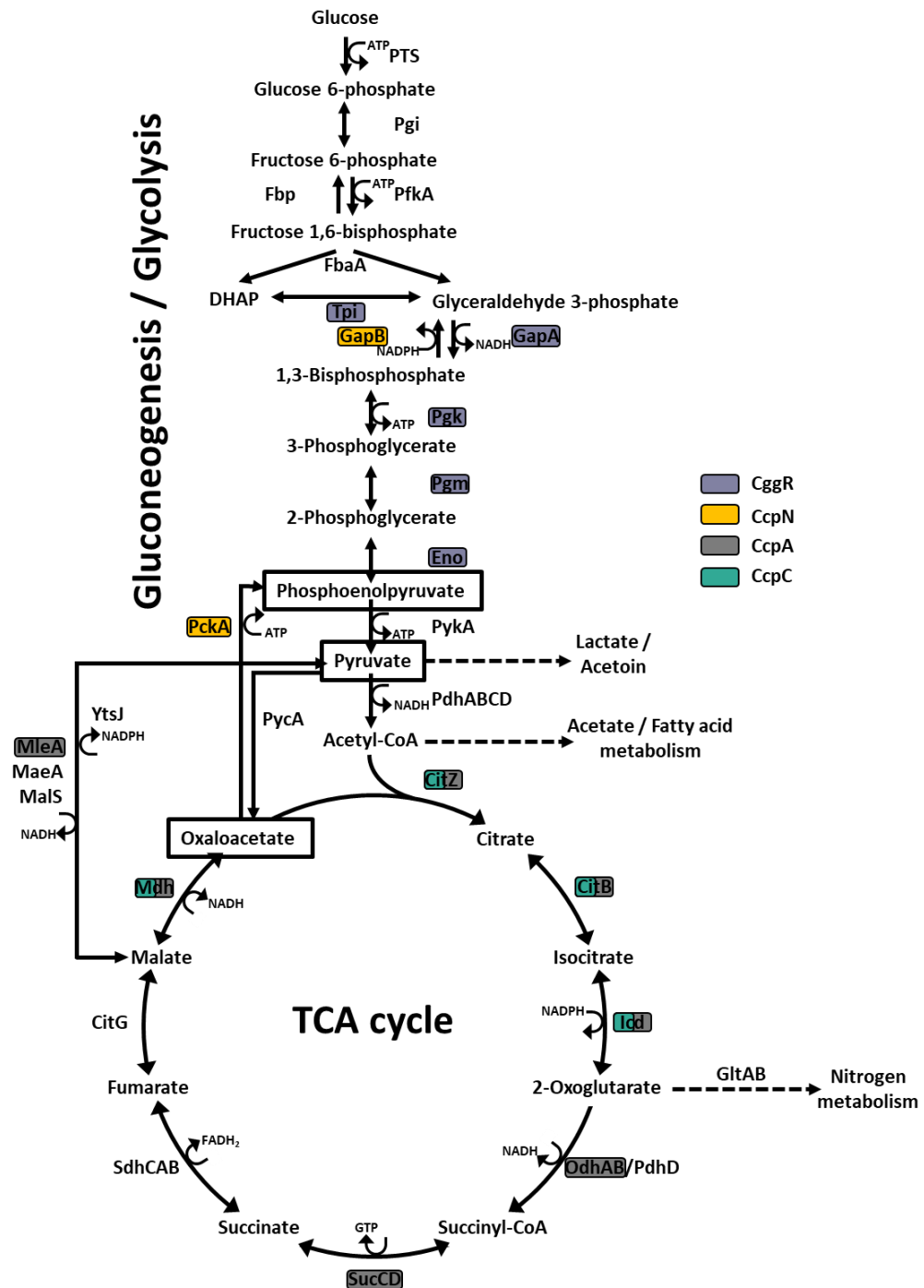


**Figure 1.1: Overview over glycolysis / gluconeogenesis and the TCA cycle in *B. subtilis*.** Proteins whose expression is regulated in a CggR dependent manner are marked in purple, proteins marked in yellow are regulated by CcpN, grey indicates regulation by CcpA and turquoise marked proteins are regulated by CcpC. Compounds of the anaplerotic node are marked in black. Abbreviations are PTS, phosphoenolpyruvate-carbohydrate phosphotransferase system; Pgi, glucose 6-phosphate isomerase; PfkA, phosphofruktokinase; Fbp, fructose 1,6-bisphosphatase; FbaA, fructose 1,6-bisphosphate aldolase; Tpi, triose phosphate isomerase; GapA, glyceraldehyde 3-phosphate dehydrogenase; GapB, glyceraldehyde 3-phosphate dehydrogenase; Pkg, phosphoglycerate kinase; Pgm, phosphoglycerate mutase; Eno, enolase; PykA, pyruvate kinase; PdhABCD, pyruvate dehydrogenase; CitZ, citrate synthase; CitB, aconitase; Icd, isocitrate dehydrogenase; OdhAB/PdhD, 2-oxoglutarate dehydrogenase; SucCD, succinyl-CoA synthetase; SdhCAB, succinate dehydrogenase; CitG, fumarase; Mdh, malate dehydrogenase; MleA, malic enzyme; MaeA, malic enzyme; MalS, malic enzyme; YtsJ, malic enzyme; PycA, pyruvate carboxylase; PckA, phosphoenolpyruvate carboxykinase; GltAB, glutamate synthase (adapted from Meyer, 2012).

### 1.2.2 The tricarboxylic acid cycle

Glycolysis is directly connected to the TCA cycle *via* the reaction performed by the pyruvate dehydrogenase complex. The cycle generates energy by complete oxidation of acetyl-CoA. Many metabolic pathways feed into or need substrates that originate from the TCA cycle. Upon growth on substrates of the TCA cycle, it can feed back into the gluconeogenesis through the enzymes involved in the anaplerotic node (Sauer & Eikmanns, 2005). As described above, this is done in order to produce glucose. If glucose is available as a carbon source, it gets metabolized through glycolysis with pyruvate. The pyruvate dehydrogenase complex then turns pyruvate into acetyl-CoA, which can have many different fates in the cell such as being used for fatty acid production to being funnelled into the TCA cycle. A detailed overview of the steps of the TCA cycle is depicted in Fig. 1.1.

Malate is, next to glucose, the second preferred carbon source in *B. subtilis*. As part of the TCA cycle, it can be oxidised by Mdh to produce oxaloacetate. Additionally, it can also be turned into pyruvate *via* one of four malic enzymes, namely MaeA, MalS, MleA, or YtsJ which enable funnelling of malate into gluconeogenesis.

To ensure smooth channelling of the intermediates through the cycle, the enzymes of the TCA cycle are often located in close proximity to each other and some can even be considered as complexes. From early on, it could already be elucidated that the sequential enzymes fumarase, malate dehydrogenase, citrate synthase, aconitase and isocitrate dehydrogenase cluster together in *E. coli* (Barnes & Weitzman, 1986). In *B. subtilis*, complex formation between the citrate synthase, the isocitrate dehydrogenase, and the malate dehydrogenase could be observed. Additionally, the aconitase and the fumarase interact with each other and with the malate dehydrogenase. Interestingly, an interaction between the malate dehydrogenase and the phosphoenolpyruvate carboxykinase was observed. Yet, this interaction only takes place under gluconeogenetic conditions and is released during growth on glucose. This makes sense since the sequential reaction of the proteins is only required if gluconeogenesis is taking place (Meyer *et al.*, 2011).

Similarly to the glycolysis, the TCA cycle is strongly regulated on a transcriptional level. One of the best studied regulatory mechanisms in bacteria is carbon catabolite repression, which regulates gene expression depending on the available carbon source. It was first observed in 1942, when the growth of *E. coli* in medium containing different carbon sources was studied. It was noted that the availability of more than one carbon source led to diauxic growth and an additional lag phase (Monod, 1942). This two-phased growth was due to the preferred carbon source being metabolized first. Once this carbon source had been exhausted, the switch to the second carbon source occurred and this adaptation led to the second lag phase. Carbon catabolite repression is the inactivation of catabolic pathways needed for utilization of a secondary carbon source if a preferred carbon source is available.



Since glucose is the preferred carbon source in most organisms, it is also known as glucose repression. Repression can be achieved through many different mechanisms such as transcriptional or translational regulation (Görke & Stülke, 2008). The magnitude of carbon catabolite repression can be illustrated by the size of this regulatory network, with 5-10 % of genes in bacteria being regulated *via* this regulatory mechanism (Blencke *et al.*, 2003; Liu *et al.*, 2005). In *B. subtilis*, there are three main enzymatic players involved in carbon catabolite repression, namely the histidine protein HPr which belongs to the PTS transport-phosphorylation system, the catabolite control protein CcpA, and the HPr kinase/phosphorylase HPrK. The PTS is involved in the import and phosphorylation of sugars and sugar derivatives (Erni, 2013). It consists of two phosphocarrier proteins, namely enzyme I (EI), HPr and additionally a sugar specific permease enzyme II (EII). EII is located at the membrane and enables import of the sugar. Phosphorylation of the sugar *via* the PTS system is PEP dependent. Here, the enzymes form a phosphorylation cascade, where EI functions as a phosphoryl acceptor from PEP. This allows the phosphorylation of HPr which then passes the phosphoryl group to EII. This leads to the subsequent phosphorylation of the EII bound carbohydrate (Deutscher *et al.*, 2014). Theoretically, there is no need for a whole cascade to phosphorylate one substrate. This mechanism has evolved due to the additional regulatory functions that are carried out by the proteins of the PTS. The HPr protein, which is involved in the regulation of carbon catabolite repression contains two phosphorylation sites namely His15 and Ser46. His15 is phosphorylated in the cascade described above. This has an enzymatic effect while the phosphorylation of Ser46 has a regulatory effect. The phosphorylation of Ser46 occurs if glycolytic intermediates, especially glucose 6-phosphate and fructose 1,6-bisphosphate, are present in abundance within the cell (Poncet *et al.*, 2004) and is performed by the bifunctional HPr kinase/phosphorylase in an ATP dependent manner (Fieulaine *et al.*, 2002; Poncet *et al.*, 2004). The transcription regulator CcpA is constitutively expressed and not regulated on a transcriptional level. Thus, regulation happens post translationally (Miwa *et al.*, 1994). This is achieved by binding of HPr-Ser46-P to CcpA, which leads to a conformational change in CcpA that allows the binding of the catabolite responsive element (*cre*) (Schumacher *et al.*, 2007). The CcpA- HPr-Ser46-P complex regulates the expression of over 300 genes, while repressing the expression of most of them. It can also have an activating effect on expression of some genes. These genes are mostly involved in amino acid synthesis and overflow metabolism (Fujita, 2009; Görke & Stülke, 2008). Interestingly, HPr is not able to bind CcpA if only His15 is phosphorylated (Deutscher *et al.*, 1995).

Next to the transcriptional regulation imposed by CcpA dependent carbon catabolite repression, additional mechanisms are in place to ensure the best control of the central carbon metabolism.

One CCR independent mechanism of regulation was discovered when the expression of *citZ* and *citB* was studied. It came to light that CcpA only directly represses the expression of the citrate synthase *citZ*, while it only has an indirect effect on the aconitase *citB* (Kim *et al.*, 2002). CitB was discovered to be regulated by an alternative regulator, the catabolite control protein CcpC. Binding of CcpC to the DNA upstream region of *citB* is modulated by the citrate concentration, with CcpC inducing expression of *citB* under high citrate concentrations and repressing it at low concentrations (Mittal *et al.*, 2013). It could also be shown that CcpC is an additional regulator for *citZ* (Jourlin-Castelli *et al.*, 2000). Furthermore, the expression of *citB* is controlled by the pleiotropic repressor CodY in the presence of branched chain amino acids. This regulation is partially competitive to CcpC (Kim *et al.*, 2003). It has been described that the transcription factor TnrA, which is involved in nitrogen metabolism, plays a role in the regulation of *citB* and activates its transcription in the absence of glutamine linking the TCA cycle to the nitrogen metabolism. The molecular mechanism of this control remains to be uncovered (Blencke *et al.*, 2006). Interestingly, *citB* not only underlies regulation, but also has regulation properties itself. It is able to bind the mRNA of *citZ* and by doing so, destabilizing it, thereby creating an autoregulation loop for citrate metabolism (Pechter *et al.*, 2013). The RNA binding activity of CitB also comes into play during iron metabolism which will be focused on later.

Interestingly, the enzyme activity of PycA, which catalyses the carboxylation of pyruvate to oxaloacetate, is regulated by direct protein-protein interaction. This regulation is achieved by binding of the c-di-AMP binding protein DarB to the pyruvate carboxylase. Binding only occurs if no c-di-AMP is bound by DarB, which is the case during potassium limitation. The interaction between DarB and PycA stimulates the activity of the pyruvate carboxylase leading to an increased activity of the TCA cycle and thus restoration of higher TCA cycle intermediate levels (Krüger *et al.*, 2022). As mentioned before, PycA is not the only enzyme that connects glycolysis with the TCA cycle. The major step connecting the two pathways is catalysed by the pyruvate dehydrogenase complex.

### 1.2.3 The pyruvate dehydrogenase

The pyruvate dehydrogenase is a multienzyme complex that catalyses the irreversible oxidative decarboxylation of pyruvate leading to the formation of acetyl-CoA. This step is the linker between the glycolytic pathway and the tricarboxylic acid (TCA) cycle and provides important precursors for fatty acid biosynthesis (Patel & Roche, 1990).

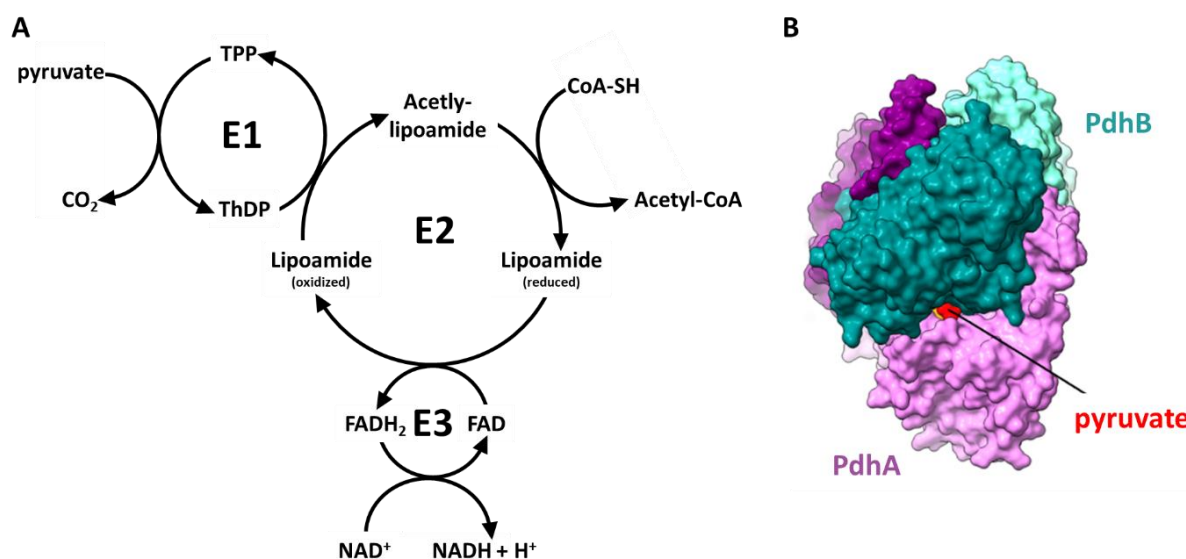
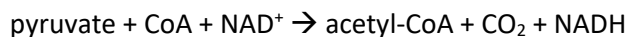


**Figure 1.2: The pyruvate dehydrogenase.** **A** Schematic illustration of the reactions catalysed by the different subunits of the pyruvate dehydrogenase complex. **B** Model of the surface of the pyruvate dehydrogenase including the pyruvate binding site (O'Reilly *et al.*, 2022).

The pyruvate dehydrogenase complex is formed by multiple copies of three enzymes that catalyse successive steps of a multistep chemical reaction, the pyruvate dehydrogenase (E1), the dihydrolipoamide acetyltransferase (E2), and the dihydrolipoamide dehydrogenase (E3). The pyruvate dehydrogenase of *B. subtilis* consists of 30 E1, 60 E2, and 6 E3 modules (Berg & de Kok, 1997; Reed & Hackert, 1990). The dihydrolipoamide acetyltransferase (E2) forms the core of the complex. E1 is a heterotetramer ( $\alpha\beta_2$ ), which is encoded by *pdhA* and *pdhB*. The dihydrolipoamide acetyltransferase is encoded by *pdhC* and the dihydrolipoamide dehydrogenase by *pdhD*. The whole complex is arranged in an icosahedral symmetry (Neveling *et al.*, 1998). Interestingly, the pyruvate dehydrogenase of Gram-negative bacteria, such as *E. coli*, consists of a homodimer (Patel *et al.*, 2014). In principle, the mode of action is identical in every organism that contains the complex, with E1 and E2 being responsible for the formation of acetyl-coenzyme A (acetyl-CoA), while E3 is needed for redox recycling (Perham, 1991). More precisely, the pyruvate dehydrogenase binds pyruvate and thiamine pyrophosphate (TPP). The decarboxylation of pyruvate leads to the formation of an enamine bound to the thiamine diphosphate (ThDP). This enamine catalyses the reductive acetylation of lipoamide bound to E2, producing acetyl lipoamide and ThDP. This is the rate-limiting step of the pyruvate dehydrogenase complex. Next, E2 binds the CoA which ultimately leads to the formation of acetyl-CoA and reduced lipoamide, with acetyl-CoA being released from the complex. Oxidation of lipoamide is performed by E3 following a ping-pong mechanism. First, an electron is removed from lipoamide which subsequently leads to the reduction of NAD<sup>+</sup> to NADH which is dependent on the oxidation of FADH<sub>2</sub> to FAD (Fig. 1.2)

(de Kok *et al*, 1998). The net reaction performed by the pyruvate dehydrogenase complex can be described as follows:



Since the oxidative decarboxylation of pyruvate to acetyl-CoA is an irreversible reaction that is located at a crucial connection point in metabolism, it needs to be tightly controlled. Yet, regulation of this process is highly species dependent with higher eukaryotes, such as mammals, having the most complex regulatory network. A combination of mechanisms ensures proper control over the pyruvate dehydrogenase activity. The first mechanism involves post translational modification, more precisely the reversible phosphorylation / dephosphorylation of up to three potential phosphorylation sites (serine residues) of E1, leading to short term regulation (Dahl *et al*, 1987; Yeaman *et al*, 1978). The effect of these modifications is dependent on each phosphorylation site, since they are located differently in relation to the active site. This allows quick fine tuning of the activity (Korotchkina & Patel, 2001). The second important mechanism for control of the pyruvate dehydrogenase activity takes place at the level of transcription, and has a more long-term effect. For this purpose, the transcription level of enzymes, such as the dedicated kinases and phosphatases needed for the phosphorylation are regulated (Harris *et al*, 2001). In mammals, four of these kinases specific of the pyruvate dehydrogenase are encoded (Gudi *et al*, 1995; Rowles *et al*, 1996). They differ in their localization, with some only present in certain tissues, as well as in their reactivity and their specificity towards the lipoyl domains (Bowker-Kinley *et al*, 1998). There is no evidence that this mechanism of regulation exists in prokaryotes and no sequence similar to the mammalian pyruvate dehydrogenase kinases has been identified. Interestingly, some prokaryotic organisms still contain pyruvate dehydrogenases with phosphorylation sites (Patel & Korotchkina, 2006). In bacteria, regulation is achieved by allosteric mechanisms and product inhibition. It has been described that the presence of pyruvate stimulates the activity of the pyruvate dehydrogenase complex, while the accumulation of acetyl-CoA has a negative effect. Furthermore, NADH negatively affects the activity of the E3 subunit while CoA increases the activity of E2 (de Kok *et al*, 1998). In *E. coli*, expression of the operon encoding the enzymes of the pyruvate dehydrogenase is repressed by PdhR. PdhR is also encoded in said operon and autoregulates its own expression while pyruvate serves as a putative inducing co-effector (Quail *et al*, 1994; Quail & Guest, 1995). These are the only regulatory mechanisms described in bacteria up to this date.

Interestingly, the E3 subunit of the pyruvate dehydrogenase complex is shared with another complex, the 2-oxoglutarate dehydrogenase complex. Similar to the pyruvate dehydrogenase complex, this complex consists of three subunits. The E1 subunit is encoded by *odhA*, the E2 subunit by *odhB* and, as mentioned before, the E3 subunit by *pdhD* (Meyer *et al.*, 2011). This complex catalyses

the oxidative decarboxylation of 2-oxoglutarate to succinyl-CoA and CO<sub>2</sub> and consumes acetyl CoA and NAD<sup>+</sup>. It additionally requires thiamine diphosphate as a co-factor.

An additional decarboxylase that forms a large protein complex in *B. subtilis* is the oxalate decarboxylase. This complex consists of six subunits of OxdC that form two trimeric subunits and catalyses the synthesis formate and carbon dioxide from oxalate (Just *et al.*, 2004). Interestingly, the complex functions best at an acidic pH and needs manganese and oxygen to function (Conter *et al.*, 2019). It is not unusual that proteins require the presence of metals as co-factors for proper function. Therefore, metal homeostasis needs to be controlled and maintained at a certain level to allow the provision of these important co-factors in bacteria.

### 1.3 Iron metabolism

#### 1.3.1 The regulator family Fur

Many proteins involved in major metabolic pathways require co-factors to function. Once the co-factor is bound, the enzyme is referred to as holoenzyme, while the enzymatically non-active form without the co-factor is termed apo-enzyme. Co-factors can be small molecules such as ATP, NAD, or even metals like iron, zinc or manganese. The concentration of intracellular metals needs to be under tight control since they can have toxic effects upon accumulation. Especially the accumulation of iron leads to oxidative stress through the products of the Fenton reaction, for example hydroxy radicals, which results in DNA damage and ultimately cell death (Touati *et al.*, 1995; Imlay, 2003). Many of these metal uptake systems are regulated by proteins belonging to the ferric uptake regulator (Fur) family (Lee & Helmann, 2007). Transcriptional regulators of this family are involved in regulating the uptake and concentration of metals such as zinc (Zur) (Gaballa & Helmann, 1998), manganese (Mur) (Díaz-Mireles *et al.*, 2005) and nickel (Nur) (Ahn *et al.*, 2006). An additional member of the Fur family is the peroxide sensor PerR (Bsat *et al.*, 1998). These transcriptional regulators all act by binding their respective metal. This results in a conformational change that can theoretically either lead to a higher or lower DNA binding affinity of the regulator. Thus, the presence of the metal can either have an inducing or repressing effect on gene expression.

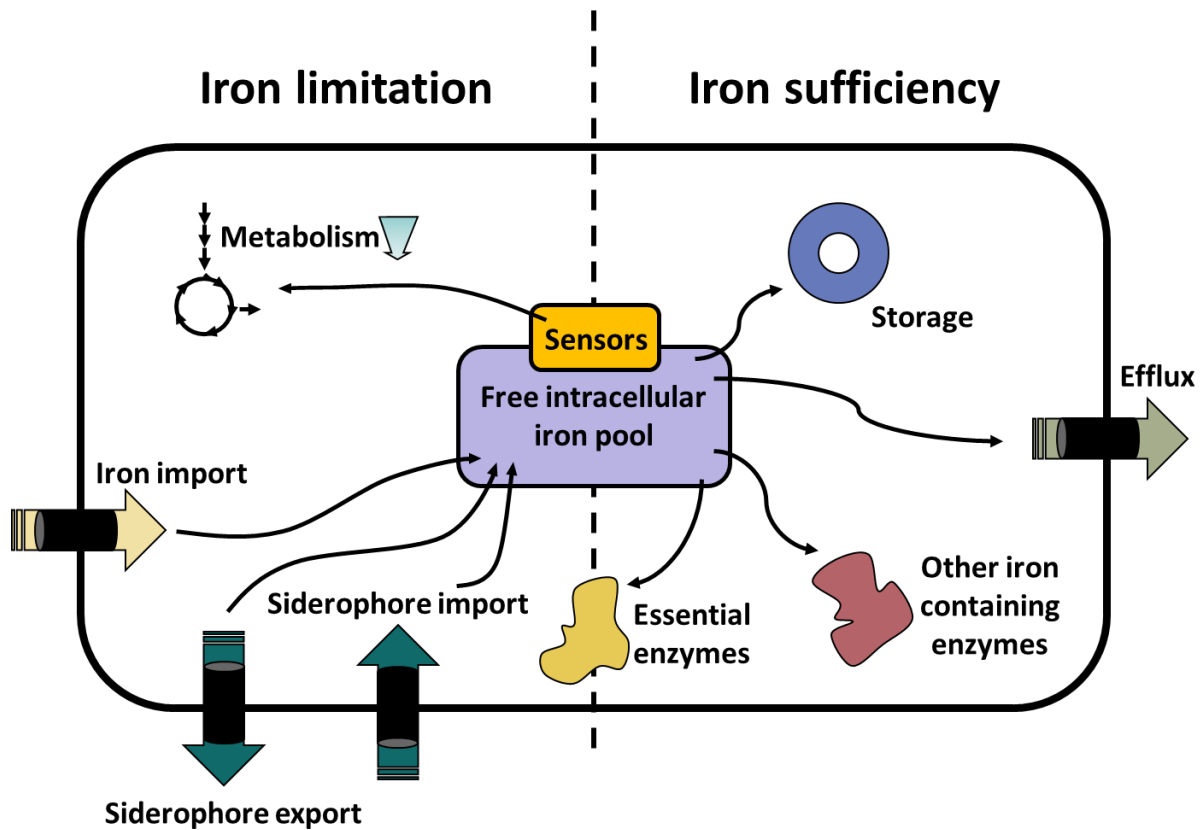


**Figure 1.3: Schematic illustration of the iron homeostasis in *B. subtilis*.** Growth under iron limitation, high affinity iron importers as well as siderophore transporters are expressed. Iron-sparing mechanisms also lead to the replacement of iron dependent enzymes by their iron independent homologs to free iron for essential iron dependent enzymes. Furthermore, central metabolism is downregulated. Spare iron can be stored in Dps like proteins or exported out of the cell to avoid the formation of RAS through the Fenton reaction. Adapted from Pi & Helmann, 2017a.

### 1.3.2 Fur

Iron containing enzymes can be divided into three classes. Firstly mono- and dinuclear iron enzymes, secondly, heme proteins and lastly iron-sulphur cluster enzymes. Life evolved in an anaerobic environment, which meant an abundance of the soluble ferrous  $\text{Fe}^{2+}$  (Anbar, 2008). Over time, the atmosphere shifted to an aerobic form which led to oxidation of the iron into its poorly soluble ferric form ( $\text{Fe}^{3+}$ ). This caused a depletion of available iron, which resulted in the evolution of iron uptake systems and other coping mechanisms (Fig. 1.3). A shortage of iron in the environment can be combatted by employing high affinity iron importers as well as siderophore synthesis and transport. Furthermore, in an iron sparing response non-essential iron containing enzymes can be replaced by their iron independent homologs.

In *B. subtilis*, Fur regulates the expression of over 50 genes involved in iron uptake, siderophore synthesis and transport as well as the expression of proteins that utilize iron (Baichoo *et al*, 2002). *B. subtilis* is not only able to synthesise its own siderophore (bacillibactin) but can also import

siderophores produced by other organisms (xenosiderophore). Fur functions as a sensor for iron sufficiency and binds  $\text{Fe}^{2+}$  in the cytosol if iron is present in excess. Once iron is bound, Fur forms homodimers and binds to a 19 bp inverted repeat sequence within the promoter region of genes involved in iron import, thus repressing their transcription. The 19 bp binding region of Fur is known as the Fur box and actually consist of two overlapping 7-1-7 heptamer repeats. This enables binding of two Fur dimers on opposite faces of the DNA helix *via* a helix-turn-helix binding motive (Baichoo & Helmann, 2002). Upon iron shortage, apo-Fur is released from the DNA and expression of genes involved in iron homeostasis is induced. This expression happens in three distinct waves. First, proteins enabling the uptake of elemental iron, petrobactin and ferric citrate are expressed. Next, bacillibactin synthesis is induced together with siderophore uptake systems. This happens parallel to the synthesis of flavodoxins in order to replace ferredoxins. As a last response to declining iron levels, the translation of abundant iron-utilizing proteins is stopped which allows the remaining iron to be made available for the most essential iron containing proteins (Pi & Helmann, 2017b).

Yet, Fur does not only have a repressing effect but can also act as an activator. This can happen in a direct or indirect fashion. Direct activation has been described for the iron efflux pump PfeT, which is repressed by PerR (Gaballa & Helmann, 2002). In this case, Fur acts as a transcriptional activator under high iron conditions and works in an antagonistic manner to PerR, which allows protection against toxic intracellular concentrations of iron (Pinochet-Barros & Helmann, 2020). Indirect activation is achieved through the regulation of the FsrA sRNA as well as the small proteins FbpA, FbpB and FbpC. Fur binds the regulatory region upstream of the sRNA as well as of the proteins but is released from the DNA once iron levels sink. This allows FsrA-mediated down regulation of the synthesis of multiple iron-containing enzymes and biosynthetic pathways consuming iron. FbpAB and FbpC function as RNA-chaperones in the process. Thus, these pathways and enzymes are active once Fur binds the regulation site of *frsA* (Gaballa *et al.*, 2008). Subject to this regulation are the iron-dependent enzymes aconitase (CitB), succinate dehydrogenase (SdhCAB) and glutamate synthase (GltAB), which all play important roles in central metabolism. Upon iron limitation, the mRNAs coding for these proteins get degraded faster which reduces the amount of the proteins that is translated and thus the metabolic flux of the TCA cycle (Smaldone *et al.*, 2012). Interestingly, the aconitase has also been described to have its own regulatory function. The protein contains an iron-sulphur cluster under standard conditions. Upon iron limitation, the cluster is unsaturated which leads to a conformational change. This change enables the binding of specific RNA regions named iron response elements (IRE), which has an effect on either translation or degradation of the mRNA, depending on the binding site. Genes that underly this regulation are for example *goxD*, *feuA* and *feuB* as well as *gerE*. It has not been determined whether binding of CitB to the RNA regions of *goxD*, *feuA* or *feuB* actually has a stabilizing

effect (Ul Haq *et al.*, 2020) but it could be shown that *greE* mRNA is stabilized by CitB binding (Serio *et al.*, 2006).

In the case of iron saturation in the cell, excess iron can be stored in specialized iron storage proteins. Here, *B. subtilis* encodes two ferritin-like proteins that belong to the class of Dps proteins (Dps and MrgA) and are able to store the metal. These proteins adapt a dodecamers conformation that results in a doughnut like structure. Iron storage is achieved by oxidation of two  $\text{Fe}^{2+}$  to  $\text{Fe}^{3+}$  in an  $\text{H}_2\text{O}_2$  dependent manner, thus avoiding the formation of ROS.  $\text{O}_2$  can also serve as an oxidant, but is in this case interestingly severely less efficient than  $\text{H}_2\text{O}_2$  (Zhao *et al.*, 2002). After oxidation with  $\text{H}_2\text{O}_2$ , up to 500 molecules of  $\text{Fe}^{3+}$  can be stored in the core of Dps. Dps can also protect the DNA by directly binding to it in a sequence independent manner (Haikarainen & Papageorgiou, 2010). To coordinate the responses to changing iron concentrations, the cells have evolved a variety of sensors. An additional iron regulator is the diphtheria toxin regulator DtxR, which in some organisms also takes part in regulating manganese transporters (Chen *et al.*, 2010). It plays a role in Gram-positive bacteria that contain a high GC content. DtxR acts as a repressor for proteins involved in iron import and as an inducer for iron storage proteins (Frunzke *et al.*, 2011; Schmitt *et al.*, 1997). Another example for a regulator involved in iron homeostasis is the rhizobial iron regulator RirA. Interestingly, it does not exhibit any sequence homology to other well studied metal sensing regulators such as Fur or DtxR (Chao *et al.*, 2005). The way this protein is activated also differs from the other regulators since it does not seem to respond to the cytosolic iron levels but rather monitors the status of the cellular iron-sulphur clusters (Andrews *et al.*, 2013). Like the other regulators, RirA controls the expression of genes that are needed for iron transport. Additionally, it also controls genes for iron-sulphur cluster formation as well as some genes involved in energy metabolism and exopolysaccharide production (Chao *et al.*, 2005).

### 1.4 Novel protein-protein interactions

It has become clear that a multitude of biological processes rely heavily on protein-protein interactions. Understanding these interactions is important to understand the function of each protein and the biological processes they are involved in. Numerous *in vivo*, *in vitro* and *in silico* methods have been developed to characterise the structure, function and interaction partners of proteins. The recent development of the artificial intelligence (AI) based network AlphaFold has allowed the accurate prediction of 3D-protein structures of completely unknown proteins (Jumper *et al.*, 2021). The further development of AlphaFold-Multimer has made it possible to predict not only the structure of a single protein but also the structure of protein complexes (Evans *et al.*, 2022). This certainly is the start of a



new era for structural biology. But where does it put the classical experimental approaches to identify protein structures such as x-ray crystallography, cross-linking mass spectrometry (CLMS) and cryo-electron microscopy (Callaway, 2020)? Combining the complementary experimental approaches of in-cell CLMS and co-fractionation mass spectrometry (CoFrac-MS) with artificial intelligence-based structure prediction of protein complexes is a workflow that could potentially bring the identification of novel protein complexes on a large scale into reach. This approach would allow the creation of interaction networks in organisms that are not easily genetically modifiable such as pathogenic bacteria and could mean a big advantage in the development of novel antibiotics. To show the functionality of this approach, the whole proteome of *B. subtilis* has recently been analysed by using this workflow which resulted in a proteome wide interaction map that interestingly also contained proteins of so far unknown function predicted with known complexes (O'Reilly *et al.*, 2022). These proteins include YabR and YugI which were found crosslinked to the ribosome, YneR which was found crosslinked to the pyruvate dehydrogenase and YlaN which was found crosslinked to Fur.

### **1.5 Objective of this thesis**

The objective of this thesis is to validate the interactions discovered by CLMS and CoFrac-MS *in vivo* and to prove that the workflow actually allows the prediction of high confidence novel protein-protein interactions. It will be focused on the interactions at the 30S subunit of the ribosome involving YabR and YugI. Furthermore, the involvement of the protein of unknown function YneR with the pyruvate dehydrogenase will be investigated. Lastly, the interaction of Fur and YlaN will be characterised. This will be approached *via* classical molecular methods such as bacterial two hybrids, genetic modifications and growth assays.



## 2. Material and Methods

### 2.1 Material

All chemicals, antibodies, equipment, commercial systems, enzymes and oligonucleotides that were used are listed in the appendix.

#### 2.1.1 Bacterial strains and plasmids

Bacterial strains and plasmids are listed in the appendix.

#### 2.1.2 Growth media

Media, solutions and buffers were prepared using deionized water and autoclaved for 20 min at 121°C and 2 bar, unless otherwise stated. Thermolabile substances were dissolved and sterile filtrated (pore size: 0.22 µm).

##### Bacterial growth media

*E. coli* was cultivated in LB medium, whereas *B. subtilis* was grown using LB, SP and MSSM minimal medium, supplemented with additives as indicated. For solidification complex media were supplemented with 1.5 % (w/v) agar and minimal media with 1.8 % Bacto agar.

##### Complex media

LB medium	10 g	Tryptone
(1 l)	5 g	Yeast extract
	10 g	NaCl
SP medium	8 g	Nutrient Broth
(1 l)	0.25 g	MgSO <sub>4</sub> x 7 H <sub>2</sub> O
	1 g	KCl
	After autoclaving add	
	1 ml	CaCl <sub>2</sub> (0.5 M)

## 2. Material and Methods

---

	1 ml	MnCl <sub>2</sub> (10 mM)
	2 ml	CAF (2.2 mg/ml)
Starch medium	7.5 g	Nutrient Broth
(1 l)	5 g	Starch
10x MN medium	136 g	K <sub>2</sub> HPO <sub>4</sub> x 3 H <sub>2</sub> O
(1 l)	60 g	KH <sub>2</sub> PO <sub>4</sub>
	10 g	Sodium citrate x 2 H <sub>2</sub> O
Minimal media		
MNGE	1 ml	10x MN-Medium
(10 ml)	400 µl	Glucose (50% (w/v))
	100 µl	Tryptophane (5 mg/ml)
	50 µl	Potassium Glutamate (40 % (w/v))
	50 µl	CAF (2.2 mg/ml)
	30 µl	MgSO <sub>4</sub> (1 M)
	(100 µl)	CAA (10 % (w/v))
5x MSSM medium stock	41 g	Na <sub>2</sub> HPO <sub>4</sub> x 3 H <sub>2</sub> O
(1 l)	18.3 g	NaH <sub>2</sub> PO <sub>4</sub> x 1 H <sub>2</sub> O
	5 g	Sodium citrate
	1 g	MgSO <sub>4</sub> x 7 H <sub>2</sub> O
MSSM medium	200 ml	5x MSSM medium stock
(1 l)	10 ml	100x Trace elements
	10 ml	100x Iron citrate
	10 ml	KCl (10 mM, if not stated otherwise)
	10 ml	Glucose (50 %)
	10 ml	Ammonium sulphate (20 % (w/v))
	10 ml	Tryptophane (5 mg/ml)

## 2. Material and Methods

100x Trace elements	0.735 g	CaCl <sub>2</sub> x 2 H <sub>2</sub> O
(1 l)	0.12 g	MnCl <sub>2</sub> x 6 H <sub>2</sub> O
	0.17 g	ZnCl <sub>2</sub>
	0.033 g	CuCl <sub>2</sub> x 2 H <sub>2</sub> O
	0.06 g	CoCl <sub>2</sub> x 6 H <sub>2</sub> O
	0.051 g	Na <sub>2</sub> MoO <sub>4</sub> x 2 H <sub>2</sub> O
100x Iron citrate	0.0135 g	FeCl <sub>3</sub> x 6 H <sub>2</sub> O
(100 ml)	0.1 g	Na <sub>3</sub> citrate x 2 H <sub>2</sub> O

### 2.1.3 Antibiotics

To select for bacterial strains and plasmids, antibiotics were prepared in 1000-fold stock solutions. If not stated otherwise they were sterile filtrated (0.22 µm pore size) and stored at -20°C. Antibiotics were added, once the medium had reached a temperature of ~50°C after autoclavation. Erythromycin and Lincomycin were used in combination to select for *ermC* (Griffith *et al.*, 1965).

**Table 2.1: Antibiotics**

Antibiotic	Solvent	Stock (mg/ml)	Working concentration (µg/ml)	
			<i>E. coli</i>	<i>B. subtilis</i>
Ampicillin	H <sub>2</sub> O	100	100	-
Kanamycin	H <sub>2</sub> O	10	50	10
Lincomycin	H <sub>2</sub> O	25	-	25
Erythromycin	70 % EtOH	2	5	2
Spectinomycin	H <sub>2</sub> O	100	-	150
Tetracycline	70 % EtOH	6.25	-	12.5
Zeocin (TermoFisher)		100		30

## 2.2 Methods

### 2.2.1 Standard methods

Some standard methods that were applied are listed in Tab. 2 together with the corresponding literature.

**Table 2.2: Standard methods**

Method	Reference
Measurement of optical density	Sambrook <i>et al.</i> , 1989
DNA gel electrophoresis	Sambrook <i>et al.</i> , 1989
Ligation of DNA fragments	Sambrook <i>et al.</i> , 1989
Plasmid isolation from <i>E. coli</i>	Green & Sambrook, 2016
Chain terminator sequencing	Sanger <i>et al.</i> , 1977

### 2.2.2 Cultivation and storage of bacteria

Unless stated otherwise, *E. coli* and *B. subtilis* strains were cultivated in LB liquid medium at 37°C and 200 rpm in tubes or flasks. For this purpose, fresh single colonies were picked from plate or cryo-cultures were used for inoculation. Growth was monitored as the optical density at 600 nm (OD<sub>600</sub>). Cultures were supplemented with the respective antibiotics and supplements if not stated otherwise. *E. coli* was kept on LB medium agar plates for up to 4 weeks at 4°C. DMSO cultures were used for long-term storage. *B. subtilis* was cultured on SP plates and were stored on these plates at room temperature. Instable strains were stored as cryo-cultures. These were prepared in 2 ml screw-cap tubes. Therefore, DMSO was mixed with a fresh overnight culture in a 1:10 ratio, subjected to rapid freezing in liquid nitrogen and stored at - 80°C.

### 2.2.3 Preparation of competent *E. coli* and transformation

#### Preparation of competent cells in SOB medium

A culture of *E. coli* DH5α cells were used to inoculate 250 ml SOB-medium over night at 18°C. After reaching an OD<sub>600</sub> of 0.5-0.9, the culture was cooled down for 10 min on ice. The cells were harvested

by centrifugation for 10 min at 4°C and 4000 rpm. Afterwards, the cell pellet was resuspended in 80 ml of ice-cold TB buffer. DMSO was added to a final concentration of 7 % and 200 µl aliquots were prepared and frozen in liquid nitrogen. The cells were stored at -80°C (modified from Klewing, 2019).

SOB medium	20 g	Tryptone
(1 l)	5 g	Yeast extract
	0.584 g	NaCl
	0.188	KCl
TB buffer	1.51 g	PIPES
(500 ml, pH 6.7)	1.1 g	CaCl <sub>2</sub> x H <sub>2</sub> O
	9.32 g	KCl
	27.5 ml	MnCl <sub>2</sub> (1 M)

### Preparation of competent cells in CaCl<sub>2</sub> solution

An overnight culture of *E. coli* DH5α was used to inoculate 10 ml of LB medium. This culture was grown at 37°C until an OD<sub>600</sub> of 0.3 was reached. The cells were then harvested for 6 min at 5000 rpm and 4°C and the resulting pellet was resuspended in 5 ml of 50 mM ice-cold CaCl<sub>2</sub> solution. The cells were incubated on ice for 30 min and then subjected to another centrifugation step as described before. The cell pellet was then resuspended in 1 ml ice-cold CaCl<sub>2</sub> solution and used for transformation.

### Transformation of *E. coli*

100 µl of competent *E. coli* cells were incubated with ligation samples on ice for 30 min. The cells were then transferred to 42°C for 90 sec as a heat shock. Subsequently, the cells were incubated on ice for 5 min. Afterwards, 500 µl of LB medium were added to the cells and they were incubated for 1 h at 37°C with agitation before being plated on LB-agar plates containing appropriate antibiotics.

## 2.2.4 Preparation of competent *B. subtilis* cells and transformation

### Preparation of competent *B. subtilis* cells

An overnight culture of *B. subtilis* was inoculated to an OD<sub>600</sub> of 0.1 in 10 ml of MNGE medium containing CAA. This culture was then incubated at 37°C and 200 rpm until an OD<sub>600</sub> of 1.3 was reached. Once this optical density was reached, the culture was diluted with 10 ml MNGE medium without CAA and incubated for an additional hour. After this incubation, the cells were either used for

transformation or prepared for long term storage. For long term storage, 15 ml of the cells were harvested by centrifugation for 5 min at 5000 rpm and resuspended in 1.8 ml of the supernatant and 1.2 ml glycerol (50%). The competent cells were stored in 300 µl aliquots at -80°C (modified from Faßhauer, 2021).

### Transformation of *B. subtilis*

Cells were either used fresh or a 300 µl aliquot was thawed on ice and mixed with 1.7 ml 1x MN medium supplemented with 43 µl glucose (20% (w/v)) and 34 µl MgSO<sub>4</sub> solution (1 M). Next, 0.1 – 1 µg genomic DNA or 2 µg plasmid DNA were added to 400 µl of competent *B. subtilis* cells. The cells were then incubated for 30 min at 37°C at agitation (200 rpm). Afterwards, 100 µl expression mix was added and incubation was continued at 37°C for an additional hour. The cells were then plated on SP medium containing the appropriate antibiotics

Expression mix	500 µl	Yeast extract
(1.05 ml)	250 µl	CAA (10 %)
	50 µl	Tryptophane

### 2.2.5 Working with DNA

#### Isolation of chromosomal and plasmid DNA from *B. subtilis* and *E. coli*

Preparation of plasmid DNA from *E. coli*

Plasmid DNA was extracted from *E. coli* utilizing the e NucleoSpin® Plasmid Kit from Machery-Nagel. For this purpose, 4-15 ml of a fresh overnight culture were harvested at 5000 rpm for 5 min and handled as described in the manufacturers' manual. The plasmids were eluted in deionized water modified from Richts, 2021).

Isolation of genomic DNA from *B. subtilis*

For isolation of genomic DNA from *B. subtilis*, 4 ml overnight culture were harvested by centrifugation for 2 min at 13 000 rpm. The resulting cell pellet was then resuspended in 100 µl lysis buffer and 100 µl TE buffer. This was followed by an incubation for 30 min at 37°C at agitation. Afterwards, the samples were subjected to centrifugation for 5 min at 4000 g. The pellet was resuspended in 300 µl DNA lysis buffer and 20 µl Proteinase K solution and 15 ml RNase A (20 mg/ml) were added. The mixture was incubated for 30 min at 70°C at agitation. From here on forward, it was continued as described in the manufacturers' manual (peqGOLD Bacterial DNA Kit from PEQLAB).



## 2. Material and Methods

---

Lysis buffer	50 mg	Lysozyme
(2.5 ml)	50 $\mu$ l	Tris-HCl pH 8.0 (1 M)
	10 $\mu$ l	Na <sub>2</sub> EDTA x 2 H <sub>2</sub> O (0.5 M)

### Determination of DNA concentrations (Nanodrop)

In order to determine the DNA concentration of a sample the optical density was measured by using a UV-Vis-Spectrophotometer, which needs only very low volumes of 1 - 2  $\mu$ l. The device measures the OD<sub>260</sub> of the sample in relation to the solution the sample is solved in and the software calculates the amount of DNA (Richts, 2021).

### Agarose gel electrophoresis

Agarose gel electrophoresis is a method used to sort DNA and RNA molecules by size. Agarose is a polysaccharide consisting of the monomers D-Galactose and 3,6-Anhydro-L-Galactose, which polymerize and form a gel, acting like a molecular sieve for the nucleic acids. The sample is loaded into small pockets and, and when a voltage is applied the negatively charged nucleic acid molecules wander through the gel towards the positive pole. Here, small molecules move faster, which separates the molecules by size. The concentration of the agarose gel is the determining factor for the resolution. 0.8 % (w/v) agarose gels were used, which can separate molecules from 0.2 to 10,000 kbp size. Agarose was solved in TAE-buffer by boiling shortly and supplemented with HDGreen™ Plus DNA stain (Intas) and poured into a gel chamber. By inserting a comb into the gel, little pockets were created in which a mixture of sample and loading dye were loaded. The gel solidifies by formation of hydrogen bridge bonds between the agarose monomers during the cooling process. In order to be able to have insights into the size of the DNA fragments a DNA ladder marker ( $\lambda$  marker) was also loaded, which consists of  $\lambda$ -DNA digested with *EcoRI* and *HindIII*. The polymerized gel was covered with 1x TAE buffer and a voltage of 120 V was applied, to enable movement of the nucleic acids. After the loading dye reached the middle of the gel, it was imaged in a GelDoc™ XR (Biorad). HDGreen™ Plus DNA stain intercalates into nucleic acids which allows their detection using UV light (254 nm) (Richts, 2021).

50x TAE buffer	242 g	Tris-base
(1 l)	57.1 ml	Acetic Acid (100 %)
	100 ml	Na <sub>2</sub> EDTA x 1 H <sub>2</sub> O (0.5 M, pH 8)

5x DNA Loading Dyer (10 ml)	5 ml 0.2 ml	Glycerol (100 %) 50 x TAE
Agarose (300 ml)	2,4 g 300 ml	Agarose 1x TAE buffer

### **Polymerase chain reaction (PCR)**

Polymerase chain reaction was used for the exponential amplification of DNA-fragments. The area which will be amplified is selected *via* a set of two primers. The reaction itself can be divided into three steps that take place at different temperatures. To achieve a quick and efficient change of temperatures, PCR is performed in a so-called thermocycler. First, the DNA is denatured which creates single strands. The necessary temperature for this step is between 95 and 98°C, depending on the polymerase that is used. Next the samples are cooled to approximately 52 °C which allows binding of the primers to the single stranded DNA (annealing). The exact temperature depends on the melting temperature ( $T_m$ ) of the primers that are being used. Basically, the ideal annealing temperature is assumed to be  $T_m - 5^\circ\text{C}$ . When the primers are bound, the temperature is increased to 72°C. This allows the amplification of the DNA fragments by the polymerase (elongation). These three steps are cycled until a sufficient amount of DNA is produced. Three additional steps are added to the PCR program in order to enhance its function: an initial denaturation step which melts the chromosomal DNA, the final elongation which ensures that the DNA polymerase can complete the elongation and the “hold” step which stops the reaction and protects the product from degradation. Two different DNA polymerases were used in this work depending on the purpose of the PCR. If the DNA was amplified for further cloning purposes, the Fusion<sup>®</sup>-polymerase was used. This polymerase originates from *Pyrococcus furiosus* and has a 50-fold lower error rate than the alternative DreamTaq-polymerase. This polymerase was used for check PCRs (Richts, 2021).

## 2. Material and Methods

**Table 2.3: Pipetting scheme for a Fusion PCR**

Volume [ $\mu$ l]	Compound
20	5 x Fusion <sup>®</sup> HF buffer
4	dNTPs (12.5 $\mu$ mol/ml)
4	fwd primer (5 pmol)
4	rev primer (5 pmol)
2	template DNA (2 ng)
0.5	Fusion <sup>®</sup> polymerase (2U/ $\mu$ l)
65.5	H <sub>2</sub> O

**Table 2.4: Cycler program of the Fusion PCR**

Step	Temp [ $^{\circ}$ C]	Time	Cycles
Initial denaturation	98	3 min	
Denaturation	98	30 sec	30x
Annealing	Primer T <sub>m</sub> -5 $^{\circ}$ C	35 sec	
Elongation	72	30 sec/kbp	
Final elongation	72	10 min	
Hold	8	$\infty$	

**Table 2.5: Pipetting scheme of the Dream Taq PCR**

Volume [ $\mu$ l]	Compound
10	10x Dream <i>Taq</i> buffer
4	dNTPs (12.5 $\mu$ mol/ml)
4	fwd primer (5 pmol)
4	rev primer (5 pmol)
2	template DNA (2 ng)
0.5	Dream <i>Taq</i> -polymerase (5U/ $\mu$ l)
75.5	H <sub>2</sub> O

**Table 2.6: Cycler program DreamTaq PCR**

Step	Temp [°C]	Time	Cycles
Initial denaturation	95	3 min	
Denaturation	95	30 sec	30x
Annealing	Primer T <sub>m</sub> -5°C	35 sec	
Elongation	72	60 sec/kbp	
Final elongation	72	10 min	
Hold	8	∞	

**DNA purification**

DNA fragments were purified using the QIAquick PCR purification Kit (QUIAGEN) as described by the manufacturer. DNA was eluted from the column using deionized water.

**Long flanking homology PCR (LFH PCR)**

The long flanking homology PCR (LFH PCR) is used to generate DNA fragments which allow the deletion or the fusion of short tags to genes in the genome of *B. subtilis*. To achieve a deletion, upstream and downstream regions of the target genes are amplified by PCR (~1000 bp). The resistance genes against chloramphenicol, kanamycin, erythromycin, spectinomycin, tetracycline and zeocin are amplified from the plasmids pGEM-cat, pDG780, pDG646, pDG1726, pDG1513 and pDG148 respectively. The flanking regions and the resistance cassette were fused together in the LFH PCR, in which the first step was the joining of the three fragments without the oligonucleotides. In a second step, the oligonucleotides were added to the reaction and the complete fragment was amplified. Complementary sequences allowed the joining of the fragments. Fusion of a tag to the gene of interest was performed following the same principle. Here, the gene was amplified as well and the tag was added *via* the primer before the fragments were fused to an antibiotic resistance cassette. Afterwards, competent *B. subtilis* cells were transformed with the LFH product and plated onto the respective selection plates (Klewing, 2019).

**Table 2.7: Pipetting scheme for a LFH PCR**

Volume	Compound
20 µl	5 x Fusion® HF buffer
4 µl	dNTPs (12.5 µmol/ml)
8 µl	fwd primer (5 pmol)
8 µl	rev primer (5 pmol)
100 ng	upstream flanking region
100 ng	downstream flanking region
200 ng	resistance gene
2 µl	DNA Fusion® polymerase (2U/µl)
ad 100 µl	H <sub>2</sub> O

**Table 2.8: Cyclor program for an LFH PCR**

Step	Temp [°C]	Time	Cycles
Initial denaturation	98	3 min	
Denaturation	98	30 sec	10x
Annealing	52	35 sec	
Elongation	72	2 min 15 sec	
Hold	15	∞	
Addition of oligonucleotides			
Denaturation	98	30 sec	30x
Annealing	52	35	
Elongation	72	3 min 30 sec + 5 sec/cycle	
Final elongation	72	10 min	
Hold	8	∞	

### Restriction digestion of DNA

The digestion of the DNA was done using FastDigest restriction endonucleases (ThermoFischer) which recognize a 4 - 10 bp palindromic sequence and cut it in a specific manner. The emerging ends can then be ligated with a vector backbone that were digested with the same enzymes. For the reaction, buffers and concentrations were used according to the manufacturers' manual. After digestion of plasmids, an additional digestion step was performed in order to prevent the digested plasmid from re-ligation.

## 2. Material and Methods

Therefore the 5'-prime end of the DNA was dephosphorylated by using FastAP (alkaline phosphatase) (ThermoFischer). 0.5  $\mu\text{l}$  of the enzyme (1 U/ $\mu\text{l}$ ) were added to the digested DNA and incubated for 10 min at 37°C. Afterwards, all reaction mixtures were purified using the QIAquick PCR purification kit (QIAGEN) as described above (Richts, 2021).

**Table 2.9: Pipetting scheme for DNA digestion**

Volume [ $\mu\text{l}$ ]		Compound
Plasmid DNA	PCR product	
4	4	10x FD buffer
4	3	enzyme 1
4	3	enzyme 2
1 $\mu\text{g}$	30	DNA
ad 40	-	H <sub>2</sub> O

### Ligation of DNA

Ligation was used to fuse the digested DNA inserts and plasmids together. The amount of vector and insert DNA was controlled prior to ligation by UV-Vis-Spectrophotometer (NanoDrop). Ligation of DNA fragments was performed using the T4 DNA ligase and buffer, as recommended by the manufacturer (ThermoFischer). The mixture was either incubated at room temperature for 2 h, or overnight at 16 °C.

**Table 2.10: Pipetting scheme for ligation of DNA fragments**

Volume [ $\mu\text{l}$ ]	Compound
2	10x ligation buffer
1	T4 DNA ligase (5 U/ $\mu\text{l}$ )
x	150 ng insert DNA
x	50 ng plasmid DNA
ad 20	H <sub>2</sub> O

### DNA sequencing

Sequencing of plasmid DNA

DNA sequencing was used to ensure that no unwanted mutations occurred. This was outsourced and done by the Microsynth which is based in Göttingen (Germany). There, the DNA sequence is determined by the chain termination method (Sanger *et al.*, 1992)

**Table 2.11: Pipetting scheme for sequencing**

Volume [ $\mu$ l]	Compound
3	primer
x	plasmid (600 – 800 ng)
ad 15	H <sub>2</sub> O

#### Whole genome sequencing

To identify the potential suppressor mutations leading to improved growth in strains, chromosomal DNA was purified using the peqGOLD Bacterial DNA Kit and send away for sequencing. The SeqCenter (Pittsburgh, USA) performed library preparation and sequencing on Illumina instruments. The reads were mapped onto the *B. subtilis* genome using the Geneious software package (Geneious Prime 2021.0.3.(<https://www.geneious.com>)). Single nucleotide polymorphisms (SNPs) were considered as significant when the total coverage depth exceeded 30 reads with a frequency variance of > 90%. Single nucleotide polymorphisms were verified by Sanger sequencing (Richts, 2021).

### 2.2.6 Phenotypic characterizations of *B. subtilis* strains

#### In liquid medium

Monitoring of the growth of different genotypes of *B. subtilis* under different growth conditions can elucidate potential phenotypes that are results of these changes. For these growth experiments, a 4 ml LB culture containing the appropriate antibiotics and facultative supplements was inoculated with a single colony. The culture was then incubated overnight at 28°C with agitation (200 rpm). If not stated otherwise, the OD<sub>600</sub> of the culture was measured and a fresh culture was inoculated to an OD<sub>600</sub> of 0.1 in MSSM minimal medium. The cells were incubated at 37°C with agitation (200 rpm) until they entered the exponential growth phase (OD<sub>600</sub> 0.5-0.8). Then, the OD<sub>600</sub> of each culture was determined and the cultures were inoculated to match an OD<sub>600</sub> of 0.1 in a 96-well plate. The growth of these cultures was monitored using an Epoch 2 Microplate Spectrophotometer (BioTek Instruments, USA). The OD<sub>600</sub> was determined every 10 min by the plate reader while the plate was incubated with agitation (200 rpm) at 37°C. If a change of medium from the fresh over day culture to the medium used in the plate reader was needed or a change of supplements, 2 ml of the cells were harvested by centrifugation (5 min, 3000 rpm, RT). The cells were then washed with 30 ml of 1x MSSM base, which did not contain any supplements. This step was repeated 3 times. Afterwards, the cells were adjusted

to an OD<sub>600</sub> of 0.1 in the desired medium used for the plate reader and it was proceeded as described earlier. The mean values of three independent experiments with each 3 technical replicates were used to compare the growth behaviour of different strains and growth conditions.

### **Drop dilution assay**

Monitoring the growth of bacterial strains using the drop dilution method can be used as an easy way to analyse phenotypes and directly compare growth of many different strains. For this purpose, overnight cultures of the strains were used to inoculate 4 ml cultures in LB. These cultures were then inoculated in MSSM minimal medium to an OD<sub>600</sub> of 0.1 and incubated at 37°C at agitation (200 rpm) until an OD<sub>600</sub> of 1 was reached. Then, the cells were adjusted to match an OD<sub>600</sub> of 1. These samples were then used for the preparation of serial dilutions of 10<sup>-1</sup> to 10<sup>-6</sup> and 3 µl of each dilution was dropped on the respective plates. If not indicated otherwise, the plates were incubated at 37°C overnight before pictures were taken with the GelDoc™ XR (Biorad).

### **Biofilm analysis**

To investigate biofilm formation, cryo cultures or a fresh single colony of the strain of interest were used to inoculate 4 ml LB medium with the appropriate antibiotics and incubated at 28°C and 200 rpm overnight. This culture was then inoculated in fresh LB to an OD<sub>600</sub> of 0.1 the following morning and incubated until an OD<sub>600</sub> of 0.5 - 0.9 was reached. Then, 5 µl of the culture were dropped on an MSgg-agar plate which was prepared as described below. The plates were incubated for 30 min under a laminar flow cabinet until all drops had dried. The plates were then transferred to 30°C and incubated for 4 days.

For the preparation of the plates, salts and additives were mixed as indicated below and H<sub>2</sub>O was added to a volume of 200 ml. The solution was warmed to 55°C. Bacto agar was prepared as indicated below with 300 ml H<sub>2</sub>O followed by autoclaving and cooling to 55°C. Both solutions were mixed and Coomassie brilliant blue and Congo red were added to a final concentration of 20 µg/ml and 40 µg/ml, respectively. 12 ml of MSgg-agar was poured in small Petri dishes. Colonies were photographed using a stereo microscope (Carl Zeiss Microscopy) equipped with digital camera AxioCam MRC (Faßhauer, 2021).



## 2. Material and Methods

---

### Mmsgg-agar

Component	Stock	Volume [ml]	Final conc.	Sterilization
Potassium phosphate buffer pH 7.0	1 M	2.5	5 mM	autoclave
MOPS pH 7.0	1 M	50	100 mM	filter sterilize, store in the dark at 4°C
Glycerol	50 %	5	0.5 %	autoclave
Thiamine	20 mM	0.05	2 µM	filter sterilize
Potassium glutamate	40 %	6.25	0.5 %	Autoclave, store at 4°C
L-Tryptophane	5 mg/ml	5	50 µg/µl	filter sterilize, store at 4°C
L-Phenylalanine	10 mg/ml	2.5	50 µg/µl	filter sterilize, store at 4°C
MgCl <sub>2</sub>	1 M	1	2 mM	filter sterilize
CaCl <sub>2</sub>	1 M	0.35	700 µM	filter sterilize
MnCl <sub>2</sub>	10 mM	2.5	50 µM	filter sterilize
FeCl <sub>3</sub> – freshly prepared	50 mM	0.5	50 µM	filter sterilize
ZnCl <sub>2</sub>	1 mM	0.5	1 µM	filter sterilize
dH <sub>2</sub> O		ad to 200		autoclave
Bacto-agar	7.5 g	300		autoclave

### Swarming motility assay

To investigate swarming motility, cryo cultures or a fresh single colony of the strain of interest were used to inoculate 4 ml LB medium with the appropriate antibiotics and was incubated at 28°C and 200 rpm overnight. The precultures were used to inoculate 20 ml LB medium containing the appropriate antibiotics to an OD<sub>600</sub> of 0.1. The cultures were incubated until an OD<sub>600</sub> of 0.8 was reached and cells were harvested by centrifugation (5 min, 3000 rpm, RT). Cells were resuspended in the supernatant and adjusted to an OD<sub>600</sub> of 10. 1 % ink (Lamy) was added to the cultures. The cells were placed in the middle of LB plates containing 0.4 % Bacto agar and left under a laminar flow cabinet for 10 min until all drops had dried. They were further incubated at 37°C and the swarming radius was measured after 24 h.

### 2.2.7 Working with proteins

#### Expression in *E. coli*

In order to produce proteins at a large, the *E. coli* strain Rosetta was transformed with expression plasmids encoding the proteins of interest. In this work, the backbones pWH844 and pETSUMO were used. pWH844 allows the expression of an N-terminally His tagged protein of interest. pETSUMO on the other hand allows the fusion of the protein of interest to an N-terminal His-SUMO tag that can be cleaved of after purification of the protein. Both plasmids are under the control of a *lac* inducible promoter which prevents the cells from expressing the protein of interest in absence of the artificial inducer IPTG. This enables the unstressed growth of the bacteria and once they reach a suitable cell density, the controlled start of the expression of the protein of interest *via* the addition of the inducer. In case the accumulation of the protein has a toxic effect on the cells, the incubation time after the addition of the inducer can be adjusted.

The Rosetta strain carrying the expression plasmid of choice was incubated overnight in 80 ml LB supplemented with the appropriate antibiotics at 37°C at agitation. The next morning, 1 l of LB was inoculated to an OD<sub>600</sub> of 0.1 and incubated at 37°C with agitation until an OD<sub>600</sub> of 0.8 was reached. Then, IPTG was added to a final concentration of 1 mM which induced the expression of the proteins. The cells were harvested after a further incubation for 2-3 h. For this purpose, the cultures were subjected to centrifugation for 15 min at 5000 rpm and 4°C. The supernatant was removed, the pellet resuspended in 15 ml 1x ZAP buffer and pelleted in another centrifugation step (8500 rpm, 10 min, 4°C). Pellets were stored at -20°C until further use (modified from Richts, 2021).

#### Expression in *B. subtilis*

For the overexpression of proteins in *bacillus*, the plasmids pGP380 and pGP382 were used. These plasmids allow the constitutive overexpression of proteins under the P<sub>degQ</sub>-promoter and the fusion of a Strep tag to the protein. *B. subtilis* strains carrying the plasmids were incubated overnight in 80 ml LB with the corresponding antibiotics. After inoculation of the main culture to an OD<sub>600</sub> of 0.1, the bacteria were incubated at 37°C at agitation until an OD<sub>600</sub> of 1 was reached. Then, they were harvested at 5000 rpm for 10 min, washed with Buffer W and stored at -20°C (Richts, 2021).

#### Cell disruption using the French press

In order to purify the overexpressed proteins, they first need to be extracted from the cells. For this purpose, the cells were lysed by subjecting them to the French press (G. Heinemann). The pellets were resuspended in 1x ZAP buffer are loaded into the precooled hollow cylinder of the so called press bomb (ThermoFischer). Then, a moveable piston was added into the cylinder. The cells were lysed by pressing

them through a narrow hole at the bottom of the cylinder. In total, a pressure of approximately 18,000 psi is reached and when the valve is opened, the cells disrupt since shear forces occur due to the smaller release opening. The cell lysate is collected and the process is repeated at least once for Gram-negative and twice for Gram-positive bacteria.

The cell debris was separated from the protein solution *via* centrifugation at 8 500 rpm for 10 min and 4°C followed by another centrifugation step (45 min, 35 000 rpm and 4°C) The supernatant was retrieved and was from there forward referred to as crude extract (CE) (modified from Richts, 2021).

### **Affinity chromatography of His-tagged proteins**

The purification of proteins from the crude extract was achieved by using affinity-tags which are amino acid sequences having a binding specificity for certain materials. Here, a 6x His tag was used that binds to a matrix consisting of Ni-NTA<sup>®</sup>. Applying the crude extract to a column containing this matrix leads to the binding of the proteins that contain the His tag to the column and the rest of the proteins passes through. By adding a ligand with a higher affinity to the stationary phase, the protein is replaced and can be collected. In case of His tag purifications, this is achieved by the addition of rising concentrations of imidazole.

More precisely, 2.5 ml of Ni-NTA<sup>®</sup> (IBA Lifescience) matrix per 1 l cell culture were filled into the affinity column (BioRad Poly-Prep<sup>®</sup> Chromatography Column) and equilibrated with 12.5 ml of 1x ZAP buffer. Next, the crude extract was loaded onto the column and the flow through (FT) was collected. The column was washed with 1x ZAP buffer until no proteins could be detected in the wash fraction. The elution steps are listed below (Richts, 2021).

**Table 2.12: Elution steps of a 6x His tag purification**

Volume [ml]	Imidazole [mM]
8	10
8	50
5	100
5	200
5	500

## 2. Material and Methods

---

10x ZAP buffer	60.57 g	Tris-base
(1 l)	116.9 g	NaCl
	Adjust the pH to 7.5 with HCl	

### Affinity chromatography of Strep-tagged proteins

The purification of Strep tagged proteins follows the same principle as the purification of His tagged proteins. Here, the proteins are bound to a Strep-Tactin® matrix and can be eluted by the addition of desthiobiotin.

1 ml of 50 % Strep-Tactin® (IBA Lifescience) suspension were used for 1 l of cell culture and equilibrated with 10 ml of buffer W. The crude extract, gathered after the cell lysis, was loaded onto the column and the flow through was collected. The column was washed with 2 ml buffer W until no protein was detectable in the wash fraction. Four elution fractions of 500 µl buffer E were collected.

10x buffer W	121.14 g	Tris base
(1 l)	87.7 g	NaCl
	3.72 g	Na <sub>2</sub> EDTA x 2 H <sub>2</sub> O
	Adjust the pH to 8.0 with HCl	

Buffer E	0.027 g	D-Desthiobiotin
(50 ml)	50 ml	1x buffer W

### Strep-protein interaction experiment (SPINE)

A SPINE experiment was used to investigate protein-protein interactions in *B. subtilis* (Herzberg *et al.*, 2007). Here, a bait-protein was fused to a Strep tag and constitutively overexpressed to facilitate interaction with a prey-protein. The cross-linker *para*-formaldehyde (PFA) was used to fix the bait-protein with its nearby interaction partner (about 2 Å). The bait-proteins were then purified using the Strep-Tactin® purification column as described above and the samples were analysed *via* SDS-PAGE. Boiling the samples before loading them onto the SDS gel not only leads to the denaturation of the proteins, but also to the dissolving of the cross-links. Therefore, the bait-protein as well as potential interaction partners can be visualized as single bands on the gel. Samples were analysed by mass spectrometry.

Expression plasmids containing N-, or C-terminal Strep-fusions to the expressed genes were introduced into a *B. subtilis* strain incubated overnight in 80 ml LB medium containing the appropriate antibiotics. The next morning, 1 l of LB was inoculated to an OD<sub>600</sub> of 0.1 and grown at 37°C with agitation to an OD<sub>600</sub> of 1 was reached. Then, the culture was split into 2x 500 ml and to one half PFA

(4 %) was added to 0.6% final concentration and incubated for an additional 20 min at 37°C. The cultures were harvested at 5000 rpm for 10 min, washed with 1x PBS to remove the PFA and pelleted by centrifugation (8500 rpm, 10 min). The cells were stored at -20°C until they were lysed by using the French press and purified by the Strep-purification system (see above). After the purification, the crosslinks were resolved by boiling the sample for 30 min in 6x PAP buffer at 95°C. The SDS gel was stained using the silver staining method, which is more sensitive than Coomassie staining (Richts, 2021).

10x phosphate buffered saline (PBS)	80 g	NaCl
(1 l)	2 g	KCl
	14.24 g	Na <sub>2</sub> HPO <sub>4</sub> x 1 H <sub>2</sub> O
	2.27 g	KH <sub>2</sub> PO <sub>4</sub>
	Adjust pH to 6.5 with HCl	

### **Determination of the protein concentration (Bradford assay)**

The Bradford assay can be used as a fast and simple way to measure the protein concentration of samples. It is based on the principle that Coomassie brilliant blue G-250 forms a complex with the proteins (Bradford, 1976) which leads to a shift in absorption of the solution. It is able to accurately measure protein concentrations ranging from 0.1 – 1.4 mg.

1 ml of 1x Bradford reagent was mixed with 2 – 20 µl of protein solution and the absorption was measured at 595 nm. A measurement performed with the elution buffer / dialysis buffer was used as a blank. A calibration curve showed the linear relation between the amount of protein and the absorption at OD<sub>595</sub>. Creation of a calibration curve revealed a slope with an incline of 0.0536. This was used as a standard value for all calculations. To calculate the amounts of protein in the sample the following equation is used:

$$c = \frac{OD_{595}}{V * 0.0536}$$

V is the volume (µl) of sample that was used for the measurement. c is the protein concentration given in mg/ml (Richts, 2021).

### **SDS polyacrylamide gel electrophoresis (SDS-PAGE)**

SDS-PAGE allows the separation of proteins according to their molecular weight. For this purpose, protein solutions are run through a discontinued polyacrylamide gel. The gel can be divided into two phases, one stacking gel and one separation gel containing different concentrations of polyacrylamide.

## 2. Material and Methods

---

In general, the gels consisted of acrylamide, water, Tris-HCl buffer, SDS, APS and TEMED. The gel starts to polymerize upon addition of APS, which acts as a radical initiator, and TEMED, which catalyses the reaction. Depending on the size of the proteins of interest, different concentrations of acrylamide are used. In this work, 12 % (w/v) (as a standard percentage) and 15 %, (w/v) (for smaller proteins) acrylamide gels were used. The stacking gel consisted of 5 % (w/v) acrylamide. By boiling the protein samples in loading dye (6 x PAP) and adding SDS to the gel, the proteins are linearized and given a negative charge (Laemmli, 1970). This allows them move through the gel towards the positive pole once voltage is applied. Here, the gel acts like a sieve. Smaller proteins move faster through the gel while bigger proteins are more likely to be retained by the gel and hence, move slower. This allows the effective separation of proteins by their molecular weight. The gels were poured in a mini-PROTEAN® (Bio-Rad) system with 1 mm thickness. The running gel was poured first and then layered with 70 % ethanol to exclude excess oxygen. After the gel was fully polymerized, the ethanol was removed and the stacking gel was poured on top of the running gel. A comp was added to the liquid gel to create pockets. The gel was run at 80 V while the proteins moved through the stacking gel. Afterwards, the voltage was increased to 120 V and the gel was run until the blue running front reached the bottom of the gel. Prestained Protein Marker (PageRuler™) (ThermoFischer) was used as a size standard (modified from Richts, 2021).

**Table 2.13: Pipetting scheme for 15 and 12 % SDS running gels**

Volume [ml]	Compound
2.3 / 3.3	H <sub>2</sub> O
5 / 4	Acrylamide
2.5	Tris-HCl pH 8.8 (1.5 M)
0.1	SDS (10 %)
0.1	APS (10 %)
0.008	TEMED

**Table 2.14: Pipetting scheme for the SDS stacking gel**

Volume [ml]	Compound
6.83	H <sub>2</sub> O
1.5	Acrylamide
0.87	Tris-HCl pH 6.8 (1.5 M)
0.1	SDS (10 %)
0.1	APS (10 %)
0.01	TEMED

6x SDS loading dye (PAP) (10 ml)	2.1 ml	Tris-HCl pH 6.8 (1.5 M)
	600 µl	β-Mercaptoethanol
	1.2 g	SDS
	6 ml	Glycerol
	6 mg	Bromphenol blue
10x PAGE buffer (PLP) (1 l)	144 g	L-Glycine
	30.3 g	Tris-base
	10 g	SDS
1.5 M Tris-HCl buffer (1 l)	181.71 g	Tris-base
	Adjust pH 6.8 or 8.8 with HCl	

### Coomassie staining of protein gels

In order to visualize the proteins separated by SDS-PAGE, the gel was stained with Coomassie. For this purpose, the gel was first incubated in fixation solution for at least 15 min. After fixation, the proteins were stained with Colloidal Coomassie staining solution in which the gel is stored for 10 – 20 min. In order to de-stain the background of the SDS gel, it is incubated overnight in de-staining solution modified from Richts, 2021).

Fixation solution (1 l)	100 ml	Acetic acid
	500 ml	Methanol

## 2. Material and Methods

---

Colloidal staining solution (1 l)	20 ml g 50 g 1 g 100 ml	Phosphoric acid Aluminium sulphate Coomassie Brilliant blue G-250 Methanol
De-staining solution (1 l)	50 ml 200 ml	Acetic Acid Ethanol

### Silver staining of protein gels

Silver staining is a more sensitive method of protein gel staining than Coomassie blue staining. Here, the amino acid residues glutamate, aspartate and cysteine form complexes with the silver ions and by that, they are reduced to silver. Even though silver staining is highly sensitive, it cannot be used for quantitative determination of proteins since the level of staining strongly depends on the amount of those residues (Richts, 2021; Winkler *et al.*, 2007).

Here, the SDS gels were incubated in fixation solution overnight and then washed 3 times for 20 min in ethanol (50 %). This was followed by a 1.5 min reduction step using a thiosulfate solution. Next, the gel was washed 3 time for 20 sec in deionized water. Then, the gel was incubated with the impregnator solution (15-25 min) and washed with deionized water as described before. The gel was incubated with the developer until sufficient staining was achieved. This was followed by another washing step with water. Lastly, the stop solution was added. All solutions were always prepared fresh (Fabian Moritz Commichau *et al.*, 2015).

Fixation solution (100 ml)	12 ml g 50 ml 100 µl	Acetic acid Methanol Formaldehyde (37 %)
Developer (100 ml)	6 g 2 ml 50 µl	Na <sub>2</sub> CO <sub>3</sub> Thiosulfate solution Formaldehyde (37 %)
Impregnator (100 ml)	0.2 g 37 µl	AgNO <sub>3</sub> Formaldehyde (37 %)



## 2. Material and Methods

---

Thiosulfate solution (100 ml)	20 mg	$\text{Na}_2\text{S}_2\text{O}_3 \times 5 \text{ H}_2\text{O}$
Stop solution (1 l)	18.612 g Adjust pH to 8.0	$\text{Na}_2\text{EDTA} \times \text{H}_2\text{O}$

### Dialysis and SUMO-protease digest

The elution of proteins from the affinity columns involves the addition of substances that replace the bound proteins. This can either be imidazole for His purifications or D-desthiobiotin for Strep purifications. Unfortunately, these small molecules are then also present in the elution fractions of the proteins and can interfere in further applications. Therefore, the buffer needs to be exchanged. This was achieved by placing the samples in a tube that consists of semi-permeable membranes (Serva MEMBRA-CEL<sup>®</sup> 22mm diameter), which allows small molecules to pass through but keeps the proteins retained inside the membrane. The membrane was cooked in deion. water containing EDTA for 10 min, before the protein solution was placed inside and sealed with clips from each side. The tube was then placed in dialysis buffer. In this work, the original buffer, so either buffer W or ZAP buffer in 1000 fold excess to the sample were used for dialysis. For proteins that were expressed using the pETSUMO vector, the SUMO-His tag was cleaved, leaving the protein without a tag after the purification. This was achieved by adding 50  $\mu\text{l}$  purified SUMO-protease into the dialysis tubes after 1 h of dialysis. The samples were incubated over night at room temperature and the next morning, applied to a Ni-NTA<sup>®</sup> affinity column which was equilibrated with the dialysis buffer. Here, the flow through was collected containing the protein of interest while the cleaved SUMO-His tag was bound to the matrix.

### Ribosome purification

For ribosome purification, selected strains were incubated overnight in 50 ml LB containing the appropriate antibiotics. The next morning, they were inoculated in 500 ml LB and incubated at 37°C at agitation (200 rpm) until an  $\text{OD}_{600}$  of 0.8 was reached. During the harvesting process, the pellets were washed with 15 ml RAPI buffer. Cell pellets were stored at -20°C. Before use, the pellets were resuspended in 15 ml RAPI buffer. Cells were lysed by subjecting them to 18,000 p.s.i. by passing them through the French press three times. After lysis, 10 U RNase free DNase was added and the solution was incubated for 20 min on ice. After incubation, the crude extract was subjected to centrifugation at 5000 rpm and 4°C for 30 min. Afterwards, the supernatant was centrifuged for 30 min at 35,000 rpm and 4°C. The resulting supernatant was then layered on top of a sucrose pillow in a ratio of 5:8 (crude extract : sucrose pillow) and centrifuged for 18 h at 40,000 rpm and 4°C. The clear pellet was washed twice with 2 ml RAPII buffer and then resuspended in 1 ml RAPII buffer. Another centrifugation step

## 2. Material and Methods

---

(10 min, 14 000 rpm and 4°C) was performed and the supernatant was transferred to a fresh 1.5 ml Eppendorf tube. Analysis of the ribosome composition was either performed by SDS-PAGE and subsequent Coomassie staining or by Western blot.

RAP I buffer	20 ml	Tris-HCl pH 7.5 (1 M)
(1 l)	5.35 g	NH <sub>4</sub> Cl
	2.03 g	MgCl <sub>2</sub>
	781 µl	β-mercaptoethanol
RAP II buffer	20 ml	Tris-HCl pH 7.5 (1 M)
(1 l)	5.35 g	NH <sub>4</sub> Cl
	1.22 g	MgCl <sub>2</sub>
	0.462 g	DTT
Sucrose pillow	2 ml	Tris-HCl pH 7.5 (1 M)
(100 ml)	2.67 g	NH <sub>4</sub> Cl
	0.203 g	MgCl <sub>2</sub>
	78.1 µl	β-mercaptoethanol
	37.65 g	sucrose

### Western blot analysis

Western blot is a highly sensitive method that is used for the detection of specific proteins in a sample. The protein samples need to first be separated *via* SDS-PAGE as described above. Then the proteins are transferred to a PVDF membrane (Bio-Rad). This membrane is then incubated in a solution that contains protein specific antibodies. After binding of the antibody to the protein, a secondary antibody is added which, on the one hand binds to the first antibody and on the other hand is linked to an alkaline phosphatase. This enzyme dephosphorylates the chemiluminescent 1,2-Dioxetane CDP-Star (Roche) which leads to light emission at a wavelength of 475 nm. This can be detected by a special ultra-sensitive CCD camera (ChemoCam Imager (Intas)).

Transfer of the proteins from the SDS gel to the PVDF membrane was done by placing the gel onto the membrane. The membrane was activated in methanol prior to assembly of the blotting machine. Three Whatman papers soaked in transfer buffer were placed underneath the membrane and on top of the gel. The whole assembly was placed in a semi dry blotting machine and bubbles were removed. A current of 200 mA was applied and the proteins were blotted for 1 h. If not stated otherwise, all the following steps were performed on a shaker at 4°C. The membrane was placed in

## 2. Material and Methods

---

Blotto in order to block free binding sites for proteins on the membrane. Next, the membrane was washed three times with 1x TBS(T) for 10 min and incubated over night with the primary antibody diluted in TBS(T). The next morning, the membrane was washed three times with 1x TBS(T) and afterwards incubated with the secondary antibody. After thirty minutes, the secondary antibody was removed and the membrane was washed three times for 20 min with 1x TBS(T). Finally, the membrane was placed in buffer III and incubated for 5 min to equilibrate the pH in preparation for the enzymatic reaction. 10 µl CDP-star were added to 990 µl of deion. water and spread equally over the membrane which started the reaction. The light signal was detected in the imager.

10x transfer buffer (1 l)	151.4 g 144 g	Tris-base Glycine
1x transfer buffer (1 l)	100 ml 200 ml	10x transfer buffer Methanol
10x TBS (1 l)	60 g 90 g Adjust pH to 7.6 with HCl	Tris-base NaCl
Blotto (1 l)	100 ml 25 g 1 ml	10x TBS Milk powder Tween 20
1x TBS(T) (1 l)	100 ml 1 ml	10x TBS Tween 20
Buffer III (1 l)	12.1 g 5.8 g	Tris-base NaCl

### **Electrophoretic mobility shift assay (EMSA) with DNA**

The electrophoretic mobility shift assay (EMSA) is often used to analyse DNA-protein interactions. The potential target DNA is incubated with the protein and then loaded onto a native polyacrylamide gel. An interaction of the DNA with the protein is visualized by an up-shift of the DNA on the gel since free DNA migrates faster.

## 2. Material and Methods

For this purpose, 10 % native gels were prepared. 200 ng DNA were used for the assay and incubated with the EMSA buffer and deion. water at 95°C for 5 min. Before the addition of 80 pmol protein, the DNA was cooled on ice for 5 min after the addition of the protein. The DNA-protein mixture was incubated for 30 min at 37°C whilst the gel was subjected to a pre-run at 90 V. Afterwards, the samples were mixed with the loading dye and loaded onto the gel which was run at 100 V for 3 h. To visualize the DNA on the gel, it was incubated in 50 ml running buffer for 2 min containing 10 µl HDGreen™ Plus DNA stain (Intas). Afterwards, the gel was imaged in a GelDoc™ XR (Biorad).

**Table 2.15: Pipetting scheme for native acrylamide gel**

Volume [ml]		Compound
5.4		H <sub>2</sub> O
4		Acrylamide
2.4		5x TBE buffer
0.2		APS (10 %)
0.01		TEMED
5x TBE buffer (running buffer) (1 l)	60.55 g	Tris-base
	30.9 g	Boric acid
	3.7 g	Na <sub>2</sub> EDTA
	Adjust pH to 8.0 with HCl	
10x EMSA buffer (200 ml)	12.1 g	Tris-base
	11.7 g	NaCl
	0.74 g	Na <sub>2</sub> EDTA
	Adjust pH to 8.0 with HCl	
10x EMSA loading dye (10 ml)	5 ml	Glycerol 50 %
	1 mg	Bromphenol blue
	1 mg	Xylene cyanol

### Determination of $\beta$ -galactosidase activity

To determine the activity of various promoters, fusions of the upstream regions of genes, including the SD sequence and part of the open reading frame, with the *lacZ* gene were constructed. This was done by using the vector pAC5. This vector can be integrated in the genome of *B. subtilis* by double-

## 2. Material and Methods

---

homologous recombination in the *amyE* site. The success of this integration was tested *via*  $\alpha$ -amylase assay. The transformants that were selected for testing as well as the wild type, that served as a positive control, were streaked out on starch plates and incubated overnight at 42°C. The next morning, the plate was covered with 1× Lugol solution. Correct integration of the vector disrupts the  $\alpha$ -amylase, which prohibits starch breakdown, leading to staining of the agar by the Lugol solution. In contrast to this, a halo is formed around the strains that still contain the intact *amyE* gene, due to the metabolization of the starch. A single colony of a strain containing the integration of the plasmid was used to inoculate 4 ml LB medium which was incubated at 28°C overnight. The next morning, 10 ml LB medium were inoculated to an OD<sub>600</sub> of 0.1 and grown at 37°C until an OD<sub>600</sub> of 0.5 - 0.8 was reached. 2 ml of the culture were harvested *via* centrifugation at 13 000 rpm and 4°C for 5 min, the supernatant was discarded, and the pellet was stored at -20°C. Lysis of the cells was achieved by re-suspension of the pellet in 400  $\mu$ l Z buffer supplemented with 20  $\mu$ l LD mix. The mixture was incubated for 10 min at 37°C at agitation. Cell debris was removed by centrifugation for 5 min at 13,000 rpm and 4°C and the supernatant was transferred to a fresh tube. 100  $\mu$ l of the cell free crude extract were mixed with 700  $\mu$ l Z buffer. This mix and 800  $\mu$ l of Z buffer, as a reference, were pre-incubated for 5 min at 28°C. The enzymatic reaction was started by addition of 200  $\mu$ l ONPG, mixing by vortexing and incubation at 28°C. As soon as the mixture turned yellow, the reaction was stopped by addition of 500  $\mu$ l stop solution. The time points where the reaction was started and stopped were noted ( $\Delta t$ ). Absorption of the samples was determined at a wavelength of 420 nm ( $A_{420}$ ) with the reference sample serving as blank. Protein amounts in 20  $\mu$ l of the crude extracts were determined *via* Bradford assay ( $A_{595}$ ) as described above (Bradford, 1976). The  $\beta$ -galactosidase activity was determined using the following equation derived from a standard curve (Faßhauer, 2021):

$$\frac{\text{units}}{\text{mg protein}} = \frac{2000 * A_{420}}{\Delta t * A_{595}}$$

5x Lugol solution (1 l)	100 g 50 g	K-Iodide Iodine
LD mix (10 ml)	100 mg 10 mg	Lysozyme DNase I
ONPG 1 ml	4 mg 1 ml	<i>o</i> -Nitrophenyl- $\beta$ -D-Galactopyranoside Z buffer (without $\beta$ -Mercaptoethanol)

## 2. Material and Methods

---

Z buffer	0.534 g	$\text{Na}_2\text{HPO}_4 \times 2 \text{H}_2\text{O}$
(50 ml)	0.276 g	$\text{NaH}_2\text{PO}_4$
	0.037 g	KCl
	50 $\mu\text{l}$	$\text{MgSO}_4$ (1 M)
	175 $\mu\text{l}$	$\beta$ -Mercaptoethanol
Stop solution	26.5 g	$\text{Na}_2\text{CO}_3$
(250 ml)		

## 3. Results

The aim of this thesis is to validate novel protein-protein interaction in *B. subtilis* that were discovered by cross-linking mass spectrometry and co-fractionating mass spectrometry. This includes proteins involved in a variety of cellular processes and functions. Some proteins were found crosslinked to proteins already known to be involved in specific functions and known to exist in characterised complexes while others involved rather understudied proteins with no specific structural or functional knowledge assigned to them.

### 3.1 YabR, YugI and the ribosome

Some of the novel protein interactions that were uncovered were located at the ribosome. Ribosomes consist of a variety of proteins and the exact composition of the ribosome can vary depending on different environmental factors. Some of these ribosomal proteins are involved in specific functions relating the activity of the ribosome while others provide stability function as scaffolding for the rRNA. The crosslinking study performed by O'Reilly *et al.* revealed two proteins of unknown function crosslinked to proteins of the 30S subunit, namely YabR and YugI. The aim of this project is the validation of these interactions and to potentially uncover the biological function of the two proteins.

#### 3.1.1 Phenotypic characterization

YabR was found crosslinked to four proteins of the 30S ribosomal subunit with ten crosslinks in total, having the most crosslinks to S6 (RpsF) and S18 (RpsR). YugI had a total of thirty-four crosslinks to eight proteins of the 30S ribosomal subunit, with the most crosslinks to S3 (RpsC) and S10 (RpsJ) (O'Reilly *et al.*, 2022). Both YabR and YugI are highly conserved in Firmicutes, share a 41 % sequence identity and have a molecular weight of ~14 kDa. They also have similar expression patterns even though they are not encoded in the same operon (Fig. 3.1). Recently, an impact of YabR on swarming motility has been described (Sanchez *et al.*, 2022). The paralog of YabR, YugI, has already been found bound to the ribosome in the presence of S14 (Natori *et al.*, 2007). Furthermore, YugI, has also been hypothesised to be involved in a general shock response and to function in a similar manner to cold shock proteins. Therefore it is also referred to as GSP13 (general stress protein 13) (Yu *et al.*, 2009). Supporting this hypothesis is the fact that expression of *yugI* is increased during heat shock, salt stress, ethanol stress, glucose starvation, oxidative stress and cold shock, yet the stringent response leads to a 10 fold

decrease in expression (Eymann *et al*, 2002). Interestingly, YugI belongs to the 100 most abundant proteins in *B. subtilis* and still, no definite function could be assigned to the protein (Eymann *et al*, 2004).

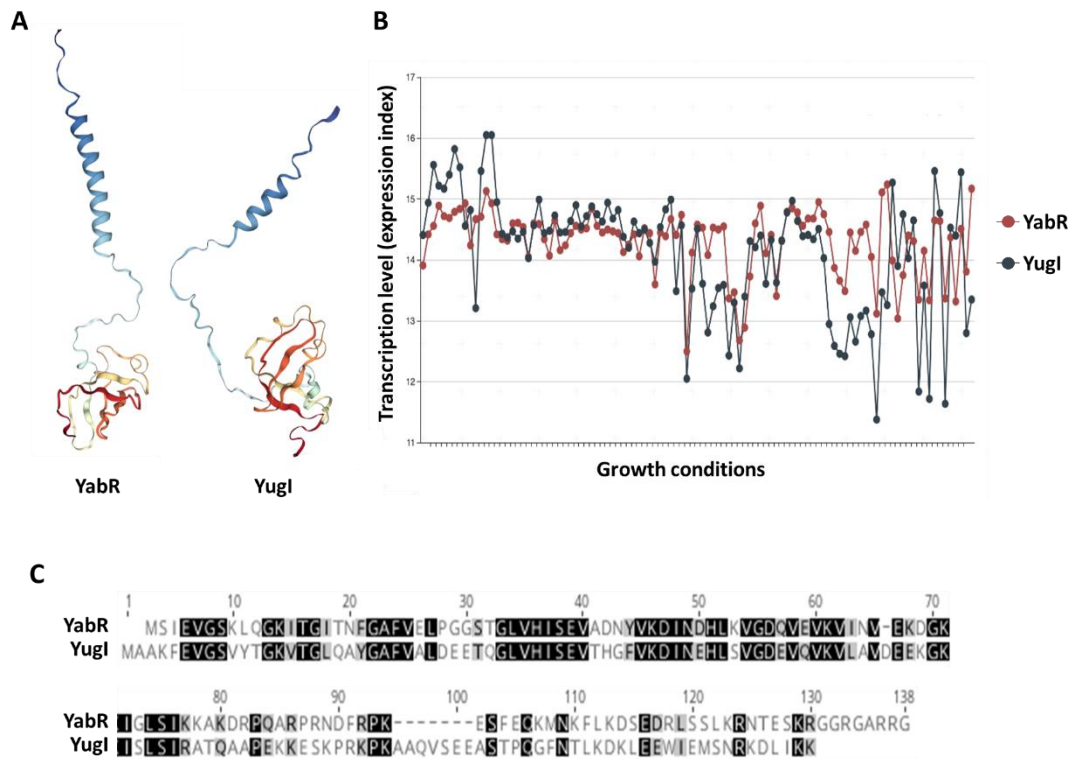


**Figure 3.1: Similarities of YabR and YugI.** **A** Protein structures of YabR and YugI as predicted by AlphaFold. The S1 RNA binding domain is located at the N-terminus and assumes a secondary structure while the C-terminus, which is coloured in blue, remains disordered. **B** A comparison of the expression pattern of *yabR* and *yugI*. Each point demonstrates the expression level under a certain growth condition (SubtiWiki). **C** Sequence alignment of YabR (S1 domain annotated from 6-74 aa, disordered region from 72-128 aa) and YugI (S1 domain annotated from 8-77 aa, disordered region from 76-109 aa). Identical amino acids are marked in black while similar amino acids are marked in grey (annotation according to UniProt, sequence alignment performed by Geneious).

The strong similarities between the two proteins suggest that they are paralogous proteins that are able to perform similar functions and might therefore be able to functionally replace each other. To test this hypothesis, deletion strains were constructed *via* LFH. Here the upstream and downstream regions of the genes of interest were amplified and fused to an antibiotic resistance cassette *via* LFH PCR. Transformation of *B. subtilis* with the PCR product leads to an integration of the resistance cassette in the locus of the gene of interest *via* homologous recombination, thus knocking the gene out. Deletions of *yugI* (GP3597) and *yabR* (GP3598) individually as well as in combination (GP3694) were possible. This indicates that the hypothesis of homologs that can carry out the same essential function is false. This does not exclude that they both are involved in the same process, yet it shows that the process is not essential. To gather information about the biological relevance of these proteins, the deletion strains were further phenotypically characterized by assessing their growth



under different conditions screening for conditions where the gene deletions might have an effect on the growth or the general phenotype of the strains. Fresh cultures of the strains were adjusted to an OD<sub>600</sub> of 1 and dilutions ranging from 10<sup>-1</sup> to 10<sup>-5</sup> were dropped on agar plates. All strains showed wild type (WT) like growth on complex medium (SP). The deletion of *yabR* negatively affected growth on MSSM minimal medium containing 0.1 mM KCl while the *yugI* knockout strains grew similar to the WT. Interestingly, the deletion of *yugI* in combination with *yabR* led to an improvement of growth compared to the single deletion of *yabR* (Fig. 3.2 A). This is an indication of a potential link between the two proteins. Since *yugI* expression is known to be upregulated under heat shock conditions (Yu *et al.*, 2009), growth was also investigated *via* drop dilution assay at 50°C. This led to no significant changes in growth compared to growth at 37°C (data not shown). Additionally, the strains were incubated on minimal medium with varying potassium and phosphate conditions, as well as under ethanol and salt stress which also led to no significant change of the phenotype (data not shown). To summarize, it can be stated that YabR and YugI fulfil separate functions in the cell since deletions result in different phenotypes. Since the double deletion strain shows improved growth compared to the *yabR* single deletion strain, it is possible that the proteins are in a regulatory relationship towards each other.

Furthermore, the effects of ribosome acting antibiotics were tested to see whether the deletions of *yabR* and *yugI* have an effect on the stress susceptibility of the ribosome. Growth was monitored in a liquid culture in a 96-well plate after the addition of tetracycline and spectinomycin. Tetracycline inhibits protein synthesis by preventing the attachment of aminoacyl-tRNA to the A site of the ribosome while spectinomycin acts by blocking the translocation of messenger RNA and transfer RNA on the 30S subunit of the ribosome (Borovinskaya *et al.*, 2007; Chopra & Roberts, 2001). Growth of the strains in minimal medium in the presence of 5.2 mM tetracycline, which is roughly one fifth of the selective concentration for *B. subtilis*, was monitored using the plate reader. Here, the *yugI* deletion strain showed faster growth compared to the wildtype. The *yabR* deletion strain exhibited the longest lag phase while the growth of the WT and the double deletion strain was similar (Fig. 3.2 B). This was expected since the deletion of *yabR* already leads to a growth defect in minimal medium. Growth of the strains in presence of spectinomycin was analysed *via* drop dilution assay on minimal medium. Here, we used 46 µM, 23 µM and 11.5 µM of the antibiotic. These concentrations correspond to roughly 1/8<sup>th</sup>, 1/16<sup>th</sup> and 1/32<sup>nd</sup> of the selective concentration of this antibiotic for *B. subtilis*, respectively. Growth on the plates containing 11.5 µM of spectinomycin was identical to growth on minimal plates without the addition of spectinomycin. While spectinomycin slowed down the growth of all strains at higher concentrations, no difference between the strains after the incubation with the antibiotic could be observed (data now shown). The fact that the deletion of *yugI* had an effect on

growth in presence of the ribosome acting antibiotic tetracycline is a first confirmation of a functional connection between Yugl and the ribosome. It can therefore be stated, that Yugl plays a role in the susceptibility of the ribosome towards tetracycline.

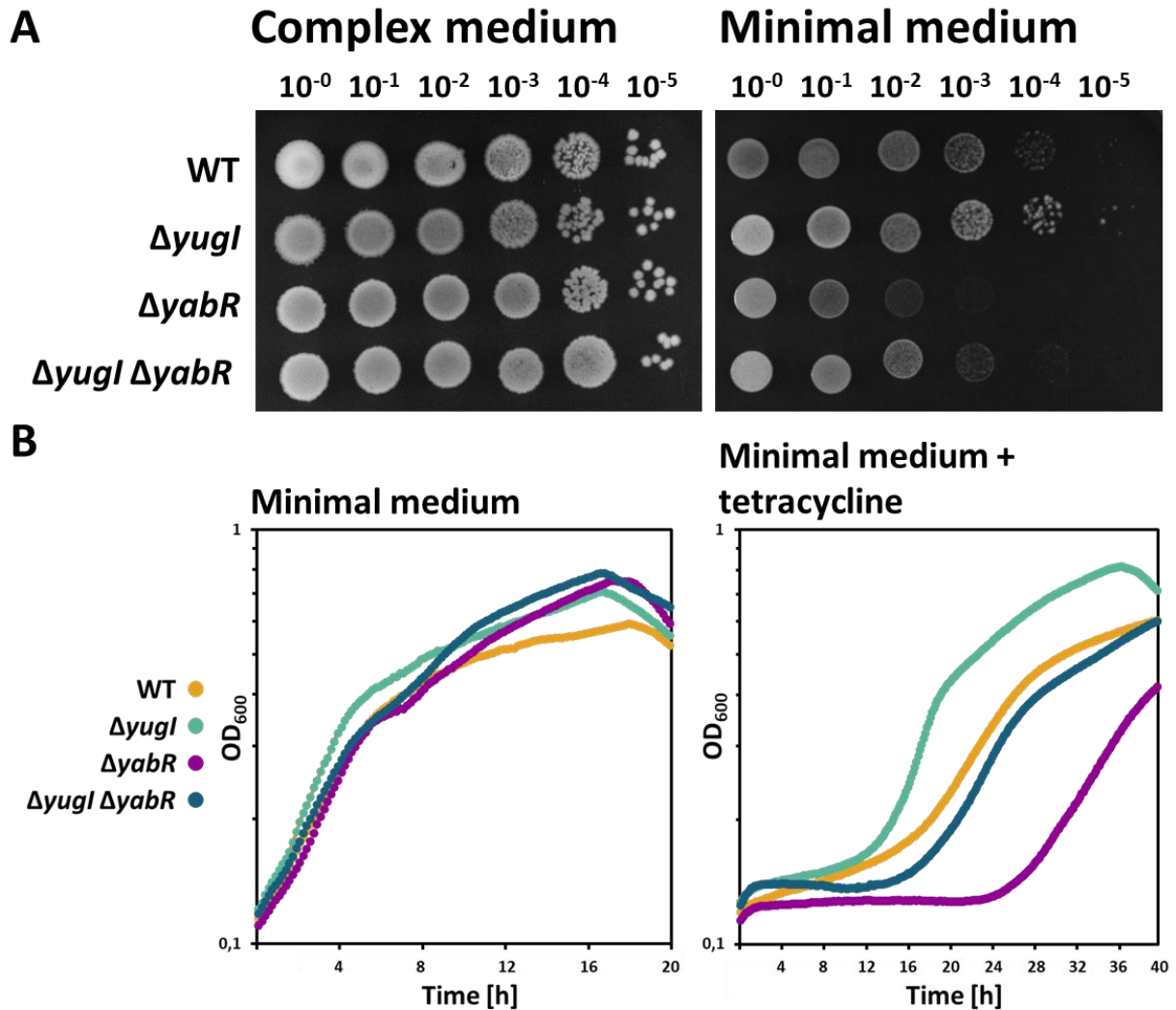


**Figure 3.2: Phenotypic characterisation of *yabR* and *yugl* deletion strains** **A** Drop dilution assay to compare growth of WT and the *yugl* (GP3597), *yabR* (GP3598), and *yugl yabR* (GP3694) deletion strains on complex medium and minimal medium after overnight incubation at 37°C. **B** Plate reader experiment showing the effect of tetracycline on the growth of the WT (orange), the *yugl* deletion strain (GP3597, green), the *yabR* deletion strain (GP3589, purple) and the *yugl yabR* double deletion strain (GP3694, blue). The strains were cultivated in MSSM minimal medium. Tetracycline was supplemented to a final concentration of 5.2 mM.

### 3.1.1.1 Investigation of the potential connection between YabR and RsbP

Growth defects of genetically altered strains under certain conditions allow the isolation of suppressors. To generate suppressor mutants, the strain is cultivated under unfavourable conditions until it evolves and is able to grow at a faster rate again. The colonies that show improved growth, the so called suppressors, can then be isolated and sequenced to identify the mutations that lead to the improved growth. Here, the  $\Delta yabR$  strain was cultivated on minimal medium until rise of one

suppressor (GP3307) that showed WT like growth (Fig. 3.3 A). The genomic DNA of this strain was isolated and sent to whole genome sequencing (WGS). Inspection of the genome sequence revealed that the suppressor had a mutation in the C-terminal region of the *rsbP* gene (D393G) which resulted in improved growth on minimal medium (Fig. 3.3 A). RsbP is a protein phosphatase involved in regulating the SigB dependent stress response together with its partner, the  $\alpha/\beta$  hydrolase RsbQ. RsbP consist of three domains, a N-terminal Per-Arnt-Sim (PAS) domain followed by a central coiled coil domain and finally a C-terminal PPM-type phosphatase domain (Vijay *et al.*, 2000). Working conjointly with RsbQ, the PAS domain is able to sense the depletion of ATP and then conveys the signal to the phosphatase domain which leads to dephosphorylation of RsbV and a continuation of the signalling cascade (Brody *et al.*, 2009; Nadezhdin *et al.*, 2011). To check whether this mutation led to a disruption of the function of RsbP, a strain with a single deletion of *rsbP* (GP3323) as well as *yabR rsbP* double deletion strain (GP3332) were constructed *via* LFH. The double deletion of *yabR* and *rsbP* led to an even more severe growth inhibition than the single *yabR* deletion strain suggesting that the mutation in *rsbP* is a gain-of-function mutation. A single deletion strain of *rsbP* showed wild type like growth when investigated in a drop dilution experiment. The growth of the precultures was not homogenic, therefore it can be assumed that suppressor formation occurs at a fast rate in this strain and the growth that was observed during the drop dilution assay is actually the growth of a suppressor strain.

Since RsbP is involved in regulating SigB dependent stress response which heavily entails biofilm formation, the ability of the wild type, the *yabR* deletion strain and the suppressor strain to produce biofilm was investigated (Bartolini *et al.*, 2019). Biofilm is an extracellular matrix that allows the cells to adhere to surfaces and withstand harsh environmental conditions. There are three types of biofilms that can form (I) the colony biofilm that is formed at a solid surface-air interface, (II) a pellicle biofilm that is formed at a liquid-air interface and (III) a biofilm that is formed at a solid surface while submerged in liquid (Hamon & Lazazzera, 2002; Sanchez-Vizueté *et al.*, 2015). The main biofilm components are an exopolysaccharide (EPS) (Branda *et al.*, 2001), the amyloid fibre forming protein TasA (Romero *et al.*, 2010) and the protein BlsA (Kobayashi & Iwano, 2012). While biofilm formation of the undomesticated WT strain NCIB 3610 has been heavily studied, the laboratory strain 168 has lost most of the ability to produce a complex extracellular matrix (McLoon *et al.*, 2011). Yet, expression of the genes coding for the main components of the biofilm, mainly *epsABDIJMNO*, *tasA* and *blsA* are heavily induced if 168 is grown on MSgg medium leading to increased biofilm formation, yet still not comparable to the levels that are present in NCIB 3610 (Nicolas *et al.*, 2012). Therefore, all strains were grown on the biofilm-inducing MSgg agar plates and the dyes Coomassie brilliant blue and Congo red were added to visualize the morphology of the biofilm (Fig. 3.3 B). The dye congo red binds specifically to the amyloid fibres of the biofilm. Coomassie brilliant blue was added as a counter stain (Kiersztyn

*et al.*, 2017; Romero *et al.*, 2010). All strains were able to form amyloid fibres, which is visualized by red staining of the biofilms. The wild type and the *rsbP* deletion strain formed very similar biofilms. Interestingly, the deletion of *yabR* seemed to lead to the formation of a white domed circle at the border of the biofilm. This could also be observed for the suppressor strain carrying the mutation in *rsbP*. It was expected that the deletion of *rsbP* would affect the biofilm formation, yet this does not seem to be the case.

Since the potential relation of YabR and RsbP can not only take place at protein level but also at a transcriptional level,  $\beta$ -galactosidase assays were performed to investigate the expression of the genes. It was checked whether RsbP potentially regulates the expression of *yabR*, or *vice versa*. This was done by determining the expression levels in strains carrying the respective deletion. Therefore the promoter regions of *yabR* (GP3327) and *rsbP* (GP3328) were fused to the *lacZ* gene and brought into the genome of *B. subtilis* by double homologous integration into the *amyE* site. These constructs were also used to bring the  $P_{yabR}$ -*lacZ* fusion into the *rsbP* deletion strain (GP3333) and the  $P_{rsbP}$ -*lacZ* fusion into the *yabR* deletion strain (GP3334). The strains were incubated in LB until an  $OD_{600}$  of 0.5-0.8 was reached, which corresponds to the exponential growth phase of *B. subtilis*. Then the cells were lysed and the  $\beta$ -galactosidase activity was calculated in relation to the total amount of protein within the sample. It could be determined that *yabR* is expressed at a low level in LB. No significant change in the expression of *yabR* in the *rsbP* deletion strain could be observed. Even though *rsbP* seems to be expressed at a higher level than *yabR*, there is also no significant change in the expression of *rsbP* detectable upon the deletion of *yabR* (Fig. 3.3 C). This indicates that there is no link between the transcription of the two genes.

YabR has been identified to play a role in swarming motility in the undomesticated *B. subtilis* strain NCIB 3610 (Kearns *et al.*, 2004). Swarming is a flagella mediated form of motility on top of a solid surface that additionally requires the production of surfactant to reduce surface tension (Connelly *et al.*, 2004; Henrichsen, 1972). Again, the laboratory strain 168 has lost most of its ability to swarm and under some conditions, a complete arrest of swarming can be observed (Julkowska *et al.*, 2005). Literature disagrees if 168 can exhibit swarming motility at all and some attribute the swarming that can be observed for 168 due to spontaneous mutations and is not reproducible (Patrick & Kearns, 2009). It was attempted to characterize the swarming of the *yabR* deletion strain as well as the *rsbP* deletion strain and the suppressor mutant (Fig. 3.3 D). First experiments were performed by incubating the strains on LB containing 0.7% agar. No swarming motility could be observed (data not shown). Therefore, the percentage of agar was reduced to 0.4 %. Under this condition, the WT was able to swarm and cover the whole plate within 24 h after incubation at 37°C. Similar to the biofilm assay, the no difference in the ability to swarm between the wild type and the *rsbP* deletion strain could be

observed. Both strains were able to cover a substantial area of the agar plate within the 24 h of incubation. Both, the *yabR* deletion strain and the suppressor strain seem to be inhibited in their swarming motility since the area that these strains covered after 24 h was comparably smaller than the area covered by the wild type and the *rsbP* deletion strain. The preparation of more replicates could lead to a more significant confirmation of this result. Yet, the trend that could be observed

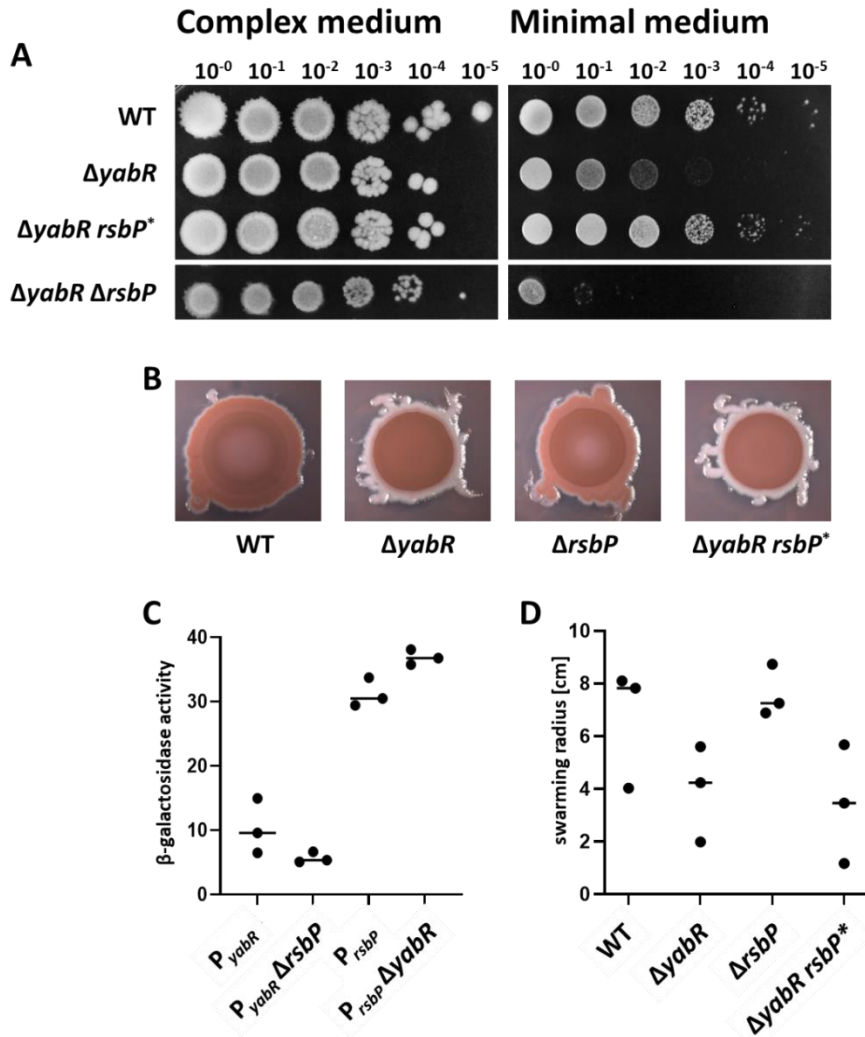


**Figure 3.3: Characterization of YabR and RsbP.** **A** Growth of the wild type, the *yabR* deletion strain (GP3598) and *yabR* suppressor strain carrying a mutation in the *rsbP* gene (GP3307, RsbP<sup>D393G</sup>) as well as the *yabR rsbP* double deletion strain (GP3332) on SP complex medium and MSSM minimal medium. **B** To investigate the biofilm formation of the WT, the *yabR* deletion strain (GP3598), the *rsbP* deletion strain (GP3323) and the *yabR* deletion suppressor strain (GP3307), they were cultivated on Mmsg medium containing Coomassie blue and congo red to stain the biofilm matrix. The plates were incubated for 4 days at 30°C before the pictures were taken with the stereo microscope (Carl Zeiss Microscopy) equipped with digital camera AxioCam MRC. **C** The promoter activities of *yabR* (GP3327) in the wild type and in the *rsbP* deletion strain (GP3333) and *rsbP* in the wild type (GP3328) and in the *yabR* deletion strain (GP3334), were investigated in a  $\beta$ -galactosidase assay. The strains were cultivated in LB medium and harvested during the exponential growth phase.  $\beta$ -Galactosidase activities are given in units per milligram of protein. **D** Swarming motility of the wild type as well as the *yabR* deletion strain (GP3598), the *rsbP* deletion strain (GP3323) and the *yabR* deletion suppressor strain (GP3307) was investigated on 4 % LB agar plates. The radius of the colonies was measured after incubation for 24 h at 37°C.

supports the recent identification of an involvement of YabR in swarming motility (Sanchez *et al.*, 2022).

To summarize, the mutation in RsbP is most likely a gain-of-function mutation since the double deletion of *yabR* and *rsbP* does not improve growth compared to the *yabR* single deletion strain. Furthermore, no connection between RsbP and YabR could be identified besides the mutation of *rsbP* in the *yabR* deletion strain. It remains to be elucidated what effect this mutation has on the phosphatase activity of RsbP. It can be stated that the involvement of YabR and RsbP most likely does not take place at the level of transcription. It is possible that the mutation in RsbP is a more general response to the elevated stress levels caused by the deletion of *yabR*. On a different note, results could be obtained that support the role of YabR in swarming motility.

#### 3.1.2 Searching for potential interaction partners

To check whether YabR and YugI potentially have additional interaction partners in *B. subtilis*, a Strep-protein interaction experiment (SPINE) was performed. For this purpose, the YugI expression plasmids pGP3523 and pGP3524 were constructed adding a N- and C-terminal Strep tag to the protein, respectively. For YabR, the plasmid pGP3522 was constructed, adding N-terminal Strep tag. The plasmids were introduced into the respective deletion strains of the genes while the empty vector control was brought into the WT. The strains were incubated in LB until an OD<sub>600</sub> of 0.8 was reached. Then the cultures were split in half and the crosslinker *para*-formaldehyde (PFA) was added to one of the cultures. After incubation for an additional 20 min, the cultures were harvested and cell pellets were subjected to lysis by French press and the crude extract applied to a Strep-tag®/Strep-Tactin® affinity purification column. The matrix was washed intensively to remove unbound proteins until the detection of proteins in the wash fraction was no longer possible using Bradford reagent. Afterwards, proteins were eluted and the crosslinks resolved by boiling of the samples. Fractions were analysed by SDS-PAGE and subsequent silver staining. As shown in Fig.3.4 A, minimal amounts of protein were still present in the wash fractions. The empty plasmid control showed only three main proteins that were bound to the column, which could be naturally biotinylated proteins such as AccB or PycA that bind the Strep column unspecifically. Interestingly, a multitude of proteins could be detected in the elution fractions of YabR and YugI, especially after the addition of PFA. This could be due to potential RNA interaction of YabR and YugI since both proteins contain a S1 RNA binding domain. Interestingly, both the purification of YabR and YugI showed a long smear on the gel indicating the presence of a multitude of bound nucleic acids, potentially RNA. Since the gels were run for a long time to ensure proper separation of the proteins, YabR and YugI were not present on the gel any longer due to their small

### 3. Results

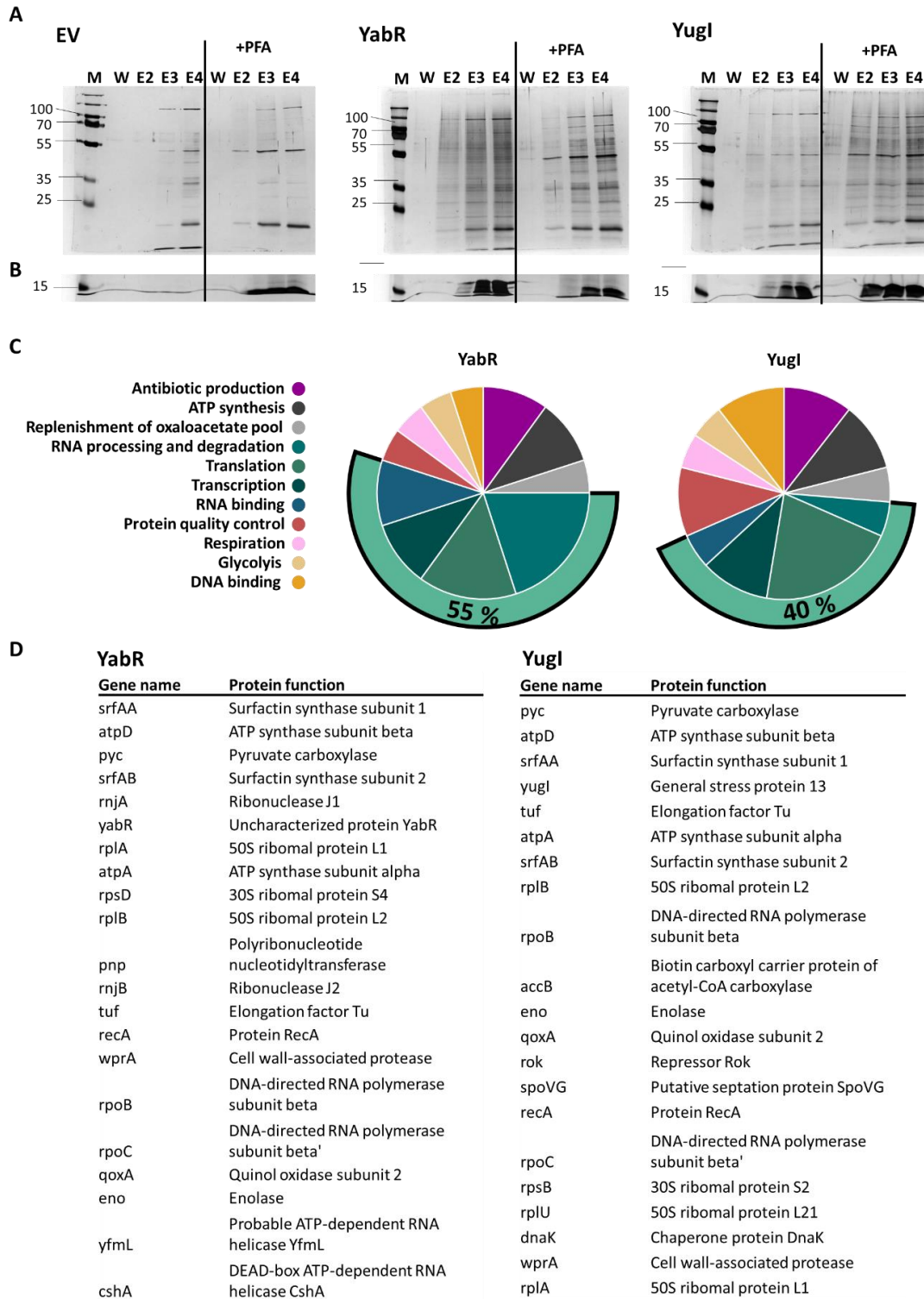


**Figure 3.4: Protein pulldown experiment** **A** SDS PAGEs after pulldown of proteins interacting with YabR and Yugi. YabR and Yugi were fused to a Strep tag and expressed in *B. subtilis*. 20 min before harvesting, cultures were split in two and one half was incubated with the crosslinker PFA. After harvesting, the cultures were subjected to the French press which lead to lysis. Crude extract was applied to a Strep matrix and bound proteins were eluted. Crosslinks were dissolved by boiling and proteins were analysed by SDS PAGE and subsequent silver staining. To achieve proper separation of the purified proteins, gels were run until the 15 kDa marker band reached the bottom of the gel. **B** Gel after shorter run time confirming the expression of YabR and Yugi. **C** Pie chart illustrating the biological functions the top twenty hits that were identified in the LC-MS were attributed to. Percentages of processes involving RNA are highlighted. **D** Table of the 20 most abundant protein identified in the YabR and Yugi Strep purification samples that were send for LC-MS.

size. Expression of the proteins was checked on an additional gel (Fig 3.4 B). To check what proteins were eluted together with YabR and YugI, the purification of YabR and YugI in *B. subtilis* was repeated and given away for liquid-chromatography mass-spectrometry (LC-MS). The twenty most abundant proteins were sorted by their biological function and their distribution is depicted in Fig. 3.4 C. YabR and YugI were excluded from the list. The exact 20 most abundant proteins that were discovered, including YabR and YugI, are listed in Fig. 3.4. D. Among them were the biotinylated PycA and AccB that bind the matrix unspecifically. A multitude of biological functions were represented and there were strong similarities between the two data sets. While for YabR, the most abundant group of proteins were proteins involved in RNA processing and degradation, proteins involved in translation were the group most present for YugI. These proteins include a multitude of ribosomal proteins from both subunits. Since YabR and YugI both contain a S1 RNA binding domain, it is possible that other RNA binding proteins were pulled through the interaction with the RNA. In total, 55 % of the top twenty proteins that eluted together with YabR have a connection to RNA processing. This is the case for 40 % of the proteins that eluted with YugI. This brings a potential RNA binding activity of YabR and YugI next to protein-protein interactions even further into the focus.

#### **3.1.3 Validation of binding of YabR and YugI to the ribosome**

There is a vast assortment of methods to prove PPIs. Since the ribosome is a multiprotein complex that also heavily involves nucleic acids, proving the interaction of YabR and YugI with the complex is a bit more challenging. To simplify the process, it was first focused on the ribosomal proteins that YabR and YugI had the most crosslinks with. To analyse the interactions, bacterial two-hybrid assays were performed. This meant testing the interaction of YabR with S6 and S18 and YugI with S3 and S10. For this purpose, fusions of all proteins of interest with either the T18 or T25 domain of the adenylate cyclase were constructed. During the bacterial two-hybrid assay, interaction of the proteins of interest leads to the functional complementation of the adenylate cyclase which results in  $\beta$ -galactosidase activity. This subsequently leads to the expression of the *lacZ* gene, which results in the degradation of x-gal and dark colonies. As shown in Fig. 3.5 A, strong interaction of S6 and S18 in addition to self-interaction of the two ribosomal proteins could be detected. The interaction of S6 and S18 is feasible since they are located in close proximity to each other on the ribosome. Furthermore, S3 and S10 showed self-interaction. Co-expression of YabR and S18 led to reconstruction of the adenylate cyclase confirming this interaction. The same can be stated for YugI and S10. None of the proteins showed interaction with the leucine zipper protein that was used as a negative control. Therefore this bacterial-two hybrid already provides a first confirmation of the interaction of YabR and YugI with the ribosome.



### 3. Results

Since the interaction of YabR and YugI with the ribosome is potentially not limited to one single protein but most likely takes place involving a variety of interaction partners as well as possibly nucleic acids, a validation of this interaction *in vivo* in *B. subtilis* would be more conclusive. For this purpose, strains were created where *yabR* was C-terminally fused to a His tag (GP3315) and *yugI* was C-terminally fused to a 3xFLAG tag (GP3700) in their native locus in the genome. Fusion of *yugI* to the 3xFLAG tag was performed utilizing the plasmid pGP1331. The construction of *yabR*-His was done by amplifying *yabR* and the respective upstream region and fusing the His tag to the gene through the reverse primer. This fragment was then fused to an antibiotic resistance cassette and the downstream region of *yabR* via LFH PCR. Transformation of the WT with the LFH product leads to homologous recombination and the integration of the His tag and the resistance cassette at the C-terminus of *yabR*. The ribosomes of these strains were isolated using a sucrose cushion. A strain encoding *rocF* fused to a FLAG tag (GP3930, constructed by R. Warneke) was used as a negative control. The crude extract (CE) and the ribosomal proteins were separated by SDS PAGE and blotted onto a membrane. Antibodies against the respective tags were used to detect the proteins of interest. YabR was enriched in the ribosome fraction

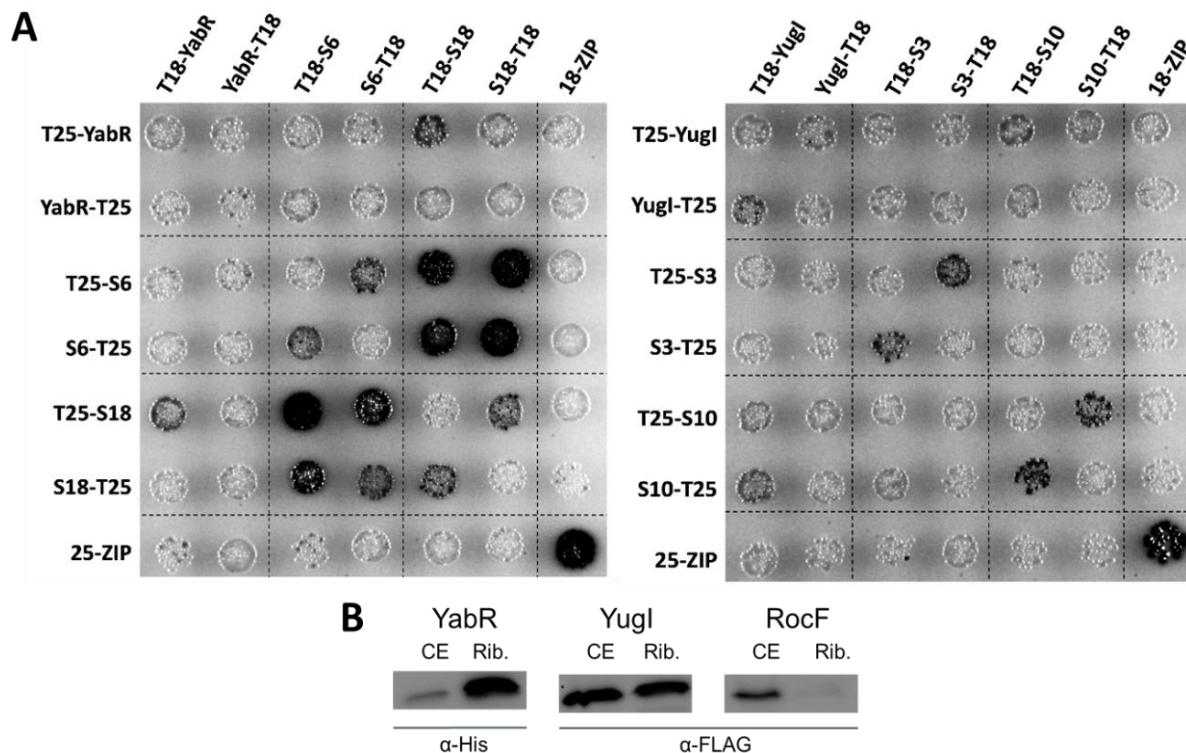


**Figure 3.5: Interaction of YabR and YugI with the ribosome.** **A** Bacterial two-hybrid experiment to identify interactions between YabR and the ribosomal proteins S6 and S18 as well as between YugI and S3 and S10. All proteins of interest were fused to the T18 and T25 domains of the adenylate cyclase CyaA and interactions were tested in the *E. coli* strain BTH101. Protein interaction leads to functional complementation of the adenylate cyclase which results in  $\beta$ -galactosidase activity visualized by dark colonies. A leucine zipper was used as a positive control **B** *B. subtilis* strains expression either YabR-His (GP3315), YugI-FLAG (GP3700) or RocF-FLAG (GP3930) were used for purification of the ribosome. The crude extract (CE) and the purified ribosomes were analysed by Western blot analysis using anti-His and anti-FLAG antibodies, respectively.

compared to the crude extract while YugI was present equally in both fractions. RocF was only detectable in the crude extract proving the functionality of this method (Fig. 3.5 B). A YabR-FLAG fusion was constructed additionally, yet here no interaction with the ribosome was detectable, probably due to the larger size of the tag (data not shown). To rule out that the FLAG tag fused to YugI had an effect on the interaction with the ribosome, a YugI-His strain (GP3322) was constructed *via* LFH as described for YabR. No changes in the binding to the ribosome could be detected compared to the binding of YugI-FLAG. This gives direct prove that YabR and YugI are actually associated with the ribosome *in vivo*. Furthermore, it suggests that the C-terminus of YabR might be heavily involved in the interaction since the fusion of the comparably large 3xFLAG tag lead to a disruption of the interaction. This is an interesting observation since the RNA binding domain of YabR is located at the N-terminus.

These results are supported by a similar experiment performed by O'Reilly *et al.*. They purified the ribosome of *B. subtilis* in a sucrose gradient which allowed the separation of the small and large subunit as well as the functional 70S ribosome. It could be shown that both, YabR and YugI are present in the fraction containing the 30S subunit. Small amounts of YabR could also be detected in the fractions corresponding to the 50S and 70S ribosome (O'Reilly *et al.*, 2022).

Two summarize, it could be conclusively prove that YabR and YugI are localized at the ribosome. Yet the function of this interaction still remains to be elucidated.

## 3.2 YneR as a novel interactor of the pyruvate dehydrogenase

The pyruvate dehydrogenase takes part in a crucial and irreversible step linking the glycolysis with the TCA cycle. Therefore, the activity of this enzymatic complex needs to be tightly controlled. So far, regulation of this complex has been attributed to allosteric mechanisms and product inhibition (de Kok *et al.*, 1998). In the study performed by O'Reilly *et al.*, in 2022, the protein of unknown function YneR was found to co-elute with the E1 module of the pyruvate dehydrogenase complex. It was also discovered to be crosslinked to both subunits (PdhA and PdhB) of the module indicating that the protein binds the multienzyme complex (O'Reilly *et al.*, 2022). To investigate the biological relevance of this interaction, a *yneR* deletion strain (GP3317) was constructed by LFH. Growth of this strain was characterised *via* drop dilution assay as described above. The minimal medium plates were incubated at 37°C and 48 °C while the growth on complex medium was only examined at 37°C. Furthermore, growth on minimal medium containing 5 mM KCl was investigated. As shown in Fig. 3.6 A, the deletion of *yneR* had no effect on the growth of *B. subtilis* under any tested condition. After prolonged incubation on standard minimal medium containing 0.1 mM KCl, colonies arose that exhibited a changed and pinkish phenotype (Fig 3.6 B). This phenotype has already been described to be caused

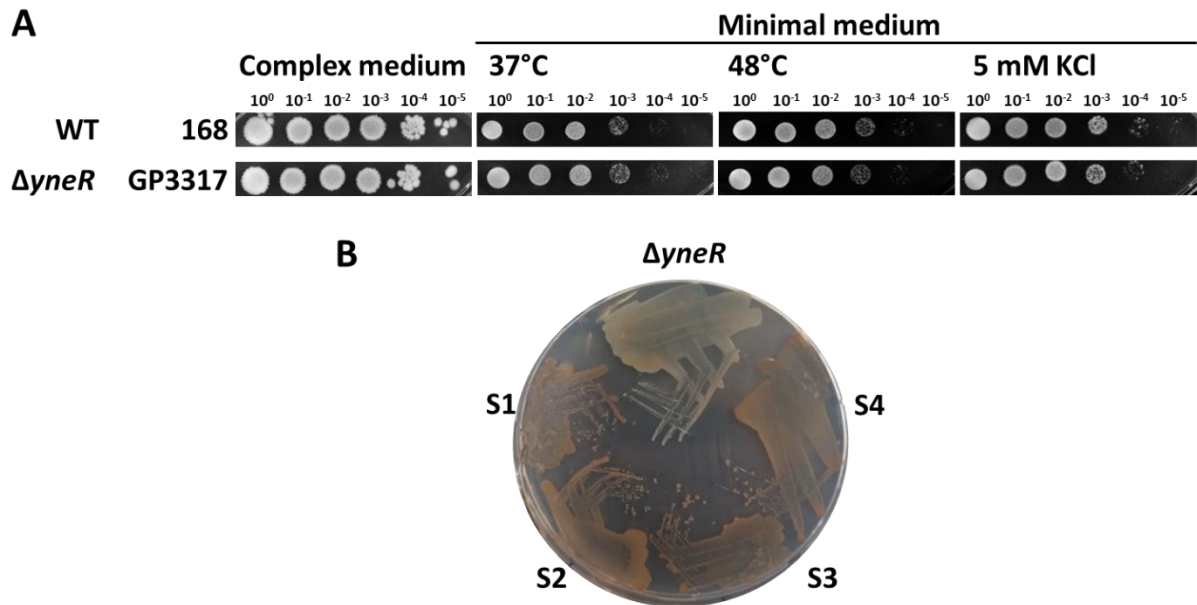


**Figure 3.6: Growth of *yneR* deletion strain.** **A** Drop dilution assay comparing the growth of the *yneR* deletion strain (GP3317) with the WT performed on complex medium as well as minimal medium under different conditions. **B** Suppressors of *yneR* deletion strain isolated on minimal medium exhibiting a pinkish phenotype caused by a frameshift mutation in *odhA*.

by mutations in *odhAB* in *B. subtilis*. To check if this was also the case for these strains, the DNA was isolated and the *odhAB* genes were sequenced. This in fact revealed mutations in the *odhA* gene, proving the suspicions right. Even though OdhA is a subunit of the 2-oxoglutarate dehydrogenase that is involved in the TCA cycle and interacts with a protein that is part of the E3 module of the pyruvate dehydrogenase complex, this mutation was not characterised further since it occurs with a high frequency in *B. subtilis* and has been observed in the past under unrelated conditions. Therefore it is probably not a specific effect caused by the deletion of *yneR*. To test a further condition, a strain was constructed allowing overexpression of *yneR* via the plasmid pBQ200. Growth was compared in a plate reader experiment including the WT and the WT carrying the empty pBQ200 vector (Fig. 3.7). The strains were incubated in MSSM minimal medium with 5 mM KCl containing either glucose, malate, citrate or pyruvate as the sole carbon source. Malate and citrate were chosen due to the fact, that they are both metabolites of the TCA cycle. The choice of the metabolite allows the identification of potential metabolic bottlenecks that might occur due to the deletion or overexpression of *yneR*. All strains showed WT like growth when glucose was available as the carbon source. The same could be observed for incubation with malate as the sole carbon source. This was expected, since malate is another preferred carbon source of *B. subtilis*. When only pyruvate was available, a pronounced growth deficit of the strain overexpressing *yneR* could be observed. Interestingly, the overexpression of *yneR* lead to increased growth with citrate as carbon source compared to the other strains. Taken together, these results show that YneR has an inhibitory effect on the enzymatic activity of the

pyruvate dehydrogenase. This aligns with the predicted structure of the complex that shows YneR covering the active site of the pyruvate dehydrogenase (see discussion, Fig. 4.1). Thus, YneR was renamed to pyruvate dehydrogenase inhibitor I (Pdhi).

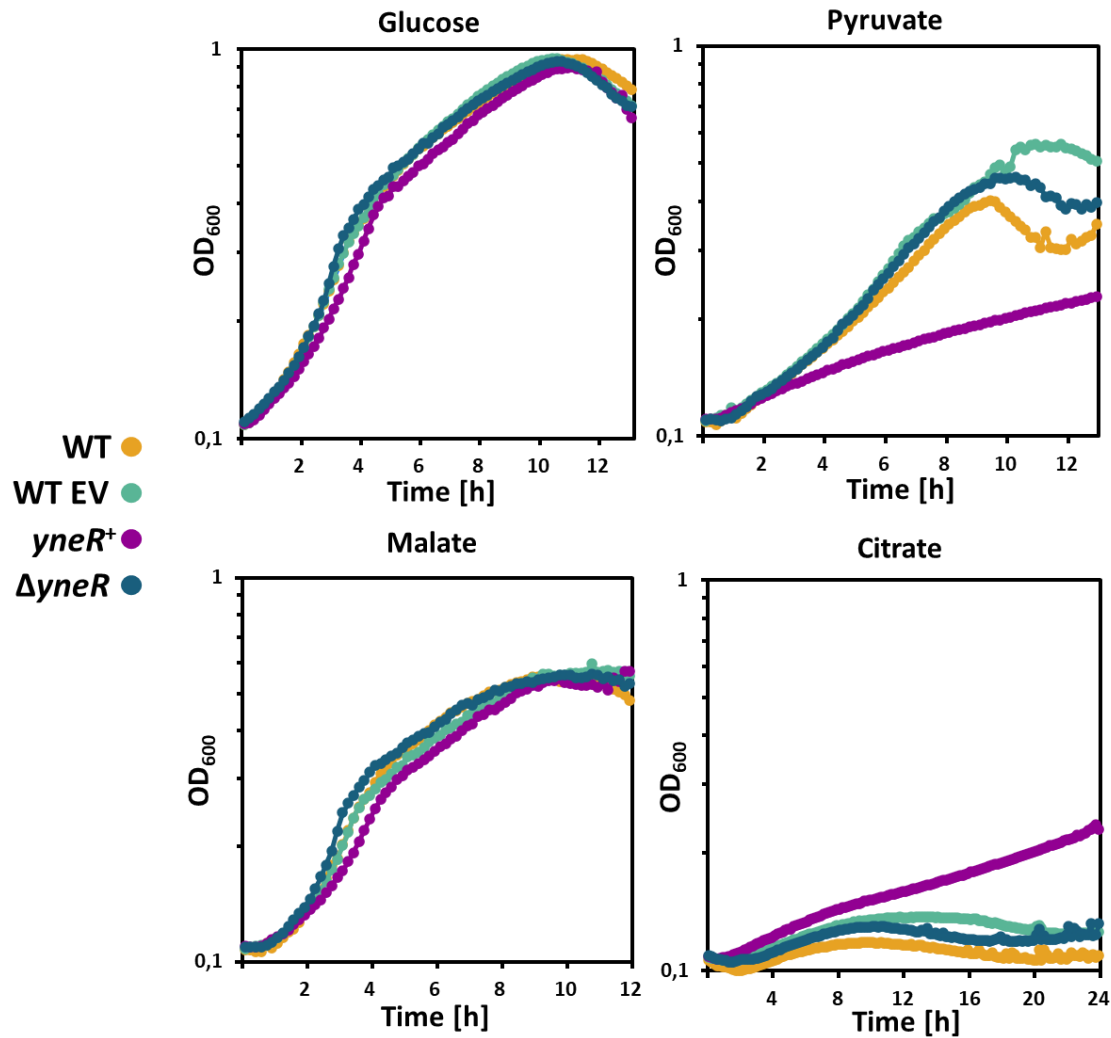


**Figure 3.7: Growth assay of the *yneR* overexpression and deletion strain.** Growth curves were performed in minimal medium containing 5 mM KCl with either glucose, pyruvate, malate or citrate as the sole carbon source. Growth was measured for the WT (orange), the strain overexpression *yneR* (pgP3588, purple) and the *yneR* knockout strain (GP3317, blue). The empty vector (EV) control is depicted in green. Growth with citrate was measured for 24 h while growth for all other conditions was measured for 12 h. Incubation was performed at 37°C at agitation and the OD<sub>600</sub> was determined in ten minute intervals.

### 3.3 Regulation of iron homeostasis

Iron is an essential micronutrient that is needed for cells in all domains of life since it functions as a co-factor for many enzymes. However, intracellular accumulation can lead to the rise of reactive oxygen species that cause great damage in the cell (Cabisco *et al.*, 2000). These reactive oxygen species are

generated by the Fenton reaction which involves iron and hydrogen peroxide. Reactive oxygen species can then destroy metalloenzymes and cause DNA damage (Imlay, 2013). Iron homeostasis in *B. subtilis* is therefore tightly regulated by the transcriptional regulator Fur. Fur was now found crosslinked to the protein of unknown function YlaN (O'Reilly *et al.*, 2022). So far, Fur is only known to bind itself and a specific DNA sequence also known as Fur box (Baichoo & Helmann, 2002). Binding of the Fur box occurs if Fe<sup>2+</sup> is available in a sufficient concentration and therefore bound by Fur, leading to the repression of genes involved in iron uptake. The aim of this chapter is to elucidate what biological function this novel interaction could potentially fulfil.

#### 3.3.1 Deletion of YlaN and suppressor screen

YlaN is an essential protein of unknown function, meaning that is crucial to sustain life under standard growth conditions and cannot be deleted. Yet, a study was able to reveal that deletion of *ylaN* is possible if Fe<sup>3+</sup> is supplemented to the medium (Peters *et al.*, 2016), already suggesting that YlaN might be involved in iron homeostasis. Finding YlaN now crosslinked to Fur further supports this hypothesis. Fur itself is not essential in *B. subtilis* and a deletion strain was already present in the laboratory strain collection (GP879, constructed by H. Eilers). To test whether the interaction of YlaN with Fur is the cause for its essentiality, the deletion of *ylaN* was attempted under standard conditions, with Fe<sup>2+</sup> or Fe<sup>3+</sup> supplemented to the medium as well as in a *fur* knockout strain. Both, deletion under standard conditions and with Fe<sup>2+</sup> supplemented to the medium were unsuccessful. As expected, deletion after supplementation of Fe<sup>3+</sup> was possible (GP3324). Interestingly, deletion of *ylaN* in the *fur* deletion strain was also successful (GP3321).

The single deletion strain of *ylaN* is not able to survive on complex medium without the addition of Fe<sup>3+</sup>. This fact was used for the isolation of suppressors. For this purpose, the strain was streaked out on standard complex medium or medium only containing Fe<sup>2+</sup> and incubated until colonies formed. These colonies were then singularized until they exhibited a stable and homogenous phenotype. The genomic DNA of these suppressor strains was isolated and the *fur* gene was sequenced. Previous sequence alignments of Fur from different prokaryotic organisms revealed the existence of highly conserved regions (Fig 3.8 A). According to the UniProt database, the region that is involved in DNA binding spans from 6<sup>th</sup> to the 91<sup>st</sup> amino acid while the region from amino acid 92 until amino acid 147 is needed for dimerization. All but one isolated suppressors had acquired mutations in the *fur* gene located in conserved regions in the DNA binding site potentially hindering Fur-DNA interaction (Fig. 3.8 A). The sites that were mutated in multiple suppressors always contained the same base-pair exchange. This was independent from the cultivation condition of the suppressors and the same

mutations arose on SP and SP containing Fe<sup>2+</sup>. A detailed list of the isolated suppressors can be found in the supplementary (Tab. 6.1). While most of the suppressors exhibited a WT like phenotype, some turned a reddish colour, leading to a colour change of the medium as well. This phenotype could also be observed in all *fur* knockout strains when they were grown in the presence of iron (Fig. 3.8 B). It can be hypothesised that the suppressors that show this phenotype contain mutations that lead to a complete abolishment of the Fur activity compared to an only partial inhibition in the other suppressor strains. An example of a mutation in Fur that led to a WT growth is the mutation of tyrosine 44 to cysteine (Y44C). On the other hand, the mutation of arginine 23 to cysteine led to the red phenotype (R23C). The one suppressor that did not contain a mutation in the *fur* gene accumulated a multitude

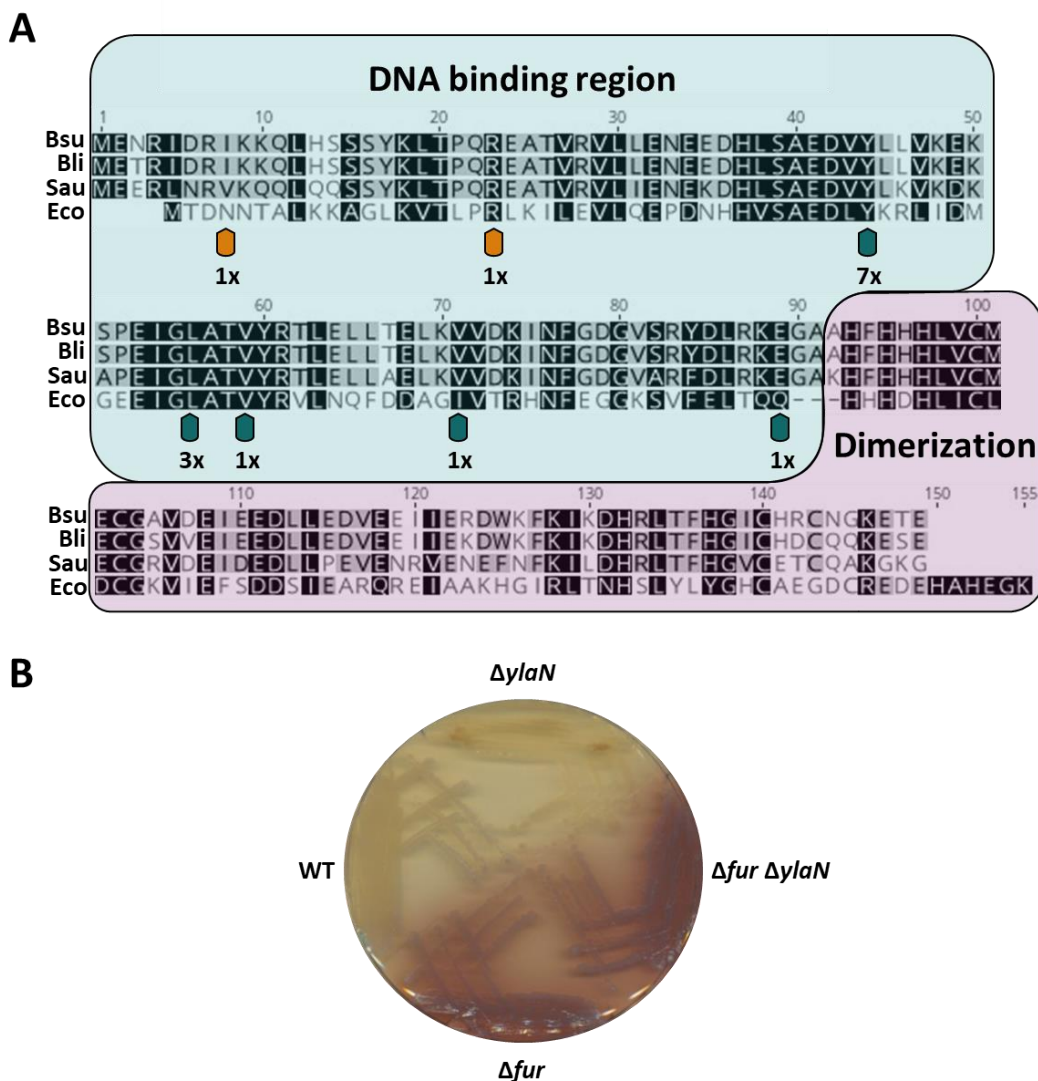


**Figure 3.8: The relationship between Fur and YlaN.** **A** Alignment of Fur from different prokaryotic organisms. Identical amino acids are marked in black and similar amino acids in grey Bsu *Bacillus subtilis*, Bli *Bacillus licheniformis*, Sau *Staphylococcus aureus* and Eco *Escherichia coli*. Mutation sites that were identified during the suppressor screen of the *ylaN* knockout strain are marked with arrows. The mutations that caused a red phenotype similar to a *fur* deletion are marked with red arrows. Numbers indicate the number of suppressor strains that had a mutation at the indicated site **B** Agar plate containing 2.5 mM Fe<sup>3+</sup> illustrating the red phenotype that can be observed after the deletion of *fur*.

of mutations in the upstream region of *fur*, probably leading to a strong reduction of *fur* expression (data not shown). Additional to the mutations in the upstream region of *fur*, a mutation in *bkdB* (G319D) could be observed. BkdB is part of the branched chain  $\alpha$ -keto acid dehydrogenase complex (BCDH complex) which turns branched chain amino acids (Leu, Ile, and Val) into branched-chain  $\alpha$ -ketoacyl-coenzyme A starters (BCCSs). These BCCSs can then be utilized for fatty acid synthesis (Wang *et al.*, 2020). Interestingly, leucine can also serve as a precursor for the production of pulcherriminic acid which is a cyclodipeptide that turns into the red insoluble pulcherrimin upon iron chelation leading to iron depletion in the environment. This makes pulcherriminic acid a promising substance for biocontrol (Uffen & Canale-Parola, 1972). Therefore, it can be hypothesised that the deletion of *fur* has an effect on the production of pulcherriminic acid, which would explain the red phenotype.

Taken together, these results indicate that YlaN plays an essential role in the regulation of Fur-DNA binding activity in *B. subtilis*.

#### 3.3.2 The role of YlaN in regulating Fur-DNA binding

To investigate the role of the essential protein of unknown function YlaN in the regulation of the DNA binding activity of the ferric uptake regulator Fur further, an electrophoretic mobility shift assay (EMSA) was performed. Fur binds the regulatory regions of genes involved in iron homeostasis as a homodimer (Ma *et al.*, 2012). The crystal structure of YlaN isolated from *S. aureus* could already be solved and revealed that the protein self-interacts and also assumes the conformation of a homodimer. It has further been hypothesised that the protein does not carry out an enzymatic function but rather binds a so far unidentified ligand (Xu *et al.*, 2007). It could already be determined that a deletion of *ylaN* is possible in combination with *fur* and that a single deletion of *ylaN* can only be achieved if  $\text{Fe}^{3+}$  is supplemented to the medium. Incubation of the *ylaN* knockout strain on medium without  $\text{Fe}^{3+}$  led to an accumulation of mutations in the DNA binding region of Fur. Therefore, it was hypothesized, that the essential function of YlaN is to sequester Fur from the DNA under low iron conditions. To test this hypothesis plasmids were constructed that allowed the overexpression and purification of Fur. YlaN was already available in the plasmid pWH844 which allows the overexpression of the protein fused to a His tag (constructed by F. Mehne during his PhD thesis). Fur was cloned into the plasmid pETSUMO which allowed fusion of the protein to a His-SUMO tag, which can be cleaved off after purification. Not only WT Fur was overexpressed and purified in this way but also the mutated Fur variants Fur<sub>Y44C</sub> and Fur<sub>R23C</sub>, which were identified during a suppressor screen and allowed growth of an *ylaN* deletion strain on medium without  $\text{Fe}^{3+}$  supplemented to it. Due to the reddish phenotype of the strain containing Fur<sub>R23C</sub>, which was similar to the *fur* deletion strain, it is suspected that this

mutant is unable to bind the DNA while Fur<sub>Y44C</sub>-DNA binding activity is potentially only partially inhibited. Fur-DNA binding was assayed using the Fur box located in the regulatory region of *dhbA*. When incubated with Fur during the EMSA, the DNA shifted upwards, indicating Fur-DNA binding. The incubation of the DNA with YlaN did not lead to a shift. When incubating Fur with YlaN and the DNA, no shift could be observed. Purified FabF was used as a negative control. This protein was chosen as a negative control due to the fact that it has a similar isoelectric point to Fur and YlaN (all ~5) and the protein has no known DNA binding activity. As expected, incubation of FabF with the DNA did not lead

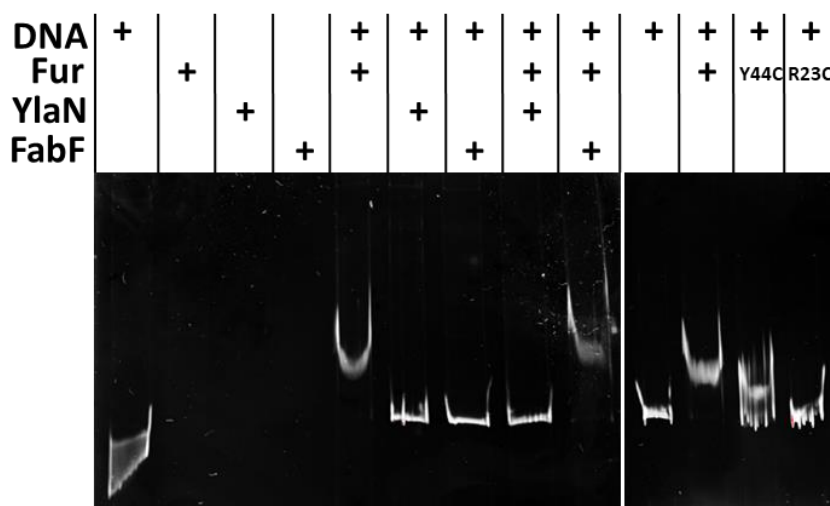


**Figure 3.9: The effect of YlaN on Fur-DNA binding.** EMSA assay performed with the regulatory Fur box amplified from in the upstream region of the *dhbA* gene DNA-protein interaction is indicated by an upshift of the DNA on the gel. The first lane shows unbound DNA. + signs indicate the addition of the respective compound. Y44C and R23C stand for the use of the respective mutated Fur. FabF was used as a negative control.

to any shift while the incubation of Fur with FabF and the DNA still resulted in an upshift of the DNA (Fig 3.9). Thus Fur-DNA binding is specifically inhibited by YlaN. To check the effect of the Fur mutations on DNA binding, the purified mutant versions of Fur were incubated with the DNA and binding was checked *via* shift assay. As hypothesized, Fur<sub>Y44C</sub> was only able to partially shift the DNA while the incubation of the Fur box with Fur<sub>R23C</sub> resulted in a nearly complete abolishment of the DNA shift.

To gain insights into the potential conformation of the Fur-YlaN complex, the complex was modelled using AlphaFold. Different ratios of the proteins were analysed. The model that was predicted for a 1:1 ratio of Fur and YlaN received an iPTM score of 0.15, indicating a very low confidence of AlphaFold in the prediction of the interaction site of the two proteins. The best scoring model for the prediction of the complex in a 2:1 ratio of Fur:YlaN also only received an iPTM score of 0.45. Finally AlphaFold was run predicting the conformation of the complex in a 2:2 ratio, since both proteins are known to form homodimers. This model received the highest iPTM score of 0.773, ranking it as a fairly confident prediction. The functional dimer of Fur is arranged in a way that exposes the N-terminal DNA binding domains but leads to a contrasted orientation of the two domains (Pohl *et al.*, 2003). Interestingly, the



model that was predicted for the complex of Fur and YlaN suggests that the interaction leads to a total conformational change in the Fur morphology, as depicted in Fig. 3.10. The regions that facilitate DNA binding are easily accessible in the Fur homodimer while the interaction with YlaN seems to lead to a 180° turn of each Fur protein. This results in a blockage of the DNA binding regions of Fur by YlaN. This would be a possible explanation of how YlaN hinders Fur from binding of the DNA.

Taken together, these results demonstrate that YlaN inhibits Fur-DNA binding. YlaN is dispensable in a *fur* deletion strain and Fur variants isolated from suppressor strains that contained an *ylaN* deletion exhibited reduced DNA-binding capability. It is therefore highly likely that the essential function of YlaN is fine tuning the DNA binding activity of Fur under low iron concentrations.

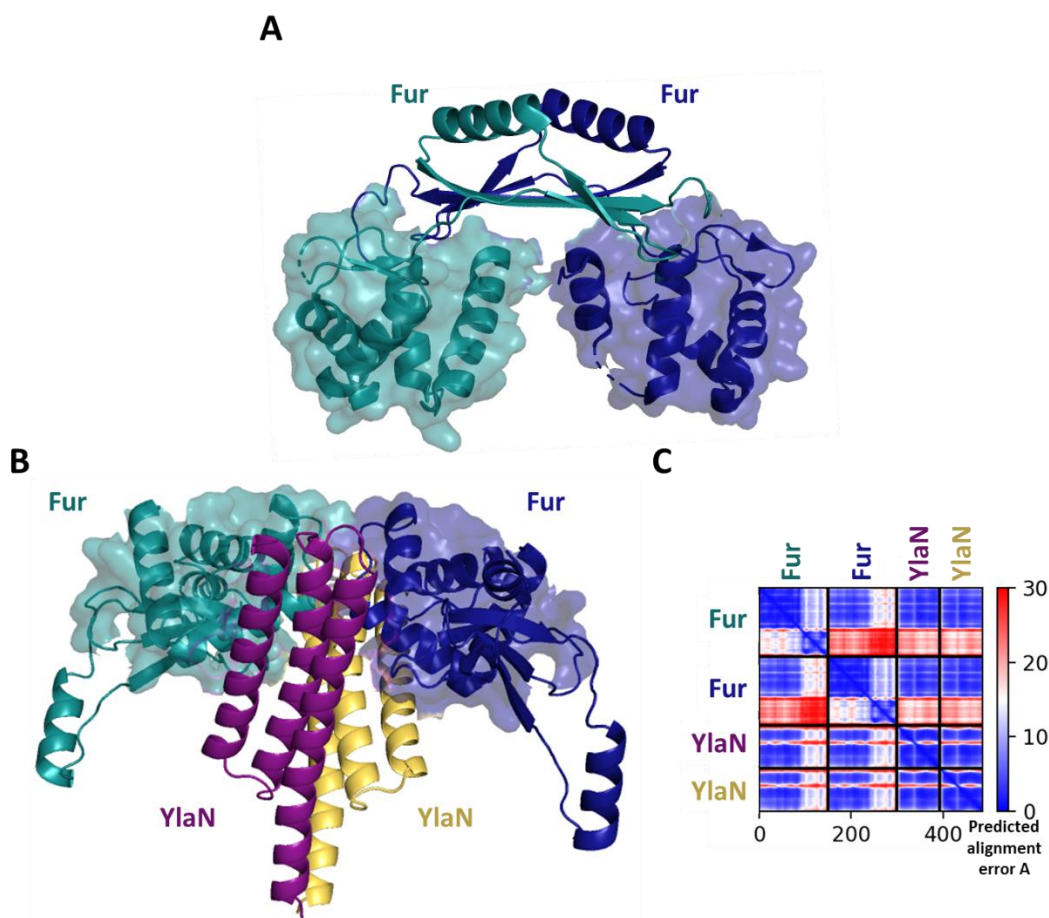


**Figure 3.10: Prediction of the structure of the Fur-YlaN complex.** **A** Crystal structure of the Fur homodimer of *Campylobacter jejuni* (Butcher *et al.*, 2012). The surface of the DNA binding region is illustrated. **B** Fur-YlaN complex in a 2:2 ratio as predicted by AlphaFold Multimer. The surface of the DNA binding region of Fur is illustrated. The Fur proteins are depicted in blue and green while YlaN is depicted in purple and orange. **C** Predicted alignment error plot of the prediction of the Fur-YlaN complex submitting both proteins as homodimers.

### 3.4 Interactions of binary complexes

While the protein interactions that are described above were analysed further to characterize the biological relevance of the complexes, some interactions were studied with merely the aim of validating their existence. Therefore, they were only subjected to bacterial two-hybrid analysis and no further research was performed. One interaction discovered during CLMS involved the essential alanine-tRNA synthetase AlaS and the protein of unknown function YozC. The structure of AlaS has already been solved for organisms such as *E. coli* or *Aquifex aeolicus*. It has been described that the protein forms a cradle-like structure that enables movement after ligand binding. It also contains a C-terminal  $\alpha$ -helix bundle that accommodates the tRNA recognition motif (Guo *et al.*, 2009). There is a specific aminoacyl-tRNA synthetase for each amino acid and the control and specificity of these synthetases is just as important for correct translation as the function of the ribosome (Döring *et al.*, 2001). Therefore, the potential interaction of AlaS with YozC could be of great interest. The size of YozC compared to AlaS is rather small with YozC only having a molecular weight of 7.93 kDa while AlaS has 97.08 kDa meaning that YozC would only cover a small fraction of the surface of AlaS upon interaction. The crosslinking data show that YozC binds to the N-terminal domain of AlaS, where the catalytic domain is located (Guo *et al.*, 2009; O'Reilly *et al.*, 2022). To verify this interaction, a bacterial two-hybrid experiment was performed. For this purpose, fusions of AlaS and YozC to either the T18 or T25

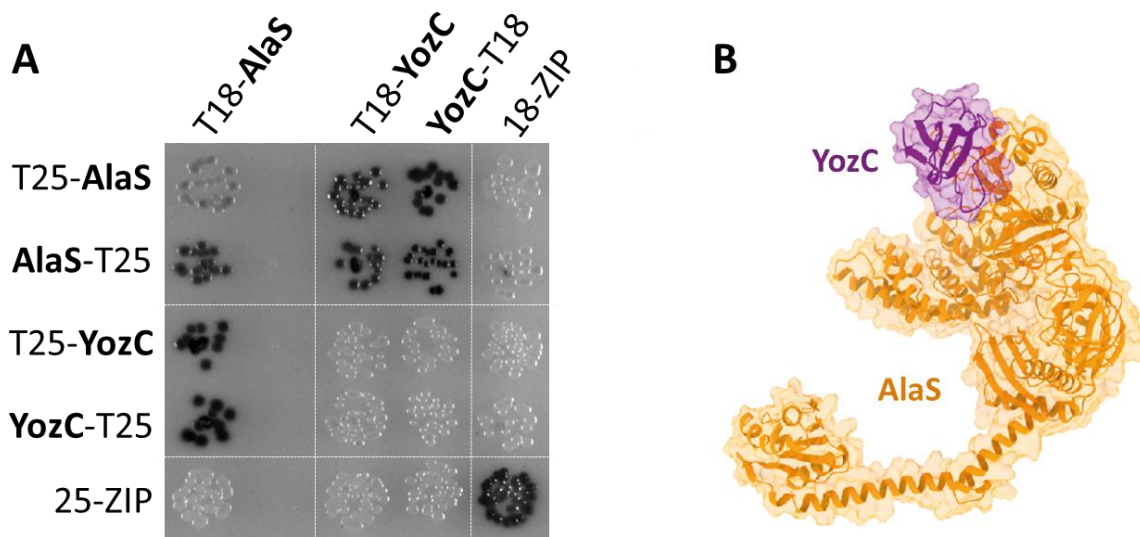


**Figure 3.11: The interaction of AlaS and YozC.** **A** Bacterial two-hybrid with the alanine-tRNA synthetase AlaS and the protein of unknown function YozC. N- and C terminal fusion of the two proteins with the T18 and T25 domains of the adenylate cyclase Cya were constructed. The construction of AlaS-T18 was unsuccessful. Interaction leads to the complementation of the adenylate cyclase which results  $\beta$ -galactosidase activity. Therefore, interaction is indicated by dark colonies. A leucine zipper was used as a positive control. **B** Prediction of the structure of the AlaS-YozC complex performed by AlphaFold. The prediction received an iPTM score of 0.97 (O'Reilly *et al.*, 2022).

domain of the adenylate cyclase (CycA) were constructed. The construction of the fusion of the T18 domain of CycA to the C-terminus of AlaS was unsuccessful. Interactions of the proteins are visualized by blue colonies which occur due to the functional complementation of the adenylate cyclase and subsequent  $\beta$ -galactosidase activity. As shown in Fig. 3.11 A, AlaS exhibited self-interaction which has not been previously described. Furthermore, a strong interaction could be observed for AlaS and YozC while none of the proteins interacted with the Zip protein. This indicates specific interaction of the alanine-tRNA synthetase AlaS with YozC. The complex was predicted using AlphaFold (Fig. 3.11 B) (O'Reilly *et al.*, 2022). The prediction received a remarkably high iPTM score (0.97) reflecting a high confidence of AlphaFold in the prediction of the interaction surface. In this model, YozC is predicted to bind to the N-terminal domain of AlaS which corresponds to the crosslinking results. This could indicate a potential inhibition of AlaS by YozC.

Additionally, the two proteins DhaS and GabD were found crosslinked to each other. Therefore it was aimed to validate the potential interaction of the proteins using the bacterial two-hybrid assay. DhaS is an aldehyde dehydrogenase that is able to produce 3-hydroxypropionic acid (3-HP) from 3-hydroxypropionaldehyde (3-HPA). 3-HPA is an industrially important raw chemical that can be used for the production of novel polymer materials (Su *et al.*, 2015). GabD is a dehydrogenase that catalyses the conversion of succinic semialdehyde to succinate in a NAD-dependent manner (Amidani *et al.*, 2017). It is one of the two enzymes needed for the alternative glutamate synthesis pathway *via*  $\gamma$ -aminobutyric acid (GABA) (Belitsky & Sonenshein, 2002) In *B. subtilis*, GABA is only used as an extracellular nitrogen source while it cannot be synthesized by the microorganism due to the lack of a suitable glutamate decarboxylase. The accumulation of GABA can be toxic which makes degradation to glutamate very important (Arst, 1976). While these two proteins have an assigned function, the biological link between the two dehydrogenases is unknown. Interestingly, succinate can be used as a precursor in the production of 3-HP (Luo *et al.*, 2016). As described above, both proteins were fused to the T18 and T25 subunit of CycA and checked for interaction. DhaS exhibited weak self-interaction while GabD showed strong self-interaction. This has not been described previously. No interaction with the leucine zipper could be detected. The suspected interaction of GabD and DhaS could not be validated using this method.

Furthermore, the two proteins YcgL and YurR were found crosslinked to each other. Both proteins so far have no function assigned to them. YurR has a molecular weight of 39.29 kDa and is homologous to the NAD-dependent oxidoreductase YurR in *B. licheniformis* (Pedreira *et al.*, 2022). YcgL, that has a molecular weight of 30.72 kDa but otherwise remains completely uncharacterised. The proteins of interest were fused to the T18 and T25 domains of the adenylate cyclase CycA as described above. Both YcgL and YurR showed strong self-interaction (Fig. 3.1 B). Similar to DhaS and GabD, no

dimer formation for these two proteins has been described up to this point. Furthermore, no interaction between YcgL and YurR could be verified, independent of the location of the adenylate cyclase domains relative to the protein. No interaction of any of the proteins with the leucine zipper could be detected.

Lastly, the proteins NusA and YkuJ were found crosslinked by O'Reilly *et al.*. NusA is an extensively studied essential transcription termination factor of the RNA polymerase (Schmidt & Chamberlin, 1987; Yang *et al.*, 2009) that has recently been described to play a role in RNA polymerase pausing *in vitro* as well as *in vivo*. This allows the synchronization of transcription and translation as well as for other regulatory mechanisms to take place (Jayasinghe *et al.*, 2022; Mondal *et al.*, 2017). On the contrary, not much is known about the function of the small protein YkuJ. While NusA is conserved among all bacterial kingdoms and even in Archaea, the presence of YkuJ is limited to some members of the class of Bacilli. A bacterial two-hybrid experiment was performed to check the interaction of the two proteins (Fig.3.1 C). As described previously, NusA and YkuJ were fused to the T18 and T25 domains of the adenylate cyclase CycA. The leucine zipper served as a positive control to test the functionality of the assay since it strongly interacts with itself. It can also be regarded as a negative control for the interaction with the proteins of interest, since no interaction should be detectable here. Both proteins of interest showed self-association to varying degrees. YkuJ exhibited the strongest signal for self-interaction and the protein has already been described to form homodimers in solution while X-ray crystallography suggests that the structure is actually a tetramer, thus this bacterial two-hybrid supports these findings (Wang *et al.*, 2008). NusA has been reported to be present predominantly as a monomer in solution (Gill *et al.*, 1991). This is contradictory with the results generated by the bacterial two-hybrid experiment. No interaction of NusA and YkuJ was

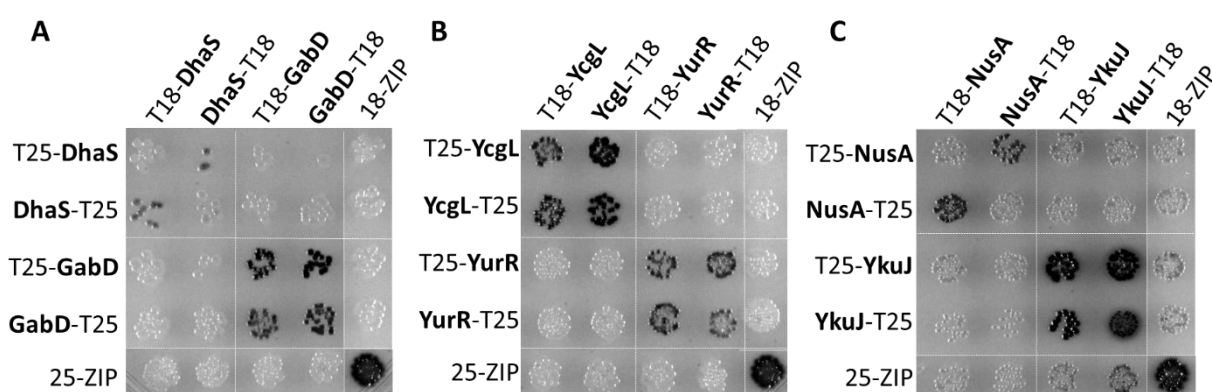


**Figure 3.12: Checking for binary interactions previously indicated by CLMS.** N- and C terminal fusion of the proteins of interest to the T18 and T25 domains of the adenylate cyclase CycA were constructed. Interaction of the proteins of interest lead to the complementation of the adenylate cyclase which results  $\beta$ -galactosidase activity. Therefore, interaction is indicated by dark colonies. A leucine zipper was used as a positive control. **A** Bacterial two-hybrid of the the dehydrogenases DhaS and GabD. **B** Test of the interaction of the proteins of unknown function YcgL and YurR via bacterial two-hybrid experiment. **C** Bacterial two-hybrid of the transcription termination factor NusA and the protein of unknown function YkuJ.

detectable. Additionally, YkuJ showed a weak signal for interaction with the leucine zipper. Some proteins are prone to interactions and are so called sticky proteins. These proteins are more likely to cause false positive results in a bacterial two-hybrid assay and interactions discovered *via* this method involving YkuJ should therefore be judged critically.

In conclusion, it can be stated that the bacterial two-hybrid approach is not suitable to identify every protein interaction. The only interaction that was identified during crosslinking that could be verified using the bacterial two-hybrid system is the interaction of the essential alanine-tRNA synthetase AlaS and the protein of unknown function YozC. All other potential interactions, namely DhaS-GabD, YcgL-YurR and NusA-YkuJ could not be verified. This does not necessarily exclude these suspected interactions but shows that for the detection of these interactions the bacterial two-hybrid experiment is unsuitable. A different approach should be used for further studying the potential binary complexes.



## 4. Discussion

*B. subtilis* is one of the best studied and understood Gram-positive microorganisms. In 1997, its genome sequence was among the first to be released (Kunst *et al.*, 1997). In total, the genome contains 4.100 protein coding genes. In an aim to further investigate the function of the proteins encoded by this soil bacterium, a large scale deletion project was initiated that aimed to create a minimal *Bacillus* strain that only encoded the proteins necessary to sustain life. As a result of these efforts, a *B. subtilis* strain could be created that only encoded 60% of the original genome (Michalik *et al.*, 2021). Even though extensive studies like this have been performed, 25% of the proteins in *B. subtilis* are still not well understood and have no function annotated to them (Michna *et al.*, 2016). This is not only the case for *B. subtilis* but a problem that is present in all model organisms. In 2015, 3.500 entries in the protein data bank (PDB) belonged to the group of proteins of unknown function (Burley *et al.*, 2017; McKay *et al.*, 2015). In an effort to shed light into this dark, sequence databases were created to potentially provide a fast solution. BLAST or HMMER can identify homologs from other organisms that have already been characterized. This provides first information about a potential function of the protein (Altschul, 1997; R. Finn *et al.*, 2011). *In vivo* or *in vitro* experiments can also be performed. This approach might be more time consuming but can potentially provide more solid predictions. The recent proteome wide crosslinking study coupled to AlphaFold Multimer based structure prediction performed by O'Reilly *et al.* revealed a couple of very interesting protein-protein interaction in *B. subtilis* (O'Reilly *et al.*, 2022). In addition to already known complexes, interactions were identified that involved proteins of so far unknown function. This is first evidence towards their function in the cell and presents a good starting point for analysis.

### 4.1 Regulation of protein complexes

#### 4.1.1 A novel inhibitor of the pyruvate dehydrogenase

The pyruvate dehydrogenase complex catalyses a reaction that is located right in the centre of central carbon metabolism and connects glycolysis to the TCA cycle *via* the oxidative decarboxylation of pyruvate. Since this reaction controls a crucial point in metabolism for organisms from all domains of life, the pyruvate dehydrogenase complex has been extensively investigated. The complex always consists of three components; the pyruvate dehydrogenase (E1), the dehydrolipoate acyltransferase (E2), and the dihydrolipoate dehydrogenase (E3), but regulatory mechanism in mammals compared to

bacteria differ (Patel *et al.*, 2014). The only regulatory mechanism that is known in bacteria is the transcriptional regulation by the repressor PdhR, which has been characterised in *E. coli*. Otherwise, no additional regulatory proteins have been described so far (Quail *et al.*, 1994). This work was able to show that an overexpression of YneR leads to a growth deficit upon growth with pyruvate as the sole carbon source. This growth deficit could not be observed if the strains were grown with glucose or malate as the carbon source, meaning that the overexpression of YneR leads to a bottleneck effect in carbon metabolism. This illustrated the inhibitory effect of YneR on the pyruvate dehydrogenase complex and therefore YneR was renamed to PdhI. PdhI was found crosslinked to both subunits of E1 in *B. subtilis*, namely PdhA and PdhB. Even though the reaction that is catalysed by E2 is the rate limiting step, it seems like controlling the activity *via* inhibition of the activity of E1 is the more conserved mechanism. In mammals, the regulation of the pyruvate dehydrogenase is achieved by the reversible phosphorylation of three different phosphorylation sites at E1. This mechanism is also present in plants and some fungi (Tovar-Mendez *et al.*, 2003; Wieland *et al.*, 1972). The regulation *via* the E1 unit could be due to the conformation of the pyruvate dehydrogenase complex. E2 is located in the middle of the complex while E1 and E3 both bind to it, potentially making E1 easier accessible for regulatory proteins.

The formation of protein complexes has also been described for other enzymes of the central carbon metabolism, like the complex formed between glycolytic enzymes like the phosphofructokinase, the phosphoglycerate mutase and the enolase. This is also the case for enzymes involved in the TCA cycle like the citrate synthase, the isocitrate dehydrogenase, and the malate dehydrogenase (Commichau *et al.*, 2009; Meyer *et al.*, 2011). In these metabolic pathways, protein interaction is presumed to lead to channelling of the substrate and increase of metabolic flux. But as demonstrated by the pyruvate dehydrogenase and PdhI, protein interactions can also have an inhibitory effect. This has already been described for other enzymes involved in important metabolic steps such as for the glutamate dehydrogenase GudB. GudB is the connection point between carbon and nitrogen metabolism and catalyses the formation of 2-oxoglutarate and ammonia from glutamate in the *B. subtilis* WT strain NCIB 3610 (Belitsky & Sonenshein, 1998). Glutamate is the most abundant metabolite in bacterial cells and an important provider of nitrogen (Bennett *et al.*, 2009). Usually, the balance of glutamate and 2-oxoglutarate lies heavily on the side of glutamate and 2-oxoglutarate is metabolized rapidly. During growth on arginine as a nitrogen source, the utilization is performed *via* glutamate and funnelled into the TCA cycle by GudB (Belitsky & Sonenshein, 1998). The reverse reaction from 2-oxoglutarate to glutamate is performed by the heterodimeric complex glutamate synthase GltAB (Belitsky, 2014). Intriguingly, the enzymes GltAB and GudB, which catalyse opposite reactions, form a transient complex, which leads to the inhibition of GudB. This prevents a futile cycle of constant synthesis and degradation of glutamate to occur. GltA inhibits the activity of GudB by



blocking the active site cleft and thus preventing co-factor binding (Jayaraman *et al.*, 2022). The crosslinking data of PdhI with PdhA and PdhB suggests a similar mechanism of inhibition. Taking the crosslinks into account, PdhI is mapped close to the active site of the dimer and potentially blocks access for pyruvate (Fig. 4.1). More precisely, Y31 of PdhI inserts itself into the active site of the pyruvate dehydrogenase and by doing so covers the entrance (O'Reilly *et al.*, 2022). Another example of interaction inhibiting the activity of one of the enzymes is the complex formed between the ornithine carbamoyltransferase ArgF and the arginase RocF. Both enzymes play a role in arginine metabolism. RocF catalyses the formation of ornithine while ArgF turns arginine into ornithine as part of the urea cycle. The inhibition of ArgF by RocF has the function of preventing unnecessary and energy expensive rounds of the urea cycle in the presence of arginine and ornithine (Issaly & Issaly, 1974).

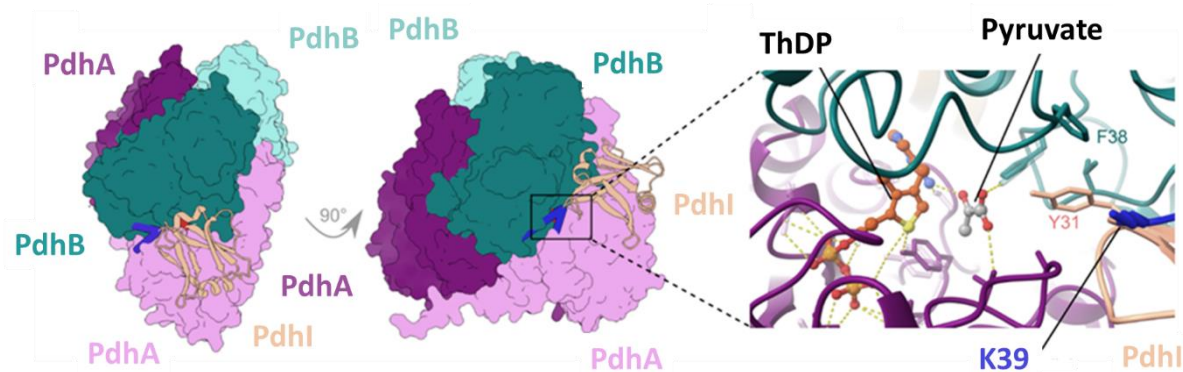


**Figure 4.1: Model of the pyruvate dehydrogenase interaction with PdhI.** Interaction of PdhI with the two subunits of the pyruvate dehydrogenase, namely PdhA and PdhB according to crosslinking data with a closer look at the active site. PdhA is depicted in purple, while PdhB is depicted in green and PdhI is depicted in pink (O'Reilly *et al.*, 2022).

The deletion of PdhI did not have any effect on growth. This suggests that the effect of PdhI on the pyruvate dehydrogenase only becomes relevant under specific conditions or that the interaction only partially inhibits the activity of the pyruvate dehydrogenase. Pyruvate could additionally be channelled into the TCA cycle through carboxylation by PycA, which would prevent the accumulation of the metabolite. It would be interesting to test what effect the deletion or overexpression of PdhI has on the metabolome of *B. subtilis*. It is also worth mentioning that PdhI is only encoded in bacteria of the class of Bacilli while the pyruvate dehydrogenase is present in all domains of life. This proposes the idea that the regulatory effect of PdhI on the pyruvate dehydrogenase is more of a fine-tuning effect that is not necessarily needed for proper control of the link between glycolysis and the TCA cycle and is therefore only conserved among this one class of bacteria. Nevertheless, this is the first time a protein regulator of the pyruvate dehydrogenase has been identified in prokaryotes and proposes the idea that also other bacteria potentially contain unidentified binders of the complex.

The growth experiments that revealed the effect of PdhI on the pyruvate dehydrogenase activity in the presence of pyruvate as the carbon source were also performed with malate and citrate. Since malate is known to be the second-best carbon source for *B. subtilis* after glucose it makes sense that the growth behaviour of all strains tested under this condition resembles the growth on glucose strongly (Doan *et al.*, 2003). To be more precise, malate gets co-utilized next to glucose if both substrates are present (Kleijn *et al.*, 2010). Previous studies have already analysed the metabolic flux in strains that were grown with malate as the sole carbon source. This analysis revealed a pronounced shift of metabolism towards the production of PEP and pyruvate from malate, which resulted in a strong increase of gluconeogenesis. Only a small fraction of the malate was actually consumed *via* the TCA cycle. But growth on malate did not only lead to a strong increase of gluconeogenesis but also to a strong overflow metabolism of pyruvate and acetate, thus heavily relying on the activity of the pyruvate dehydrogenase complex (Kleijn *et al.*, 2010; Sonenshein, 2007). Looking closely at the growth on malate, slight differences in the growth behaviour of the strains become clear. It can be observed that the strain containing the *pdhI* deletion actually shows the fastest growth while the strain overexpressing PdhI grows the slowest (Fig. 3.7). These differences are only subtle but their biological relevance should not be dismissed so easily, especially since both strains show contrary effects compared to the wild type. It is feasible that the deletion of *pdhI* increases the activity of the pyruvate dehydrogenase, which enables increased overflow metabolism *via* acetate and therefore better growth while the overexpression of *pdhI* has the opposite effect. It would be interesting to analyse, whether the deletion of *pdhI* actually leads to an accumulation of acetate in the cells if grown on malate compared to the wild type or deletion strain. Growth was additionally assayed on citrate, which is another intermediate of the TCA cycle. Theoretically all strains should be able to grow on citrate as the carbon source (Warner & Lolkema, 2002). Yet, growth of the wild type strain or the *pdhI* deletion strain could not be sustained, while very slow growth could be detected for the *pdhI* overexpression strain. Citrate is the first intermediate of the TCA cycle which connects to glycolysis and it is unclear why the overexpression leads to an increased growth compared to the wild type. One possible explanation is the acquisition of suppressor mutations in this strain that are triggered by the inhibition of the pyruvate dehydrogenase complex. But this should be apparent by a sudden increase in growth rate after a lag phase, which is not the case. Therefore, the improved growth is probably due to metabolic changes. The mechanism that led to the improved growth of the *pdhI* overexpression strain remains to be elucidated. Furthermore, it would be interesting to see whether growth on isocitrate leads to similar results.

#### 4.1.2 Regulation of the transcription regulator Fur by YlaN

Another regulatory complex that was discovered during this study involved the iron sensor Fur. Fur regulates the expression of a multitude of genes involved in iron metabolism such as transport systems and iron dependent enzymes (Pinochet-Barros & Helmann, 2018). This is achieved by binding of the Fur homodimer to the regulatory DNA region upstream of the target genes. This regulation only takes place if iron is bound by Fur which leads to DNA binding and repression of gene expression. Fur was now found crosslinked to the protein of unknown function YlaN, which is essential under standard growth conditions, but becomes dispensable under high iron concentrations (Peters *et al.*, 2016). This work shows that the deletion of *ylaN* can also be achieved independent of the iron concentration if *fur* is deleted prior. Both these results support a functional link between YlaN and iron metabolism, more precisely Fur. Investigating the exact biological relevance of this interaction revealed that YlaN disrupts Fur-DNA binding. Modelling the Fur-YlaN complex with AlphaFold showed interesting structural changes. It has been predicted that the interaction of the Fur dimer with the YlaN dimer leads to a complete switch of the Fur arrangement (Fig. 3.10 B). When not interacting with YlaN, the Fur dimer adopts a canonical V-shaped with the C-terminal domains interacting and the N-terminal DNA binding domains being exposed and easily accessible (Pohl *et al.*, 2003). According to the model predicted with high confidence by AlphaFold, binding of Fur to YlaN is mediated by the DNA binding sites of Fur and leads to a complete blockage of the DNA binding domains. This type of topological change in a dimer has been observed before in other regulatory protein-protein relationships like for the interaction with DarB and Rel. Rel is a bifunctional protein that catalyses the synthesis and degradation of guanosine tetra- and penta-phosphate ((p)ppGpp). This molecule serves as a second messenger and is heavily involved in stress response by modulating the stringent response (Ronneau & Hallez, 2019). DarB on the other hand is a regulatory signal transduction protein that binds the second messenger cyclic diadenosine monophosphate (c-di-AMP). This nucleotide is involved in many cellular processes, such as osmotic adaptation or virulence (Stülke & Krüger, 2020). In its apo-form, the DarB dimer is able to bind two Rel monomers per dimer, thereby disrupting the dimer formation of Rel. This then leads to an increase in (p)ppGpp and induction of stringent response (Krüger *et al.*, 2021). DarB additionally controls the activity of the pyruvate carboxylase PycA. Yet, the protein does not carry out an enzymatic function in the cell.

The crystal structure of YlaN has been solved in *S. aureus* and it has been hypothesised, that the protein does not have a catalytic function. The crystal also revealed a binding pocket for a so far unidentified ligand located in a shallow groove that spans the surface of each subunit. The entrance of the groove has a positive charge while the binding pocket is mostly negatively charged (Xu *et al.*, 2007). It is tempting to speculate that the so far unidentified ligand could be iron, more precisely ferric iron ( $\text{Fe}^{3+}$ ), since the deletion of YlaN is only possible if  $\text{Fe}^{3+}$  is added to the medium and the addition of ferrous iron ( $\text{Fe}^{2+}$ ) does not have the same effect. Interestingly,  $\text{Fe}^{2+}$  is the bioactive form and can be integrated into proteins to serve as a co-factor. *B. subtilis* has three main strategies to import iron.  $\text{Fe}^{3+}$  can enter the cell *via* siderophore dependent transport followed by a reduction to  $\text{Fe}^{2+}$ . This leads to a release of the iron due to a low affinity of the siderophore towards ferrous iron (Fontecave *et al.*, 1994). It can also be imported in its elemental form *via* the transport system EfeUOB (Miethke *et al.*, 2013). As a third option, the iron chelator citrate can be secreted and reimported by the FecCDEF system (Ollinger *et al.*, 2006). The reduction of  $\text{Fe}^{3+}$  to  $\text{Fe}^{2+}$  can be performed by ferric reductases (Gaines *et al.*, 1981; Lodge *et al.*, 1980). More precisely, iron gets reduced by the free reduced flavine that is produced by the ferric reductases and serves as electron donor (Schröder *et al.*, 2003). The iron availability could potentially regulate the interaction of Fur and YlaN the same way that c-di-AMP regulates the interaction of DarB and Rel. If high iron concentrations are present in the cell, Fur is

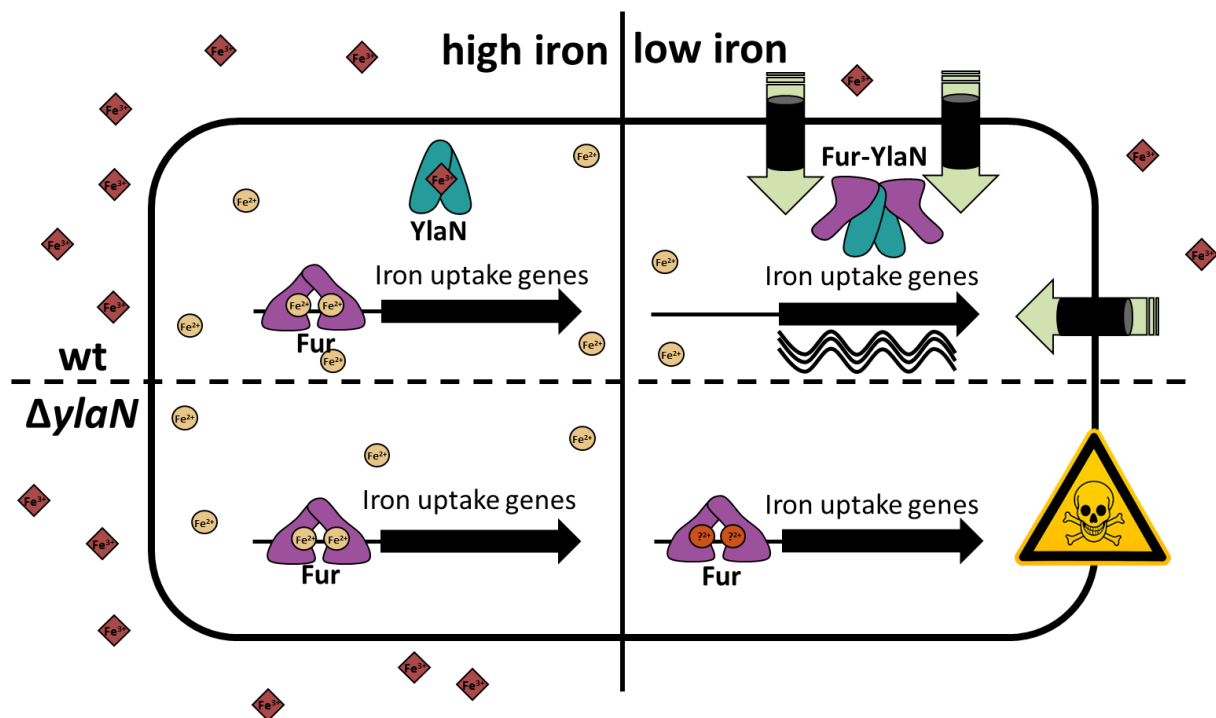


**Figure 4.2: Proposed model of the Fur regulation by YlaN.** Fur dimers are depicted in purple, while YlaN dimers are depicted in green. Soluble  $\text{Fe}^{2+}$  is depicted in beige, while  $\text{Fe}^{3+}$  is depicted in brown. High iron concentrations enable Fur-DNA binding. Deletion of YlaN is possible under high iron concentrations. If iron limitation occurs, YlaN sequesters Fur from the DNA allowing expression of the iron uptake genes. Deletion of YlaN under iron limitation leads to cell death.

bound to the DNA, repressing the expression of iron uptake genes and the iron sparing response. Therefore, the interaction between Fur and YlaN should already not be taking place and YlaN is dispensable, thus allowing its deletion. If the  $\text{Fe}^{2+}$  concentration then decreases, Fur cannot bind iron and is released from the DNA. It could be possible, that YlaN is needed in addition to sequester Fur from the DNA and allow iron uptake. Deletion of YlaN if iron is not present in excess either leads to cell death or the appearance of suppressor mutants that all either contain mutations in the DNA binding region of Fur or in the Fur promoter region. Thus, the regulatory effect of YlaN on Fur is essential for survival under iron limitation. It remains to be elucidated, why the addition of  $\text{Fe}^{2+}$  does not have the same effect as  $\text{Fe}^{3+}$  since  $\text{Fe}^{2+}$  is the bioactive and soluble form of iron. Interestingly, YlaN is only conserved in the class of Bacilli, meaning that this regulation is not conserved among many species and therefore probably evolved quite late, while Fur is conserved among all classes of bacteria and can even be found in Archaea. A model of the hypothesized interaction mechanism is depicted in Fig. 4.2.

## 4.2 Proteins still in the search for a function

### 4.2.1 Novel interactions at the ribosome

The main focus of this work was the validation of protein complexes identified during CLMS and CoFrac-MS involving proteins of unknown function. Since the interaction already provides a first hint towards the function of these proteins, this was a good starting point for further research. This work elucidated the function of the so far uncharacterised protein YlaN and YneR (now PdhI). Yet, the elucidation of the protein function was not possible for all investigated proteins.

Two proteins still in search of their function are the paralogous proteins YabR and YugI. They were identified as being crosslinked to different ribosomal proteins belonging to the 30S subunit. Both proteins have very similar sequences and contain an S1 RNA binding domain. Yet, they seem to carry out different functions in the cell. For example, the deletion of *yabR* causes a growth defect on minimal medium while this is not the case for the deletion of *yugI*. This already gives a first hint that YabR carries out a more important function in the cell compared to YugI. Further phenotypical differences could be observed. While a Western blot analysis performed with purified ribosomes was able to validate the interaction of YabR and YugI with the macromolecular complex, it also showed different affinities of the two proteins towards the ribosome. YugI was equally represented in the crude extract and the ribosome fraction while YabR was enriched in the ribosome fraction. This could be due to the different tags that were used in this experiment. Therefore, it was repeated with both proteins fused

to a His tag, which yielded the same results (data not shown). It can be stated that the interaction of YabR with the ribosome is stronger than the interaction of YugI with the ribosome. Furthermore, a sucrose gradient purification of the ribosome was performed by O'Reilly *et al.*, to elucidate if YabR and YugI are actually, as predicted, associated with the 30S subunit of the ribosome. It could be shown that both proteins can be co-purified with the 30S subunit of the ribosome. YabR could also be detected in the 50S and the 70S ribosome fractions (O'Reilly *et al.*, 2022). Interaction of the two paralogs with selected ribosomal proteins was tested in a bacterial two hybrid assay. It showed an interaction of YabR with S18 and YugI with S10. In these experiments, again the signal for the interaction of YabR with S18 was the strongest. Interestingly, YabR was found crosslinked to less r-proteins with less crosslinks in total (ten links to four proteins) while YugI had thirty-four links to eight r-proteins (O'Reilly *et al.*, 2022). This could mean that the interaction space of YugI with the ribosome is not completely fixed and that the surface YugI interacts with is bigger, but also looser. YabR on the other hand seems to be interacting in a tighter manner with the ribosome and has therefore a narrower interaction surface. The crosslinks identified for the interaction of YabR were also much shorter than the crosslinks found for YugI. Since both proteins contain RNA binding domains, the rRNA might also be heavily involved in mediating the interaction. Interestingly, YugI was already discovered crosslinked to RNA in a recent study, further indicating rRNA mediated interaction of the protein with the ribosome (Wulf, 2022). Since the ribosome is a large multiprotein complex that is dependent on the rRNA, it cannot be modelled by AlphaFold. Therefore, the interaction of YabR and YugI can also not be modelled by AlphaFold. This already illustrates a shortcoming of the AI-technology and shows the relevance of experimental techniques to characterize interactions.

It was first assumed that YabR and YugI are paralogous proteins that fulfil an essential function in the cell but are functionally able to replace each other and therefore are deemed as non-essential. This mechanism has already been described for the ribosomal proteins S14, L31 and L33 (Nanamiya *et al.*, 2008; Natori *et al.*, 2007). These are zinc dependent ribosomal proteins, but can be replaced by non-zinc dependent paralogs upon zinc limitation. In general, the ribosome is proof that all life originated from one common ancestor since it is conserved in all domains of life (Fournier & Gogarten, 2010). The three ribosomal RNAs are present in all organisms and so are seventeen out of twenty-one proteins of the small subunit and sixteen out of the thirty-two proteins of the large subunit. Furthermore, the initiation factors IF-1, IF-2 and IF-3 and the elongation factors EF-G and EF-Ts are highly conserved (McCutcheon & Moran, 2012). YabR and YugI are only conserved in a couple of bacterial phyla with the highest conservation in Firmicutes. This suggests that the interaction of the two proteins with the ribosome developed quite late during evolution and is not related to the general function of the ribosome. The hypothesis that YabR and YugI perform an essential function, but are able to functionally replace each other was refuted by a successful construction of a *yabR yugI* double

deletion strain. This does not necessarily mean that the proteins have no role in translation, since the composition of the ribosome can vary depending on the growth condition and not all ribosomal proteins are essential for the function of the macromolecular complex. Especially symbiotic bacteria and parasites often have strongly reduced ribosomes (Galperin *et al.*, 2021). The list of non-essential ribosomal proteins in *B. subtilis* and *E. coli* is quite similar (Galperin *et al.*, 2021). For example, in *B. subtilis*, the proteins S6, L1, L23 and L36 become dispensable for growth under high  $Mg^{2+}$  concentrations (Akanuma *et al.*, 2018).

### 4.2.2 The potential role of YugI

To further characterize the interaction of YabR and YugI with the ribosome, deletion strains were created and incubated in the presence of the antibiotic tetracycline, which interacts with the 30S subunit of the ribosome. This revealed that the deletion of *yugI* leads to a growth benefit when the deletion strain was incubated with the antibiotic. The mode of action of tetracycline can be summarized as inhibition of protein synthesis by disrupting the attachment of aminoacyl-tRNA to the A site of the ribosome (Chopra & Roberts, 2001). In high doses, this leads to cell death. Yet, a multitude of resistance mechanisms have been described for the antibiotic in many different bacterial species. One widespread mechanism of resistance is the export of tetracycline by efflux pumps. In total, thirty-six different genes coding for efflux pumps specific for tetracycline have been identified, most of them in Gram-negative bacteria (<http://faculty.washington.edu/marilynr/tetweb1.pdf>). The best represented group of efflux pumps in the list belongs to the major facilitator superfamily (MFS) of transporters (Chopra & Roberts, 2001). These efflux pumps facilitate the proton dependent export of the antibiotic and therefore prevent cell damage. Mutations in the efflux pumps can lead to changed substrate specificities which can either have an increasing or reducing effect on resistance (Guay *et al.*, 1994; Sapunarc & Levy, 2005). Furthermore, mutations in two-component systems that potentially regulate the efflux or permeability of tetracycline can lead to changes in resistance (Marchand *et al.*, 2004; Srinivasan *et al.*, 2012). An additional mechanism of resistance is achieved by enzymatic detoxification of tetracycline. The first evidence of tetracycline modifying proteins was described for *E. coli* (Speer & Salyers, 1988). A simple addition of a hydroxyl group at the C-11a leads to the inactivation of the antibiotic (Yang *et al.*, 2004). A last resistance mechanism takes place right at the ribosome. This is facilitated by mutations close to the binding site of tetracycline. One potential site of mutation is the 16S rRNA. This mechanism has been described for organisms such as *Helicobacter pylori* and *Mycoplasma bovis* (Amram *et al.*, 2015; Trieber & Taylor, 2002). Furthermore, mutations in r-proteins have been described. It is important to keep in mind that YugI was found crosslinked to S3

as well as S10. The r-protein S3, next to S7, S8, S14, and S19, has been shown to be involved in the binding of tetracycline to the ribosome in *E. coli* (Buck & Cooperman, 1990). Mutations in the proteins S3 and S10 in *Streptococcus pneumoniae* increase resistance to the tetracycline derivate tigecycline (Lupien *et al.*, 2015). Multiple other bacteria are able to become less susceptible to tetracycline by mutations in S10, which is the most common mutation of r-protein in context of tetracycline exposure. This has been characterised *in vitro* for bacteria such as *E. coli*, *Enterococcus faecium*, *Acinetobacter baumannii* and *S. aureus* (Beabout *et al.*, 2015). Furthermore, this mechanism of resistance has also been described for *B. subtilis* (Williams & Smith, 1979). The A site of the ribosome, which is also close to the primary binding site of tetracycline is solely formed by rRNA, but the r-proteins S4, S6, and S14 as well as S10 are involved in its scaffolding (Brodersen *et al.*, 2000). It is believed that even though S10 is not in direct contact with the 16S RNA at the point of tetracycline binding, a mutation of S10 can potentially alter the A-site conformation to a point where tetracycline cannot bind efficiently (Hu *et al.*, 2005). As mentioned above, YugI was found crosslinked to S3 as well as S10, which are both involved in conferring tetracycline resistance in multiple organisms. The deletion of *yugI* led to an increase in tetracycline resistance, which provides further proof of a functional link between the protein and the ribosome. It can be speculated that the deletion of *yugI* results in a conformational

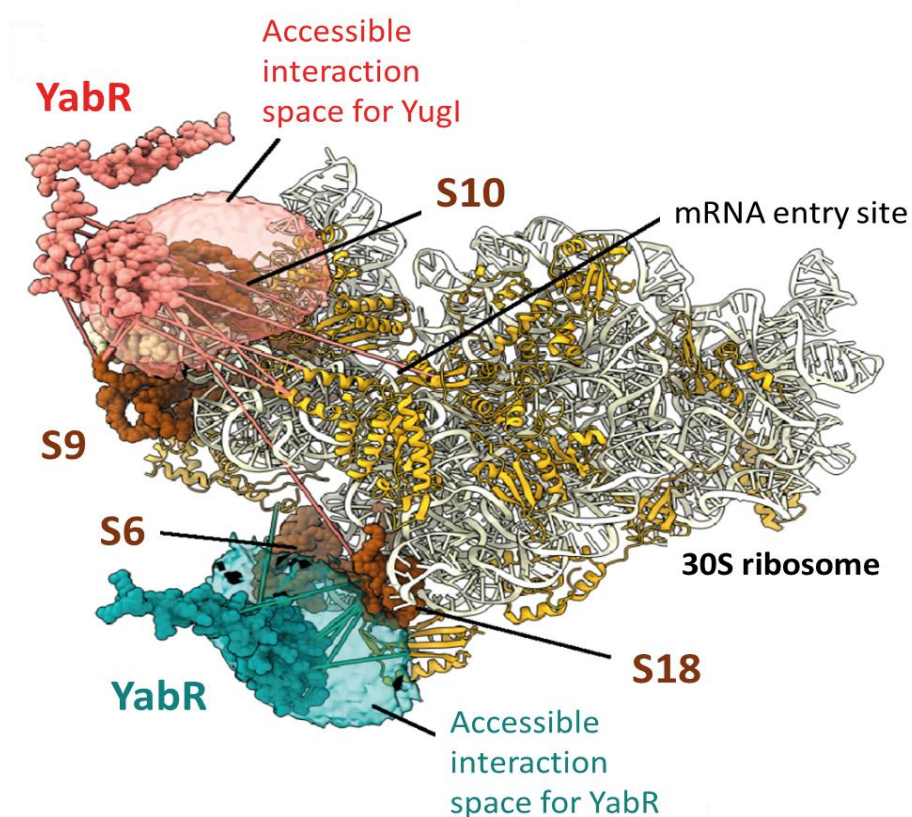


**Figure 4.3: Localization of YabR and Yugi on the ribosome.** The potential interaction space of YabR as well as Yugi with the 30S subunit of the ribosome was modelled by DisVis. (van Zundert *et al.*, 2017). Selected crosslinks are represented with lines. r-proteins are depicted in yellow or brown (interacting proteins) while the rRNA is depicted in white. The mRNA entry site is marked. (O'Reilly *et al.*, 2022)



change in either S3 or S10, or even both of the proteins. This would potentially change the conformation of the A-site of the ribosome, which would result in less efficient binding of tetracycline. Even though YabR and YugI are paralogs, the interaction space of YabR on the ribosome is removed from the interaction space of the YugI. Therefore, the presence of YabR does not affect the resistance to tetracycline (Fig 4.3).

Interestingly, YugI shows a 51 % similarity to parts of the S1 ribosomal protein of *E. coli*. This is interesting, since the S1 protein is the first protein where the S1 RNA binding domain has been described (Subramanian, 1983). In *E. coli*, the S1 protein consists of six repeats of the S1 RNA binding domain, which allows the guiding of the incoming mRNA towards the entrance of the ribosome (Laubert *et al.*, 2012). It has been determined that the N-terminal domain of S1 facilitates the interaction with the ribosome while the C-terminal domain is involved in mRNA binding (Laubert *et al.*, 2012). S1 recognises the SD sequence in the 5' UTRs of the mRNA and additionally unwinds potential secondary structures of the mRNA (Qu *et al.*, 2012). Even though the protein plays such an important role in *E. coli* and other organisms, no direct counterpart has been identified in *B. subtilis*. Since YugI is located in close proximity to the mRNA entry site of the ribosome and also contains an S1 RNA binding domain, it is thinkable that YugI contributes to mRNA recognition and guidance in *B. subtilis*. Other additional roles of YugI are of a possibility as well.

YugI is also known as GSP13, since it was first hypothesised that the protein plays a role in cold shock response (Antelmann *et al.*, 1997; Bernhardt *et al.*, 1997). Interestingly, it also gets expressed in a very similar manner to the cold shock protein CspB (*SubtiWiki*). The validation of the interaction with the ribosome poses the question of how this interaction potentially regulates the ribosome function under stress. Intriguingly, a cold shock adaptation protein that is essential for growth at low temperatures and binds to the ribosome in *E. coli* has been described, namely RbfA (Jones & Inouye, 1996). It is, just like YugI, a relatively small protein (15 kDa) and contains an KH domain. RbfA exclusively interacts with the 30S subunit of the ribosome, which was also observed for YugI during a sucrose gradient purification of the whole ribosome performed by O'Reilly *et al.* (O'Reilly *et al.*, 2022). In this work, it could be shown that YugI is equally represented in the cytosol or bound to the ribosome under standard growth conditions. Interestingly, only one third of RbfA is bound to free 30S subunits at growth at 37°C, while two-thirds bind free 30S subunits during cold shock (Xia *et al.*, 2003). RbfA is involved in ribosome maturation, especially efficient 16S RNA processing. It also potentially functions as an initiator for translation (Bylund *et al.*, 1998; Dammel & Noller, 1995). Deletion of *rbfA* therefore leads to an accumulation of 16S RNA precursors and slower adaptation to cold shock due to a reduction in protein translation (Xia *et al.*, 2003). It remains to be elucidated if this might be a function that is performed by YugI in *B. subtilis*. For this purpose, it would be interesting to determine the state of the

16S RNA in a *yugI* deletion strain in *B. subtilis* under cold shock conditions and to check if cold shock alters the localization of the protein in the cell.

### 4.2.3 YabR – the protein, the mystery

YabR seems to play a more important role in the cell, specifically for ribosome function compared to its paralog YugI. It is bound more tightly to the ribosome and deletion affects growth on minimal medium. This interaction with the ribosome is probably facilitated by the S1 domain of YabR and the ribosomal RNA. Furthermore, a mutation in the protein serine phosphatase RsbP improves growth of a *yabR* deletion strain on minimal medium. RsbP is involved in regulating the  $\sigma^B$  dependent stress response. During this work, no functional relationship between the two proteins could be established and the function of YabR remains unknown. Since the deletion of *rsbP* together with *yabR* did not lead to an improvement of growth, the suppressor mutation is likely to be a gain-of-function mutation. Phenotypic analysis of the suppressor strain revealed no changes in biofilm formation or swarming motility. Deletion of *yabR* led to reduced motility of the tested strains and therefore the recently described effect of YabR on swarming could be confirmed (Sanchez *et al.*, 2022). This hints towards a potential moonlighting function of YabR beyond the ribosome. The mutation of RsbP could potentially lead to a change in substrate specificity of the phosphatase. Gain-of-function mutations have already been identified in other Ser/Thr protein phosphatases belonging to the PPM family and have been shown to play a role in cancer development in humans (Kleiblova *et al.*, 2013). It would be interesting to see, whether mutations or deletions of the proteins downstream of RsbP in the signalling cascade also improve growth of the *yabR* deletion strain on minimal medium.

YabR contains an S1 RNA binding domain. This domain can be found in a variety of proteins that are involved in many different functions and processes. As mentioned above, the S1 ribosomal protein of *E. coli* consists of six repeats of this domain. The yeast protein S57596 contains twelve repeats of the S1 RNA binding domain. But just like YabR, no function could be assigned to this protein so far. There are also proteins that only contain one S1 domain such as the Tex (toxin expression) protein of *Bordetella pertussis* (Fuchs *et al.*, 1996), or several RNases including RNase E from *E. coli* (Bycroft *et al.*, 1997). RNase E is known to function as the scaffold for the degradosome in *E. coli*. The degradosome is responsible for RNA processing and degradation. It furthermore consists of the polyribonucleotide nucleotidyltransferase PNP, the enolase and the RNA helicase RhIB. Interestingly, PNP also contains an S1 domain as well as a KH domain. Both domains are involved in RNA binding and substrate recognition (Stickney *et al.*, 2005). The PNPase exhibits 3' to 5' exonuclease activity and degrades RNA. While YabR also contains an S1 RNA binding domain that is very similar to the one present in PNP, it is highly unlikely that they carry out the same function in the cell due to their large

difference in size. It is important to mention, that the degradosome of *B. subtilis* is assembled quite differently compared to the degradosome of *E. coli*. *B. subtilis* does not encode an equivalent to RNase E but the RNases J1, J2 and RNase Y have been identified as part of a large complex. Additionally, PnpA, the helicase CshA, the enolase and phosphofructokinase are part of the complex. The localization of the degradosome at the ribosome could be shown for both RNase E and RNase J based complexes (Redko *et al.*, 2013; Tsai *et al.*, 2012). It might be possible, that YabR is involved in the degradosome and able to facilitate an interaction between the ribosome and the degradosome by binding to both complexes. Unfortunately, no crosslinks between YabR and the components of the degradosome could be identified, making this theory highly unlikely.

Next to its potential involvement in swarming motility and its location at the ribosome, YabR has also been brought into context with sporulation, since it is encoded in close proximity to YabQ. YabQ is localized at the membrane of the forespore and plays an important role in the formation of the spore cortex. And indeed, disruption of *yabR* also leads to a 10-fold reduction of sporulation frequency (Asai *et al.*, 2001). All in all it can be stated, that YabR seems to be involved in a variety of processes and that its deletion causes pleiotropic phenotypes. It is therefore not possible to pinpoint the exact biological relevance of this protein in *B. subtilis*.

### 4.3 Challenges in protein interaction studies

The study performed by O'Reilly *et al.* led to the identification of a multitude of novel protein complexes in *B. subtilis* (O'Reilly *et al.*, 2022). This work aimed towards validating some of these interactions and characterizing the function of these complexes. Making this task even more exciting is the fact that proteins of unknown function were involved in the investigated complexes. While some complexes were studied more extensively, others were only investigated by bacterial two-hybrid assays. It was possible to validate the binary complex of essential alanine-tRNA synthetase AlaS and the protein of unknown function YozC. AlaS consists of a C-terminal  $\alpha$ -helix bundle that contains the tRNA recognition motif and a N-terminal catalytic domain (Guo *et al.*, 2009). Interestingly, the small protein YozC binds AlaS at the N-terminal catalytic domain. This would not be the first interaction of a tRNA synthetase with a regulatory protein that has been described. The Arc1p protein from yeast has been identified to bind both tRNA and the tRNA synthetase. This interaction is able to modulate the activity of the synthetase by stabilizing the tRNA-enzyme complex (Deinert *et al.*, 2001; Simos *et al.*, 1996). Homologs of the Arc1p protein are also present in some prokaryotes and are either encoded on their own or directly fused to the tRNA synthetase (Simos *et al.*, 1996). Yet, there is no significant

similarity between YozC and Arc1p. Nevertheless, it is likely that YozC plays a role in the regulation of the activity of AlaS.

Next to AlaS and YozC, three other binary interactions were analysed *via* bacterial two-hybrid, namely the interaction between DhaS with GabD, YcgL with YurR and NusA with YkuJ. It was not possible to verify any of these interactions. This does not mean that they were falsely discovered as interactors during CLMS or CoFrac-MS, but rather points out the highly complementary nature of protein interaction experiments. One drawback of bacterial two hybrid experiments is that the protein interactions are not being tested in their natural environment. If, like for the interaction of YabR and Yugi with the ribosome, protein complexes and even nucleic acids are involved in the interaction, it is quite likely that it will not be detected using this experimental setup. On the other hand, it often leads to false positive results (Battesti & Bouveret, 2012). In general, protein interactomes are highly dynamic and complexes are forming and dissociating constantly. Proteome wide crosslinking approaches have allowed the large-scale analysis of protein complexes but require high computational power and it is often challenging to achieve even crosslinking throughout the cell. Crosslinking of a sample fixes transient interactions but can also lead to the formation of very large complexes that are not analysable due to their size. An additional challenge is posed by the varying ratios of protein expression and degradation causing a detection *bias* towards the most abundant proteins. During the CoFrac-MS analysis this work is based on, a total of 667 potential interactions were identified. Out of these 667 interactions, only 4% were also established *via* the CLMS approach. To summarize, there is no such thing as one experiment that is suitable to catch all interactions. For the construction of a proteome wide interaction map, the use of complementary techniques is crucial.

### 4.4 Outlook

This project was able to show the power of predicting protein complexes by combining the complementary techniques CLMS and CoFrac-MS with the AI assisted complex modelling tool AlphaFold multimer. Multiple new protein complexes could be validated *in vivo* which opens the door for additional research on the biological relevance of these interactions. Especially the interaction between AlaS and YozC could be characterized further. Moreover, other organisms could be subjected to this workflow which would open up endless new possibilities in protein interaction studies. Especially bacteria that are hard to genetically modify should be subjected to this new approach. This could potentially open doors for studying and understanding pathogens which could lead to the development of antibiotics or other therapeutics.

This work was able to identify novel regulatory mechanisms of very well studied processes such as in carbon metabolism and iron homeostasis. Since these mechanisms remained undiscovered for so long, it would be interesting to analyse under which specific conditions they take place and what signal provokes the interactions. Furthermore, two proteins of unknown function were identified bound to the ribosome. These interactions might have an effect on ribosome maturation or translation speed. This remains to be studied in more detail. In general, the proteome wide crosslinking map revealed a multitude of novel protein-protein interactions that could be studied further. The work of understanding the biological relevance of the interactions discovered in the study from O'Reilly *et al.* is far from done (O'Reilly *et al.*, 2022).



## 5. References

- Ahn, B. E., Cha, J., Lee, E. J., Han, A. R., Thompson, C. J., & Roe, J. H. 2006. Nur, a nickel-responsive regulator of the Fur family, regulates superoxide dismutases and nickel transport in *Streptomyces coelicolor*. *Mol Microbiol*, **59**, 1848–1858.
- Akanuma, G., Nanamiya, H., Natori, Y., Yano, K., Suzuki, S., Omata, S., *et al.* 2012. Inactivation of ribosomal protein Genes in *Bacillus subtilis* reveals importance of each ribosomal protein for cell proliferation and cell differentiation. *J Bacteriol*, **194**, 6282–6291.
- Akanuma, G., Yamazaki, K., Yagishi, Y., Iizuka, Y., Ishizuka, M., Kawamura, F., & Kato-Yamada, Y. 2018. Magnesium suppresses defects in the formation of 70S ribosomes as well as in sporulation caused by lack of several individual ribosomal proteins. *J Bacteriol*, **200**, e00212-18.
- Altschul, S. 1997. Gapped BLAST and PSI-BLAST: a new generation of protein database search programs. *Nucleic Acids Res*, **25**, 3389–3402.
- Amidani, D., Tramonti, A., Canosa, A. V., Campanini, B., Maggi, S., Milano, T., *et al.* 2017. Study of DNA binding and bending by *Bacillus subtilis* GabR, a PLP-dependent transcription factor. *Biochim Biophys Acta Gen Subj*, **1861**, 3474–3489.
- Amram, E., Mikula, I., Schnee, C., Ayling, R. D., Nicholas, R. A. J., Rosales, R. S., *et al.* 2015. 16S rRNA gene mutations associated with decreased susceptibility to tetracycline in *Mycoplasma bovis*. *Antimicrob Agents Chemother*, **59**, 796–802.
- Anbar, A. D. 2008. Elements and evolution. *Science*, **322**, 1481–1483.
- Andrews, S., Norton, I., Salunkhe, A. S., Goodluck, H., Aly, W. S. M., Mourad-Agha, H., & Cornelis, P. 2013. Control of iron metabolism in bacteria. *Met. ions life sci.*, **12**, 203–239.
- Antelmann, H., Bernhardt, J., Schmid, R., Mach, H., Völker, U., & Hecker, M. 1997. First steps from a two-dimensional protein index towards a response-regulation map for *Bacillus subtilis*. *Electrophoresis*, **18**, 1451–1463.
- Arst, H. N. 1976. Integrator gene in *Aspergillus nidulans*. *Nature*, **262**, 231–234.
- Baichoo, N., & Helmann, J. D. 2002. Recognition of DNA by Fur: a reinterpretation of the Fur box consensus sequence. *J Bacteriol*, **184**, 5826–5832.
- Baichoo, N., Wang, T., Ye, R., & Helmann, J. D. 2002. Global analysis of the *Bacillus subtilis* Fur regulon and the iron starvation stimulon. *Mol Microbiol*, **45**, 1613–1629.
- Ban, N., Nissen, P., Hansen, J., Moore, P. B., & Steitz, T. A. 2000. The complete atomic structure of the large ribosomal subunit at 2.4 Å resolution. *Science*, **289**, 905–920.
- Barnes, S. J., & Weitzman, P. D. J. 1986. Organization of citric acid cycle enzymes into a multienzyme cluster. *FEBS Lett*, **201**, 267–270.

- Bartolini, M., Cogliati, S., Vileta, D., Bauman, C., Rateni, L., Leñini, C., et al.** 2019. Regulation of biofilm aging and dispersal in *Bacillus subtilis* by the alternative sigma factor SigB. *J Bacteriol*, **201**, e00473-18.
- Battesti, A., & Bouveret, E.** 2012. The bacterial two-hybrid system based on adenylate cyclase reconstitution in *Escherichia coli*. *Methods*, **58**, 325–334.
- Beabout, K., Hammerstrom, T. G., Perez, A. M., Magalhães, B. F., Prater, A. G., Clements, T. P., et al.** 2015. The ribosomal S10 protein is a general target for decreased tigecycline susceptibility. *Antimicrob Agents Chemother*, **59**, 5561–5566.
- Belitsky, B. R.** 2014. Biosynthesis of amino acids of the glutamate and aspartate families, alanine, and polyamines. In *Bacillus subtilis* and its closest relatives (pp. 203–231). Washington, DC, USA: ASM Press.
- Belitsky, B. R., & Sonenshein, A. L.** 1998. Role and regulation of *Bacillus subtilis* glutamate dehydrogenase genes. *J Bacteriol*, **180**, 6298–6305.
- Belitsky, B. R., & Sonenshein, A. L.** 2002. GabR, a member of a novel protein family, regulates the utilization of gamma-aminobutyrate in *Bacillus subtilis*. *Mol Microbiol*, **45**, 569–583.
- Bennett, B. D., Kimball, E. H., Gao, M., Osterhout, R., van Dien, S. J., & Rabinowitz, J. D.** 2009. Absolute metabolite concentrations and implied enzyme active site occupancy in *Escherichia coli*. *Nat Chem Biol*, **5**, 593–599.
- Berg, A., & de Kok, A.** 1997. 2-Oxo acid dehydrogenase multienzyme complexes. The central role of the lipoyl domain. *Biol Chem*, **378**, 617–634.
- Bernhardt, J., Völker, U., Völker, A., Antelmann, H., Schmid, R., Mach, H., & Hecker, M.** 1997. Specific and general stress proteins in *Bacillus subtilis* -- a two-dimensional protein electrophoresis study. *Microbiology*, **143**, 999–1017.
- Blencke, H.-M., Homuth, G., Ludwig, H., Mäder, U., Hecker, M., & Stülke, J.** 2003. Transcriptional profiling of gene expression in response to glucose in *Bacillus subtilis*: regulation of the central metabolic pathways. *Metab Eng*, **5**, 133–149.
- Blencke, H.-M., Reif, I., Commichau, F. M., Detsch, C., Wacker, I., Ludwig, H., & Stülke, J.** 2006. Regulation of *citB* expression in *Bacillus subtilis*: integration of multiple metabolic signals in the citrate pool and by the general nitrogen regulatory system. *Arch Microbiol*, **185**, 136–146.
- Bley Folly, B., Ortega, A. D., Hubmann, G., Bonsing-Vedelaar, S., Wijma, H. J., van der Meulen, P., et al.** 2018. Assessment of the interaction between the flux-signaling metabolite fructose-1,6-bisphosphate and the bacterial transcription factors CggR and Cra. *Mol Microbiol*, **109**, 278–290.
- Borovinskaya, M. A., Shoji, S., Holton, J. M., Fredrick, K., & Cate, J. H. D.** 2007. A steric block in translation caused by the antibiotic spectinomycin. *ACS Chem Biol*, **2**, 545–552.



- Bowker-Kinley, M. M., Davis, I. W., Wu, P., Harris, A. R., & Popov, M. K.** 1998. Evidence for existence of tissue-specific regulation of the mammalian pyruvate dehydrogenase complex. *Biochem*, **329**, 191–196.
- Bradford, M. M.** 1976. A rapid and sensitive method for the quantitation of microgram quantities of protein utilizing the principle of protein-dye binding. *Anal Biochem*, **72**, 248–254.
- Branda, S. S., González-Pastor, J. E., Ben-Yehuda, S., Losick, R., & Kolter, R.** 2001. Fruiting body formation by *Bacillus subtilis*. *PNAS*, **98**, 11621–11626.
- Bremer, H., & Dennis, P. P.** 2008. Modulation of Chemical Composition and Other Parameters of the Cell at Different Exponential Growth Rates. *EcoSal Plus*, **3**, ecosal.5.2.3.
- Brodersen, D. E., Clemons, W. M., Carter, A. P., Morgan-Warren, R. J., Wimberly, B. T., & Ramakrishnan, V.** 2000. The structural basis for the action of the antibiotics tetracycline, pactamycin, and hygromycin B on the 30S ribosomal subunit. *Cell*, **103**, 1143–1154.
- Brody, M. S., Stewart, V., & Price, C. W.** 2009. Bypass suppression analysis maps the signalling pathway within a multidomain protein: the RsbP energy stress phosphatase 2C from *Bacillus subtilis*. *Mol Microbiol*, **72**, 1221–1234.
- Bsat, N., Herbig, A., Casillas-Martinez, L., Setlow, P., & Helmann, J. D.** 1998. *Bacillus subtilis* contains multiple Fur homologues: identification of the iron uptake (Fur) and peroxide regulon (PerR) repressors. *Mol Microbiol*, **29**, 189–198.
- Buck, M. A., & Cooperman, B. S.** 1990. Single protein omission reconstitution studies of tetracycline binding to the 30S subunit of *Escherichia coli* ribosomes. *Biochem*, **29**, 5374–5379.
- Burley, S. K., Berman, H. M., Kleywegt, G. J., Markley, J. L., Nakamura, H., & Velankar, S.** 2017. Protein Data Bank (PDB): The single global macromolecular structure archive. In *Methods mol. biol*, **1607**, 627–641.
- Butcher, J., Sarvan, S., Brunzelle, J. S., Couture, J.-F., & Stintzi, A.** 2012. Structure and regulon of *Campylobacter jejuni* ferric uptake regulator Fur define apo-Fur regulation. *PNAS*, **109**, 10047–10052.
- Bycroft, M., Hubbard, T. J. P., Proctor, M., Freund, S. M. V., & Murzin, A. G.** 1997. The solution structure of the S1 RNA binding domain: a member of an ancient nucleic acid-binding fold. *Cell*, **88**, 235–242.
- Bylund, G. O., Wipemo, L. C., Lundberg, L. A. C., & Wikström, P. M.** 1998. RimM and RbfA Are essential for efficient processing of 16S rRNA in *Escherichia coli*. *J Bacteriol*, **180**, 73–82.
- Cabiscol, E., Tamarit, J., & Ros, J.** 2000. Oxidative stress in bacteria and protein damage by reactive oxygen species. *Int Microbiol*, **3**, 3–8.

- Callaway, E.** 2020. 'It will change everything': DeepMind's AI makes gigantic leap in solving protein structures. *Nature*, **588**, 203–204.
- Carpousis, A. J.** 2007. The RNA degradosome of *Escherichia coli*: an mRNA-degrading machine assembled on RNase E. *Annu Rev Microbiol*, **61**, 71–87.
- Cerullo, F., Filbeck, S., Patil, P. R., Hung, H.-C., Xu, H., Vornberger, J., et al.** 2022. Bacterial ribosome collision sensing by a MutS DNA repair ATPase paralogue. *Nature*, **603**, 509–514.
- Chadani, Y., Ito, K., Kutsukake, K., & Abo, T.** 2012. ArfA recruits release factor 2 to rescue stalled ribosomes by peptidyl-tRNA hydrolysis in *Escherichia coli*. *Mol Microbiol*, **86**, 37–50.
- Chao, T. C., Buhrmester, J., Hansmeier, N., Pühler, A., & Weidner, S.** 2005. Role of the regulatory gene *rirA* in the transcriptional response of *Sinorhizobium meliloti* to iron limitation. *Appl Environ Microbiol*, **71**, 5969–5982.
- Chen, H., Wu, R., Xu, G., Fang, X., Qiu, X., Guo, H., et al.** 2010. DR2539 is a novel DtxR-like regulator of Mn/Fe ion homeostasis and antioxidant enzyme in *Deinococcus radiodurans*. *Biochem Biophys Res Commun*, **396**, 413–418.
- Chopra, I., & Roberts, M.** 2001. Tetracycline antibiotics: mode of action, applications, molecular biology, and epidemiology of bacterial resistance. *Microbiol. Mol. Biol. Rev*, **65**, 232–260.
- Commichau, F. M., Rothe, F. M., Herzberg, C., Wagner, E., Hellwig, D., Lehnik-Habrink, M. et al.** 2009. Novel activities of glycolytic enzymes in *Bacillus subtilis*. *MCP*, **8**, 1350–1360.
- Commichau, F. M., Blötz, C., & Stülke, J.** 2015. Methods in molecular biology of bacteria. *Method Collection*.
- Connelly, B. M., Young, G. M., & Sloma, A.** 2004. Extracellular proteolytic activity plays a central role in swarming motility in *Bacillus subtilis*. *J Bacteriol*, **186**, 4159–4167.
- Conter, C., Oppici, E., Dindo, M., Rossi, L., Magnani, M., & Cellini, B.** 2019. Biochemical properties and oxalate-degrading activity of oxalate decarboxylase from *Bacillus subtilis* at neutral pH. *IUBMB Life*, **71**, 917–927.
- Conway, T.** 1992. The Entner-Doudoroff pathway: history, physiology and molecular biology. *FEMS Microbiol Lett*, **103**, 1–27.
- Cornish-Bowden, A., & Cardenas, M. L.** 1993. Channelling can affect concentrations of metabolic intermediates at constant net flux: artefact or reality? *Eur J Biochem*, **213**, 87–92.
- Cui, W., Han, L., Suo, F., Liu, Z., Zhou, L., & Zhou, Z.** 2018. Exploitation of *Bacillus subtilis* as a robust workhorse for production of heterologous proteins and beyond. *World J Microbiol Biotechnol*, **34**, 145.
- Dahl, H. H., Hunt, S. M., Hutchison, W. M., & Brown, G. K.** 1987. The human pyruvate dehydrogenase complex. Isolation of cDNA clones for the E1 alpha subunit, sequence analysis, and characterization of the mRNA. *JBC*, **262**, 7398–7403.

- Dammel, C S, & Noller, H. F.** 1995. Suppression of a cold-sensitive mutation in 16S rRNA by overexpression of a novel ribosome-binding factor, RbfA. *Genes Dev*, **9**, 626–637.
- Dandekar, T., Schuster, S., Snel, B., Huynen, M., & Bork, P.** 1999. Pathway alignment: application to the comparative analysis of glycolytic enzymes. *Biochem J*, **343**, 115-124.
- de Kok, A., Hengeveld, A. F., Martin, A., & Westphal, A. H.** 1998. The pyruvate dehydrogenase multi-enzyme complex from Gram-negative bacteria. *BBA Protein Struc Mol Enzym*, **1385**, 353–366.
- Deinert, K., Fasiolo, F., Hurt, E. C., & Simos, G.** 2001. Arc1p organizes the yeast aminoacyl-tRNA synthetase complex and stabilizes its interaction with the cognate tRNAs. *JBC*, **276**, 6000–6008.
- Deng, M., Zhang, K., Mehta, S., Chen, T., & Sun, F.** 2003. Prediction of protein function using protein–protein interaction data. *J Comput Biol*, **10**, 947–960.
- Deutscher, J., Aké, F. M. D., Derkaoui, M., Zébré, A. C., Cao, T. N., Bouraoui, H., et al.** 2014. The bacterial phosphoenolpyruvate:carbohydrate phosphotransferase system: regulation by protein phosphorylation and phosphorylation-dependent protein-protein interactions. *Microbiol Mol Biol Rev*, **78**, 231–256.
- Deutscher, J., Küster, E., Bergstedt, U., Charrier, V., & Hillen, W.** 1995. Protein kinase-dependent HPr/CcpA interaction links glycolytic activity to carbon catabolite repression in Gram-positive bacteria. *Mol Microbiol*, **15**, 1049–1053.
- Díaz-Mireles, E., Wexler, M., Todd, J. D., Bellini, D., Johnston, A. W. B., & Sawers, R. G.** 2005. The manganese-responsive repressor Mur of *Rhizobium leguminosarum* is a member of the Fur-superfamily that recognizes an unusual operator sequence. *Microbiology*, **151**, 4071–4078.
- Doan, T., Servant, P., Tojo, S., Yamaguchi, H., Lerondel, G., Yoshida, K.-I., et al.** 2003. The *Bacillus subtilis* ywA gene encodes a malic enzyme and its transcription is activated by the YufL/YufM two-component system in response to malate. *Microbiology*, **149**, 2331–2343.
- Döring, V., Mootz, H. D., Nangle, L. A., Hendrickson, T. L., de Crécy-Lagard, V., Schimmel, P., & Marlière, P.** 2001. Enlarging the amino acid set of *Escherichia coli* by infiltration of the valine coding pathway. *Science*, **292**, 501–504.
- Eilers, H.** 2010. Transcription in *Mycoplasma pneumoniae*. *Dissertation*.
- Erni, B.** 2013. The bacterial phosphoenolpyruvate: sugar phosphotransferase system (PTS): an interface between energy and signal transduction. *J Iran Chem Soc*, **10**, 593–630.
- Evans, R., O'Neill, M., Pritzel, A., Antropova, N., Senior, A., Green, T., et al.** 2022. Protein complex prediction with AlphaFold-Multimer. *BioRxiv*. 2021.10.04.463034
- Eymann, C., Dreisbach, A., Albrecht, D., Bernhardt, J., Becher, D., Gentner, S., et al.** 2004. A comprehensive proteome map of growing *Bacillus subtilis* cells. *Proteomics*, **4**, 2849–2876.

- Eymann, C., Homuth, G., Scharf, C., & Hecker, M.** 2002. *Bacillus subtilis* functional genomics: global characterization of the stringent response by proteome and transcriptome analysis. *J Bacteriol*, **184**, 2500–2520.
- Faßhauer, P.** 2021. Functions of the Cold Shock Proteins in *Bacillus Subtilis*. *Dissertation*.
- Fioulaine, S., Morera, S., Poncet, S., Mijakovic, I., Galinier, A., Janin, J., et al.** 2002. X-ray structure of a bifunctional protein kinase in complex with its protein substrate HPr. *PNAS*, **99**, 13437–13441.
- Fillinger, S., Boschi-Muller, S., Azza, S., Dervyn, E., Branlant, G., & Aymerich, S.** 2000. Two glyceraldehyde-3-phosphate dehydrogenases with opposite physiological roles in a nonphotosynthetic bacterium. *JBC*, **275**, 14031–14037.
- Finn, R. D., Clements, J., & Eddy, S. R.** 2011. HMMER web server: interactive sequence similarity searching. *Nucleic Acids Res*, **39**, 29–37.
- Fontecave, M., Covès, J., & Pierre, J. L.** 1994. Ferric reductases or flavin reductases? *Biometals*, **7**, 3-8.
- Fournier, G. P., & Gogarten, J. P.** 2010. Rooting the ribosomal tree of life. *Mol Biol Evol*, **27**, 1792–1801.
- Frunzke, J., Gätgens, C., Brocker, M., & Bott, M.** 2011. Control of heme homeostasis in *Corynebacterium glutamicum* by the two-component system HrrSA. *J Bacteriol*, **193**, 1212–1221.
- Fuchs, T M, Deppisch, H., Scarlato, V., & Gross, R.** 1996. A new gene locus of *Bordetella pertussis* defines a novel family of prokaryotic transcriptional accessory proteins. *J Bacteriol*, **178**, 4445–4452.
- Fujita, Y.** 2009. Carbon catabolite control of the metabolic network in *Bacillus subtilis*. *Biosci Biotechnol Biochem*, **73**, 245–259.
- Gaballa, A., Antelmann, H., Aguilar, C., Khakh, S. K., Song, K.-B., Smaldone, G. T., & Helmann, J. D.** 2008. The *Bacillus subtilis* iron-sparing response is mediated by a Fur-regulated small RNA and three small, basic proteins. *PNAS*, **105**, 11927–11932.
- Gaballa, A., & Helmann, J. D.** 1998. Identification of a zinc-specific metalloregulatory protein, Zur, controlling zinc transport operons in *Bacillus subtilis*. *J Bacteriol*, **180**, 5815–5821.
- Gaballa, A., & Helmann, J. D.** 2002. A peroxide-induced zinc uptake system plays an important role in protection against oxidative stress in *Bacillus subtilis*. *Mol Microbiol*, **45**, 997–1005.
- Gaines, C. G., Lodge, J. S., Arceneaux, J. E., & Byers, B. R.** 1981. Ferrisiderophore reductase activity associated with an aromatic biosynthetic enzyme complex in *Bacillus subtilis*. *J Bacteriol*, **148**, 527–533.

- Galperin, M. Y., Wolf, Y. I., Garushyants, S. K., Vera Alvarez, R., & Koonin, E. V.** 2021. Nonessential ribosomal proteins in bacteria and archaea identified using clusters of orthologous genes. *J Bacteriol*, **203**, e00058-21.
- Gill, S. C., Weitzel, S. E., & von Hippel, P. H.** 1991. *Escherichia coli*  $\sigma$ 70 and NusA proteins. *J Mol Biol*, **220**, 307–324.
- Gimpel, M., & Brantl, S.** 2016. Dual-function sRNA encoded peptide SR1P modulates moonlighting activity of *B. subtilis* GapA. *RNA Biol*, **13**, 916–926.
- Görke, B., & Stülke, J.** 2008. Carbon catabolite repression in bacteria: many ways to make the most out of nutrients. *Nat Rev Microbiol*, **6**, 613–624.
- Green, M. R., & Sambrook, J.** 2016. Preparation of plasmid DNA by alkaline lysis with sodium dodecyl sulfate: Minipreps. *Cold Spring Harb Protoc*,
- Griffith, L. J., Ostrander, W. E., Mullins, C. G., & Beswick, D. E.** 1965. Drug antagonism between lincomycin and erythromycin. *Science*, **147**, 746–747.
- Guay, G. G., Tuckman, M., & Rothstein, D. M.** 1994. Mutations in the *tetA(B)* gene that cause a change in substrate specificity of the tetracycline efflux pump. *Antimicrob Agents Chemother*, **38**, 857–860.
- Gudi, Ramavedi, Melissa, M. B.-K., Kedishvili, N. Y., Zhao, Y., & Popov, K. M.** 1995. Diversity of the pyruvate dehydrogenase kinase gene family in humans. *JBC*, **270**, 28989–28994.
- Guérout-Fleury, A.-M., Shazand, K., Frandsen, N., & Stragier, P.** 1995. Antibiotic-resistance cassettes for *Bacillus subtilis*. *Gene*, **167**, 335–336.
- Guo, M., Chong, Y. E., Shapiro, R., Beebe, K., Yang, X.-L., & Schimmel, P.** 2009. Paradox of mistranslation of serine for alanine caused by AlaRS recognition dilemma. *Nature*, **462**, 808–812.
- Haikarainen, T., & Papageorgiou, A. C.** 2010. Dps-like proteins: structural and functional insights into a versatile protein family. *CLMS*, **67**, 341–351.
- Hamon, M. A., & Lazazzera, B. A.** 2002. The sporulation transcription factor Spo0A is required for biofilm development in *Bacillus subtilis*. *Mol Microbiol*, **42**, 1199–1209.
- Hanington, P. C., Barreda, D. R., & Belosevic, M.** 2006. A novel hematopoietic granulins induces proliferation of goldfish (*Carassius auratus L.*) macrophages. *JBC*, **281**, 9963–9970.
- Harada, N., Maemura, K., Yamasaki, N., & Kimura, M.** 1998. Identification by site-directed mutagenesis of amino acid residues in ribosomal protein L2 that are essential for binding to 23S ribosomal RNA. *Biochim Biophys Acta Prot Struct Mol Enzym*, **1429**, 176–186.
- Harris, R. A., Huang, B., & Wu, P.** 2001. Control of pyruvate dehydrogenase kinase gene expression. *Adv Enzyme Regul*, **41**, 269–288.

- Henrichsen, J.** 1972. Bacterial surface translocation: a survey and a classification. *Bacteriol Rev*, **36**, 478–503.
- Herzberg, C., Weidinger, L. A. F., Dörrbecker, B., Hübner, S., Stülke, J., & Commichau, F. M.** 2007. SPINE: A method for the rapid detection and analysis of protein-protein interactions *in vivo*. *Proteomics*, **7**, 4032–4035.
- Hu, M., Nandi, S., Davies, C., & Nicholas, R. A.** 2005. High-level chromosomally mediated tetracycline resistance in *Neisseria gonorrhoeae* results from a point mutation in the *rpsJ* gene encoding ribosomal protein S10 in combination with the *mtrR* and *penB* resistance determinants. *Antimicrob Agents Chemother*, **49**, 4327–4334.
- Imlay, J. A.** 2003. Pathways of oxidative damage. *Annu Rev Microbiol*, **57**, 395–418.
- Imlay, J. A.** 2013. The molecular mechanisms and physiological consequences of oxidative stress: lessons from a model bacterium. *Nat Rev Microbiol*, **11**, 443–454.
- Issaly, I. M., & Issaly, A. S.** 1974. Control of ornithine carbamoyltransferase activity by arginase in *Bacillus subtilis*. *Eur J Biochem*, **49**, 485–495.
- Jayaraman, V., Lee, D. J., Elad, N., Vimer, S., Sharon, M., Fraser, J. S., & Tawfik, D. S.** 2022. A counter-enzyme complex regulates glutamate metabolism in *Bacillus subtilis*. *Nat Chem Biol*, **18**, 161–170.
- Jayasinghe, O. T., Mandell, Z. F., Yakhnin, A. v., Kashlev, M., & Babitzke, P.** 2022. Transcriptome-wide effects of NusA on RNA Polymerase pausing in *Bacillus subtilis*. *J Bacteriol*, **204**, e00534-21.
- Jones, P. G., & Inouye, M.** 1996. RbfA, a 30S ribosomal binding factor, is a cold-shock protein whose absence triggers the cold-shock response. *Mol Microbiol*, **21**, 1207–1218.
- Jourlin-Castelli, C., Mani, N., Nakano, M. M., & Sonenshein, A. L.** 2000. CcpC, a novel regulator of the LysR family required for glucose repression of the *citB* gene in *Bacillus subtilis*. *J Mol Biol*, **295**, 865–878.
- Julkowska, D., Obuchowski, M., Holland, I. B., & Séror, Simone. J.** 2005. Comparative analysis of the development of swarming communities of *Bacillus subtilis* 168 and a natural wild type: critical effects of surfactin and the composition of the medium. *J Bacteriol*, **187**, 65–76.
- Jumper, J., Evans, R., Pritzel, A., Green, T., Figurnov, M., Ronneberger, O., et al.** 2021. Highly accurate protein structure prediction with AlphaFold. *Nature*, **596**, 583–589.
- Just, V. J., Stevenson, C. E. M., Bowater, L., Tanner, A., Lawson, D. M., & Bornemann, S.** 2004. A closed conformation of *Bacillus subtilis* oxalate decarboxylase OxdC provides evidence for the true identity of the active site. *JBC*, **279**, 19867–19874.
- Karimova, G., Pidoux, J., Ullmann, A., & Ladant, D.** 1998. A bacterial two-hybrid system based on a reconstituted signal transduction pathway. *PSNA*, **95**, 5752–5756.

- Karzai, A. W., Roche, E. D., & Sauer, R. T. 2000. The SsrA–SmpB system for protein tagging, directed degradation and ribosome rescue. *Nat Struct Biol*, **7**, 449–455.
- Kearns, D. B., Chu, F., Rudner, R., & Losick, R. 2004. Genes governing swarming in *Bacillus subtilis* and evidence for a phase variation mechanism controlling surface motility. *Mol Microbiol*, **52**, 357–369.
- Keiler, K. C., Waller, P. R. H., & Sauer, R. T. 1996. Role of a peptide tagging system in degradation of proteins synthesized from damaged messenger RNA. *Science*, **271**, 990–993.
- Kiersztyn, B., Siuda, W., & Chróst, R. 2017. Coomassie Blue G250 for visualization of active bacteria from lake environment and culture. *Pol J Microbiol*, **66**, 365–373.
- Kim, H. J., Kim, S. I., Ratnayake-Lecamwasam, M., Tachikawa, K., Sonenshein, A. L., & Strauch, M. 2003. Complex regulation of the *Bacillus subtilis* aconitase gene. *J Bacteriol*, **185**, 1672–1680.
- Kim, H. J., Roux, A., & Sonenshein, A. L. 2002. Direct and indirect roles of CcpA in regulation of *Bacillus subtilis* Krebs cycle genes. *Mol Microbiol*, **45**, 179–190.
- Kleiblova, P., Shaltiel, I. A., Benada, J., Sevcík, J., Pecháčková, S., Pohlreich, P., *et al.* 2013. Gain-of-function mutations of PPM1D/Wip1 impair the p53-dependent G1 checkpoint. *J Cell Biol*, **201**, 511–521.
- Kleijn, R. J., Buescher, J. M., le Chat, L., Jules, M., Aymerich, S., & Sauer, U. 2010. Metabolic fluxes during strong carbon catabolite repression by malate in *Bacillus subtilis*. *JBC*, **285**, 1587–1596.
- Klewing, A. 2019. *MiniBacillus* - the construction of a minimal organism. *Dissertation*.
- Kobayashi, K., & Iwano, M. 2012. BslA(YuaB) forms a hydrophobic layer on the surface of *Bacillus subtilis* biofilms. *Mol Microbiol*, **85**, 51–66.
- Korotchkina, L. G., & Patel, M. S. 2001. Probing the mechanism of inactivation of human pyruvate dehydrogenase by phosphorylation of three sites. *JBC*, **276**, 5731–5738.
- Krüger, L., Herzberg, C., Wicke, D., Bähre, H., Heidemann, J. L., Dickmanns, A., *et al.* 2021. A meet-up of two second messengers: the c-di-AMP receptor DarB controls (p)ppGpp synthesis in *Bacillus subtilis*. *Nat Commun*, **12**, 1210.
- Krüger, L., Herzberg, C., Wicke, D., Scholz, P., Schmitt, K., Turdiev, A., *et al.* 2022. Sustained control of pyruvate carboxylase by the essential second messenger cyclic di-AMP in *Bacillus subtilis*. *MBio*, **13**, e03602-21.
- Kunst, F., Ogasawara, N., Moszer, I., Albertini, A. M., Alloni, G., Azevedo, V., *et al.* 1997. The complete genome sequence of the Gram-positive bacterium *Bacillus subtilis*. *Nature*, **390**, 249–256.

- Laemmli, U. K.** 1970. Cleavage of structural proteins during the assembly of the head of bacteriophage T4. *Nature*, **227**, 680–685.
- Lauber, M. A., Rappsilber, J., & Reilly, J. P.** 2012. Dynamics of ribosomal protein S1 on a bacterial ribosome with cross-linking and mass spectrometry. *MCP*, **11**, 1965–1976.
- Lauber, M. A., Running, W. E., & Reilly, J. P.** 2009. *B. subtilis* ribosomal proteins: structural homology and post-translational modifications. *J Proteome Res*, **8**, 4193–4206.
- Lee, J.-W., & Helmann, J. D.** 2007. Functional specialization within the Fur family of metalloregulators. *BioMetals*, **20**, 485–499.
- Lehnik-Habrink, M., Pförtner, H., Rempeters, L., Pietack, N., Herzberg, C., & Stülke, J.** 2010. The RNA degradosome in *Bacillus subtilis*: Identification of CshA as the major RNA helicase in the multiprotein complex. *Mol Microbiol*, **77**, 958–971.
- Licht, A., Preis, S., & Brantl, S.** 2005. Implication of CcpN in the regulation of a novel untranslated RNA (SR1) in *Bacillus subtilis*. *Mol Microbiol*, **58**, 189–206.
- Liu, M., Durfee, T., Cabrera, J. E., Zhao, K., Jin, D. J., & Blattner, F. R.** 2005. Global transcriptional programs reveal a carbon source foraging strategy by *Escherichia coli*. *JBC*, **280**, 15921–15927.
- Lodge, J. S., Gaines, C. G., Arceneaux, J. E. L., & Byers, B. R.** 1980. Non-hydrolytic release of iron from ferrienterobactin analogs by extracts of *Bacillus subtilis*. *Biochem Biophys Res Commun*, **97**, 1291–1295.
- Loveland, A. B., & Korostelev, A. A.** 2018. Structural dynamics of protein S1 on the 70S ribosome visualized by ensemble cryo-EM. *Methods*, **137**, 55–66.
- Lu, J., & Deutsch, C.** 2008. Electrostatics in the ribosomal tunnel modulate chain elongation rates. *J Mol Biol*, **384**, 73–86.
- Luo, H., Zhou, D., Liu, X., Nie, Z., Quiroga-Sánchez, D. L., & Chang, Y.** 2016. Production of 3-hydroxypropionic acid *via* the propionyl-CoA pathway using recombinant *Escherichia coli* strains. *PLoS One*, **11**, e0156286.
- Lupien, A., Gingras, H., Leprohon, P., & Ouellette, M.** 2015. Induced tigecycline resistance in *Streptococcus pneumoniae* mutants reveals mutations in ribosomal proteins and rRNA. *J Antimicrob Chemother*, **70**, 2973–2980.
- Ma, Z., Faulkner, M. J., & Helmann, J. D.** 2012. Origins of specificity and cross-talk in metal ion sensing by *Bacillus subtilis* Fur. *Mol Microbiol*, **86**, 1144–1155.
- Marchand, I., Damier-Piolle, L., Courvalin, P., & Lambert, T.** 2004. Expression of the RND-Type efflux pump AdeABC in *Acinetobacter baumannii* is regulated by the AdeRS two-component system. *Antimicrob Agents Chemother*, **48**, 3298–3304.



- Martin-Verstraete, I., Débarbouillé, M., Klier, A., & Rapoport, G.** 1992. Mutagenesis of the *Bacillus subtilis* “-12, -24” promoter of the levanase operon and evidence for the existence of an upstream activating sequence. *J Mol Biol*, **226**, 85–99.
- McCutcheon, J. P., & Moran, N. A.** 2012. Extreme genome reduction in symbiotic bacteria. *Nat Rev Microbiol*, **10**, 13–26.
- McKay, T., Hart, K., Horn, A., Kessler, H., Dodge, G., Bardhi, K., et al.** 2015. Annotation of proteins of unknown function: initial enzyme results. *J Struct Funct Genomics*, **16**, 43–54.
- McLoon, A. L., Guttenplan, S. B., Kearns, D. B., Kolter, R., & Losick, R.** 2011. Tracing the domestication of a biofilm-forming bacterium. *J Bacteriol*, **193**, 2027–2034.
- Mehne, F.** 2014. Bildung und Homöostase von c-di-AMP in *Bacillus subtilis*. *Dissertation*.
- Meyer, F.** 2012. Regulatory interactions of enzymes of the citric acid cycle in *Bacillus subtilis*. *Dissertation*.
- Meyer, F. M., Gerwig, J., Hammer, E., Herzberg, C., Commichau, F. M., Völker, U., & Stülke, J.** 2011. Physical interactions between tricarboxylic acid cycle enzymes in *Bacillus subtilis*: Evidence for a metabolon. *Metab Eng*, **13**, 18–27.
- Michalik, S., Reder, A., Richts, B., Faßhauer, P., Mäder, U., Pedreira, T., et al.** 2021. The *Bacillus subtilis* minimal genome compendium. *ACS Synth Biol*, **10**, 2767–2771.
- Michels, P. A. M., Bringaud, F., Herman, M., & Hannaert, V.** 2006. Metabolic functions of glycosomes in trypanosomatids. *Biochim Biophys Acta Mol Cell Res*, **1763**, 1463–1477.
- Michna, R. H., Zhu, B., Mäder, U., & Stülke, J.** 2016. SubtiWiki 2.0—an integrated database for the model organism *Bacillus subtilis*. *Nucleic Acids Res*, **44**, 654–662.
- Miethke, M., Monteferrante, C. G., Marahiel, M. A., & van Dijk, J. M.** 2013. The *Bacillus subtilis* EfeUOB transporter is essential for high-affinity acquisition of ferrous and ferric iron. *Biochim Biophys Acta Mo Cell Res*, **1833**, 2267–2278.
- Mittal, M., Pechter, K. B., Picossi, S., Kim, H.-J., Kerstein, K. O., & Sonenshein, A. L.** 2013. Dual role of CcpC protein in regulation of aconitase gene expression in *Listeria monocytogenes* and *Bacillus subtilis*. *Microbiology*, **159**, 68–76.
- Miwa, Y., Saikawa, M., & Fujita, Y.** 1994. Possible function and some properties of the CcpA protein of *Bacillus subtilis*. *Microbiology*, **140**, 2567–2575.
- Mondal, S., Yakhnin, A. v., & Babitzke, P.** 2017. Modular organization of the NusA- and NusG-stimulated RNA polymerase pause signal that participates in the *Bacillus subtilis* *trp* operon attenuation mechanism. *J Bacteriol*, **199**, e00223-17 .
- Monod, J.** 1942. Recherches sur la croissance des cultures bactériennes. *Ann. Inst. Pasteur*, **69**

- Müller, C., Crowe-McAuliffe, C., & Wilson, D. N. 2021. Ribosome rescue pathways in bacteria. *Front Microbiol*, **12**, 652980.
- Nadezhdin, E. V., Brody, M. S., & Price, C. W. 2011. An  $\alpha/\beta$  Hydrolase and associated Per-ARNT-Sim domain comprise a bipartite sensing module coupled with diverse output domains. *PLoS One*, **6**, e25418.
- Nanamiya, H., Akanuma, G., Natori, Y., Murayama, R., Kosono, S., Kudo, T., *et al.* 2008. Zinc is a key factor in controlling alternation of two types of L31 protein in the *Bacillus subtilis* ribosome. *Mol Microbiol*, **52**, 273–283.
- Natori, Y., Nanamiya, H., Akanuma, G., Kosono, S., Kudo, T., Ochi, K., & Kawamura, F. 2007. A fail-safe system for the ribosome under zinc-limiting conditions in *Bacillus subtilis*. *Mol Microbiol*, **63**, 294–307.
- Neveling, U., Bringer-Meyer, S., & Sahm, H. 1998. Gene and subunit organization of bacterial pyruvate dehydrogenase complexes. *Biochim Biophys Acta Prot Struct Mol Enzym*, **1385**, 367–372.
- Nicolas, P., Mäder, U., Dervyn, E., Rochat, T., Leduc, A., Pigeonneau, N., *et al.* 2012. Condition-dependent transcriptome reveals high-level regulatory architecture in *Bacillus subtilis*. *Science*, **335**, 1103–1106.
- Nissen, Poul, Hansen, J., Ban, N., Moore, P. B., & Steitz, T. A. 2000. The structural basis of ribosome activity in peptide bond synthesis. *Science*, **289**, 920–930.
- Nooren, I. M.A. 2003. Diversity of protein-protein interactions. *EMBO J*, **22**, 3486–3492.
- Ollinger, J., Song, K.-B., Antelmann, H., Hecker, M., & Helmann, J. D. 2006. Role of the Fur regulon in iron transport in *Bacillus subtilis*. *J Bacteriol*, **188**, 3664–3673.
- O'Reilly, F. J., Graziadei, A., Forbrig, C., Bremenkamp, R., Charles, K., Lenz, S., *et al.* 2022. Protein complexes in *Bacillus subtilis* by AI-assisted structural proteomics. *BioRxiv*, 2022.07.26.501605
- Patel, M.S., & Korotchkina, L. G. 2006. Regulation of the pyruvate dehydrogenase complex. *Biochem Soc Trans*, **34**, 217.
- Patel, M. S., Nemeria, N. S., Furey, W., & Jordan, F. 2014. The pyruvate dehydrogenase complexes: structure-based function and regulation. *JBC*, **289**, 16615–16623.
- Patel, Mulchand S., & Roche, T. E. 1990. Molecular biology and biochemistry of pyruvate dehydrogenase complexes. *The FASEB Journal*, **4**, 3224–3233.
- Patrick, J. E., & Kearns, D. B. 2009. Laboratory strains of *Bacillus subtilis* do not exhibit swarming motility. *J Bacteriol*, **191**, 7129–7133.
- Pechter, K. B., Meyer, F. M., Serio, A. W., Stülke, J., & Sonenshein, A. L. 2013. Two roles for aconitase in the regulation of tricarboxylic acid branch gene expression in *Bacillus subtilis*. *J Bacteriol*, **195**, 1525–1537.

- Pedreira, T., Eifmann, C., & Stülke, J.** 2022. The current state of *SubtiWiki*, the database for the model organism *Bacillus subtilis*. *Nucleic Acids Res*, **50**, 875–882.
- Perham, R. N.** 1991. Domains, motifs, and linkers in 2-oxo acid dehydrogenase multienzyme complexes: a paradigm in the design of a multifunctional protein. *Biochemistry*, **30**, 8501–8512.
- Peters, J. M., Colavin, A., Shi, H., Czarny, T. L., Larson, M. H., Wong, S., et al.** 2016. A comprehensive, CRISPR-based functional analysis of essential genes in bacteria. *Cell*, **165**, 1493–1506.
- Pi, H., & Helmann, J. D.** 2017a. Ferrous iron efflux systems in bacteria. *Metallomics*, **9**, 840–851.
- Pi, H., & Helmann, J. D.** 2017b. Sequential induction of Fur-regulated genes in response to iron limitation in *Bacillus subtilis*. *PNAS*, **114**, 12785–12790.
- Pinochet-Barros, A., & Helmann, J. D.** 2018. Redox sensing by Fe<sup>2+</sup> in bacterial Fur family metalloregulators. *Antioxid Redox Signal*, **29**, 1858–1871.
- Pinochet-Barros, A., & Helmann, J. D.** 2020. *Bacillus subtilis* Fur Is a transcriptional activator for the PerR-repressed *pfeT* gene, encoding an iron efflux pump. *J Bacteriol*, **202**, e00697-19.
- Pohl, E., Haller, J. C., Mijovilovich, A., Meyer-Klaucke, W., Garman, E., & Vasil, M. L.** 2003. Architecture of a protein central to iron homeostasis: crystal structure and spectroscopic analysis of the ferric uptake regulator. *Mol Microbiol*, **47**, 903–915.
- Poncet, S., Mijakovic, I., Nessler, S., Gueguen-Chaignon, V., Chaptal, V., Galinier, A., et al.** 2004. HPr kinase/phosphorylase, a Walker motif A-containing bifunctional sensor enzyme controlling catabolite repression in Gram-positive bacteria. *Biochim Biophys Acta Proteins Proteom*, **1697**, 123–135.
- Qu, X., Lancaster, L., Noller, H. F., Bustamante, C., & Tinoco, I.** 2012. Ribosomal protein S1 unwinds double-stranded RNA in multiple steps. *PNAS*, **109**, 14458–14463.
- Quail, M. A., & Guest, J. R.** 1995. Purification, characterization and mode of action of PdhR, the transcriptional repressor of the *pdhR-aceEF-lpd* operon of *Escherichia coli*. *Mol Microbiol*, **15**, 519–529.
- Quail, M. A., Haydon, D. J., & Guest, J. R.** 1994. The *pdhR-aceEF-lpd* operon of *Escherichia coli* expresses the pyruvate dehydrogenase complex. *Mol Microbiol*, **12**, 95–104.
- Ray, B. K., & Apirion, D.** 1979. Characterization of 10S RNA: a new stable RNA molecule from *Escherichia coli*. *Mol Gen Genet*, **174**, 25–32.
- Redko, Y., Aubert, S., Stachowicz, A., Lenormand, P., Namane, A., Darfeuille, F., et al.** 2013. A minimal bacterial RNase J-based degradosome is associated with translating ribosomes. *Nucleic Acids Res*, **41**, 288–301.

- Reed, L. J., & Hackert, M. L.** 1990. Structure-function relationships in dihydrolipoamide acyltransferases. *JBC*, **265**, 8971–8974.
- Richts, B.** 2021. Vitamin B6 metabolism and underground metabolic routes in the Gram-positive bacterium *Bacillus subtilis*. *Dissertation*.
- Romero, D., Aguilar, C., Losick, R., & Kolter, R.** 2010. Amyloid fibres provide structural integrity to *Bacillus subtilis* biofilms. *PNAS*, **107**, 2230–2234.
- Ronneau, S., & Hallez, R.** 2019. Make and break the alarmone: regulation of (p)ppGpp synthetase/hydrolase enzymes in bacteria. *FEMS Microbiol Rev*, **43**, 389–400.
- Rowles, J., Scherer, S. W., Xi, T., Majer, M., Nickle, D. C., Rommens, J. M., et al.** 1996. Cloning and characterization of on 7q21.3 encoding a fourth pyruvate dehydrogenase kinase isoenzyme in human. *JBC*, **271**, 22376–22382.
- Sambrook, J., Fritsch, E. F., & Maniatis, T.** 1989. *Molecular cloning: a laboratory manual*, Cold Spring Harbor Laboratory, Cold Spring Harbor, NY
- Sanchez, S., Snider, E. v., Wang, X., & Kearns, D. B.** 2022. Identification of genes required for swarming motility in *Bacillus subtilis* using transposon mutagenesis and high-throughput sequencing (TnSeq). *J Bacteriol*, **204**, e0008922.
- Sanchez-Vizueté, P., le Coq, D., Bridier, A., Herry, J.-M., Aymerich, S., & Briandet, R.** 2015. Identification of *ypqP* as a new *Bacillus subtilis* biofilm determinant that mediates the protection of *Staphylococcus aureus* against antimicrobial agents in mixed-species communities. *Appl Environ Microbiol*, **81**, 109–118.
- Sanger, F., Nicklen, S., & Coulson, A. R.** 1977. DNA sequencing with chain-terminating inhibitors. *Proc Natl Acad Sci U S A*, **74**, 5463–5467.
- Sapunaric, F. M., & Levy, S. B.** 2005. Substitutions in the interdomain loop of the Tn10 TetA efflux transporter alter tetracycline resistance and substrate specificity. *Microbiology*, **151**, 2315–2322.
- Sauer, U., & Eikmanns, B. J.** 2005. The PEP—pyruvate—oxaloacetate node as the switch point for carbon flux distribution in bacteria. *FEMS Microbiol Rev*, **29**, 765–794.
- Schirmer, F., Ehrh, S., & Hillen, W.** 1997. Expression, inducer spectrum, domain structure, and function of MopR, the regulator of phenol degradation in *Acinetobacter calcoaceticus* NCIB8250. *J Bacteriol*, **179**, 1329–1336.
- Schmalisch, M., Langbein, I., & Stülke, J.** 2002. The general stress protein Ctc of *Bacillus subtilis* is a ribosomal protein. *J Mol Microbiol Biotechnol*, **4**, 495–501.
- Schmidt, M. C., & Chamberlin, M. J.** 1987. NusA Protein of *Escherichia coli* is an efficient transcription termination factor for certain terminator sites. *J Mol Biol*, **195**, 809–818.

- Schmitt, M. P., Talley, B. G., & Holmes, R. K.** 1997. Characterization of lipoprotein IRP1 from *Corynebacterium diphtheriae*, which is regulated by the diphtheria toxin repressor (DtxR) and iron. *Infect Immun*, **65**, 5364–5367.
- Schröder, I., Johnson, E., & de Vries, S.** 2003. Microbial ferric iron reductases. *FEMS Microbiol Rev*, **27**, 427–447.
- Schumacher, M. A., Seidel, G., Hillen, W., & Brennan, R. G.** 2007. Structural mechanism for the fine-tuning of CcpA function by the small molecule effectors glucose 6-phosphate and fructose 1,6-bisphosphate. *J Mol Biol*, **368**, 1042–1050.
- Sengupta, J., Agrawal, R. K., & Frank, J.** 2001. Visualization of protein S1 within the 30S ribosomal subunit and its interaction with messenger RNA. *PNAS*, **98**, 11991–11996.
- Serio, A. W., Pechter, K. B., & Sonenshein, A. L.** 2006. *Bacillus subtilis* aconitase Is required for efficient late-sporulation gene expression. *J Bacteriol*, **188**, 6396–6405.
- Servant, P., le Coq, D., & Aymerich, S.** 2005. CcpN (YqzB), a novel regulator for CcpA-independent catabolite repression of *Bacillus subtilis* gluconeogenic genes. *Mol Microbiol*, **55**, 1435–1451.
- Sharma, K., Sultana, T., Dahms, T. E. S., & Dillon, J. A. R.** 2020. CcpN: a moonlighting protein regulating catabolite repression of gluconeogenic genes in *Bacillus subtilis* also affects cell length and interacts with DivIVA. *Can J Microbiol*, **66**, 723–732.
- Shimokawa-Chiba, N., Müller, C., Fujiwara, K., Beckert, B., Ito, K., Wilson, D. N., & Chiba, S.** 2019. Release factor-dependent ribosome rescue by BrfA in the Gram-positive bacterium *Bacillus subtilis*. *Nat Commun*, **10**, 5397.
- Shoji, S., Dambacher, C. M., Shajani, Z., Williamson, J. R., & Schultz, P. G.** 2011. Systematic chromosomal deletion of bacterial ribosomal protein genes. *J Mol Biol*, **413**, 751–761.
- Simos, G., Segref, A., Fasiolo, F., Hellmuth, K., Shevchenko, A., Mann, M., & Hurt, E. C.** 1996. The yeast protein Arc1p binds to tRNA and functions as a cofactor for the methionyl- and glutamyl-tRNA synthetases. *EMBO J*, **15**, 5437–5448.
- Smaldone, G. T., Revelles, O., Gaballa, A., Sauer, U., Antelmann, H., & Helmann, J. D.** 2012. A global investigation of the *Bacillus subtilis* iron-sparing response identifies major changes in metabolism. *J Bacteriol*, **194**, 2594–2605.
- Sohmen, D., Chiba, S., Shimokawa-Chiba, N., Innis, C. A., Berninghausen, O., Beckmann, R., et al.** 2015. Structure of the *Bacillus subtilis* 70S ribosome reveals the basis for species-specific stalling. *Nat Commun*, **6**, 6941.
- Sonenshein, A. L.** 2007. Control of key metabolic intersections in *Bacillus subtilis*. *Nat Rev Microbiol*, **5**, 917–927.

- Speer, B. S., & Salyers, A. A.** 1988. Characterization of a novel tetracycline resistance that functions only in aerobically grown *Escherichia coli*. *J Bacteriol*, **170**, 1423–1429.
- Srinivasan, V. B., Venkataramaiah, M., Mondal, A., Vaidyanathan, V., Govil, T., & Rajamohan, G.** 2012. Functional characterization of a novel outer membrane porin KpnO, regulated by PhoBR two-component system in *Klebsiella pneumoniae* NTUH-K2044. *PLoS One*, **7**, e41505.
- Stickney, L. M., Hankins, J. S., Miao, X., & Mackie, G. A.** 2005. Function of the conserved S1 and KH domains in polynucleotide phosphorylase. *J Bacteriol*, **187**, 7214–7221.
- Stülke, J., & Hillen, W.** 2000. Regulation of carbon catabolism in *Bacillus* species. *Annu Rev Microbiol*, **54**, 849–880.
- Stülke, J., & Krüger, L.** 2020. Cyclic di-AMP signalling in bacteria. *Annu Rev Microbiol*, **74**, 159–179.
- Su, M., Li, Y., Ge, X., & Tian, P.** 2015. 3-Hydroxypropionaldehyde-specific aldehyde dehydrogenase from *Bacillus subtilis* catalyzes 3-hydroxypropionic acid production in *Klebsiella pneumoniae*. *Biotechnol Lett*, **37**, 717–724.
- Subramanian, A. R.** 1983. Structure and functions of ribosomal protein S1. *Prog Nucleic Acid Res Mol Biol*, **28**, 101–142.
- Suzuki, S., Tanigawa, O., Akanuma, G., Nanamiya, H., Kawamura, F., Tagami, K., et al.** 2014. Enhanced expression of *Bacillus subtilis* *yaaA* can restore both the growth and the sporulation defects caused by mutation of *rplB*, encoding ribosomal protein L2. *Microbiology*, **160**, 1040–1053.
- Takada, H., Crowe-McAuliffe, C., Polte, C., Sidorova, Z. Y., Murina, V., Atkinson, G. C., et al.** 2021. RqcH and RqcP catalyze processive poly-alanine synthesis in a reconstituted ribosome-associated quality control system. *Nucleic Acids Res*, **49**, 8355–8369.
- Touati, D., Jacques, M., Tardat, B., Bouchard, L., & Despied, S.** 1995. Lethal oxidative damage and mutagenesis are generated by iron in delta fur mutants of *Escherichia coli*: protective role of superoxide dismutase. *J Bacteriol*, **177**, 2305–2314.
- Tovar-Mendez, A., Miernyk, J. A., & Randall, D. D.** 2003. Regulation of pyruvate dehydrogenase complex activity in plant cells. *Eur J Biochem*, **270**, 1043–1049.
- Trieber, C. A., & Taylor, D. E.** 2002. Mutations in the 16S rRNA genes of *Helicobacter pylori* mediate resistance to tetracycline. *J Bacteriol*, **184**, 2131–2140.
- Tsai, Y.-C., Du, D., Domínguez-Malfavón, L., Dimastrogiovanni, D., Cross, J., Callaghan, A. J., et al.** 2012. Recognition of the 70S ribosome and polysome by the RNA degradosome in *Escherichia coli*. *Nucleic Acids Res*, **40**, 10417–10431.
- Uffen, R. L., & Canale-Parola, E.** 1972. Synthesis of pulcherriminic acid by *Bacillus subtilis*. *J Bacteriol*, **111**, 86–93.

- Ul Haq, I., Müller, P., & Brantl, S.** 2020. Intermolecular communication in *Bacillus subtilis*: RNA-RNA, RNA-protein and small protein-protein interactions. *Front Mol Biosci*, **7**, 178.
- Ul Haq, I., Müller, P., & Brantl, S.** 2021. SR7 – a dual-function antisense RNA from *Bacillus subtilis*. *RNA Biol*, **18**, 104–117.
- van Zundert, G. C. P., Trellet, M., Schaarschmidt, J., Kurkcuoglu, Z., David, M., Verlato, M., et al.** 2017. The DisVis and PowerFit web servers: explorative and integrative modelling of biomolecular complexes. *J Mol Biol*, **429**, 399–407.
- Vijay, K., Brody, M. S., Fredlund, E., & Price, C. W.** 2000. A PP2C phosphatase containing a PAS domain is required to convey signals of energy stress to the sigmaB transcription factor of *Bacillus subtilis*. *Mol Microbiol*, **35**, 180–188.
- Wang, S., Wang, H., Zhang, D., Li, X., Zhu, J., Zhan, Y., et al.** 2020. Multistep metabolic engineering of *Bacillus licheniformis* to improve pulcherriminic acid production. *Appl Environ Microbiol*, **86**.
- Wang, X., Bansal, S., Jiang, M., & Prestegard, J. H.** 2008. RDC-assisted modeling of symmetric protein homo-oligomers. *Protein Sci*, **17**, 899–907.
- Warner, J. B., & Lolkema, J. S.** 2002. Growth of *Bacillus subtilis* on citrate and isocitrate is supported by the Mg<sup>2+</sup>-citrate transporter CitM. *Microbiology*, **148**, 3405–3412.
- Weinrauch, Y., Msadek, T., Kunst, F., & Dubnau, D.** 1991. Sequence and properties of *comQ*, a new competence regulatory gene of *Bacillus subtilis*. *J Bacteriol*, **173**, 5685–5693.
- Wen, J. D., Lancaster, L., Hodges, C., Zeri, A. C., Yoshimura, S. H., Noller, H. F., et al.** 2008. Following translation by single ribosomes one codon at a time. *Nature*, **452**, 598–603.
- Wieland, O. H., Hartmann, U., & Siess, E. A.** 1972. *Neurospora crassa* pyruvate dehydrogenase: interconversion by phosphorylation and dephosphorylation. *FEBS Lett*, **27**, 240–244.
- Williams, G., & Smith, I.** 1979. Chromosomal mutations causing resistance to tetracycline in *Bacillus subtilis*. *Mol Gen Genet*, **177**, 23–29.
- Winkler, C., Denker, K., Wortelkamp, S., & Sickmann, A.** 2007. Silver- and Coomassie-staining protocols: detection limits and compatibility with ESI MS. *Electrophoresis*, **28**, 2095–2099.
- Wulf A.** 2022. Investigating chemical crosslinking of protein-RNA complexes by mass spectrometry. *Dissertation*.
- Xia, B., Ke, H., Shinde, U., & Inouye, M.** 2003. The role of RbfA in 16S rRNA processing and cell growth at low temperature in *Escherichia coli*. *J Mol Biol*, **332**, 575–584.
- Xu, L., Sedelnikova, S. E., Baker, P. J., Hunt, A., Errington, J., & Rice, D. W.** 2007. Crystal structure of *S. aureus* YlaN, an essential leucine rich protein involved in the control of cell shape. *Proteins: Struct Funct Genet*, **68**, 438–445.

- Yang, W., Moore, I. F., Koteva, K. P., Bareich, D. C., Hughes, D. W., & Wright, G. D.** 2004. TetX is a flavin-dependent monooxygenase conferring resistance to tetracycline antibiotics. *JBC*, **279**, 52346–52352.
- Yang, X., Molimau, S., Doherty, G. P., Johnston, E. B., Marles-Wright, J., Rothnagel, R., et al.** 2009. The structure of bacterial RNA polymerase in complex with the essential transcription elongation factor NusA. *EMBO Rep*, **10**, 997–1002.
- Yeaman, S. J., Hutcheson, E. T., Roche, T. E., Pettit, F. H., Brown, J. R., Reed, L. J., et al.** 1978. Sites of phosphorylation on pyruvate dehydrogenase from bovine kidney and heart. *Biochemistry*, **17**, 2364–2370.
- Yu, W., Hu, J., Yu, B., Xia, W., Jin, C., & Xia, B.** 2009. Solution structure of GSP13 from *Bacillus subtilis* exhibits an S1 domain related to cold shock proteins. *J Biomol NMR*, **43**, 255–259.
- Zhao, G., Ceci, P., Ilari, A., Giangiacomo, L., Laue, T. M., Chiancone, E., & Chasteen, N. D.** 2002. Iron and hydrogen peroxide detoxification properties of DNA-binding protein from starved cells. *JBC*, **277**, 27689–27696.



## 6. Appendix

### 6.1 Supplementary information

Table 6.1: Suppressor mutations found in  $\Delta ylaN$  strain when cultivated on standard SP or containing  $Fe^{2+}$

Mutation	SP	$Fe^{2+}$	Total Mutations
Ile8Cys	-	1 x	1
Arg23Cys	-	1 x	1
Tyr44Cys	4 x	3 x	7
Leu56Phe	1 x	2 x	3
Val59Leu	1 x	-	1
Val71Gly	-	1 x	1
Glu89Gly	1 x	-	1

## 6.2 Materials

### 6.2.1 Chemicals

Acrylamide	Roth, Karlsruhe
Agar	Roth, Karlsruhe
Agarose	Biozym Scientific GmbH, Hessisch Oldendorf
Antibiotics	Sigma-Aldrich, Munich
$\beta$ -Mercaptoethanol	Merck, Darmstadt
Bacto agar	Becton, Dickinson and Company, Heidelberg
Bromphenol blue	Serva, Heidelberg
CDP*	Roche Diagnostics, Mannheim
Coomassie Brilliant Blue, G250	Roth, Karlsruhe
Desthiobiotin	IBA, Göttingen
DMSO	Roth, Karlsruhe
dNTPs	Roche Diagnostics, Mannheim
DTT	Roth, Karlsruhe
Ethidium bromide	Roth, Karlsruhe

HDGreen™	Intas, Göttingen
Ni-NTA Agarose	Macherey-Nagel, Düren
N,N-Dimethylformamide	Sigma-Aldrich, Munich
Nutrient broth	Merck, Darmstadt
ONPG	AppliChem, Darmstadt
Skim milk powder, fat-free	Roth, Karlsruhe
Step-Tactin Sepharose	IBA, Göttingen
TEMED	Roth, Karlsruhe
Tween 20	Sigma-Aldrich, Munich
x-Gal	Preqlab, Erlangen
Yeast extract	Oxoid, Heidelberg

Further chemicals were purchased from Carl Roth, Merck, Peqlab or Sigma-Aldrich

### 6.2.2 Enzymes

DNase I	Roche Diagnostics, Mannheim
DreamTaq DNA Polymerase	ThermoFisher, Waltham, USA
FastAP	ThermoFisher, Waltham, USA
Lysozyme	Merck, Darmstadt
Restriction endonucleases	ThermoFisher, Waltham, USA
RNase A	Roche Diagnostics, Mannheim
RNase Inhibitor 40 U	Roche Diagnostics, Mannheim
S7 Fusion High-Fidelity DNA Polymerase	Biozym, Hessisch Oldendorf
T4-DNA ligase	Roche Diagnostics, Mannheim

### 6.2.3 Commercial systems

NucleoSpin Plasmid-Kit	Macherey-Nagel, Düren
PageRuler™ Plus Prestained Protein Ladder	ThermoFisher, Waltham, USA

peqGOLD Bacterial DNA Kit	PeqLab, Erlangen
QIAquick PCR purification kit	Quiagen, Düsseldorf

#### 6.2.4 Instruments / Equipment

Autoclave	Zirbus technology, Bad Grund
Biofuge fresco	Amersham, Freiburg
ChemoCam imager	Intas, Göttingen
Electronic scale	Sartorius, Göttingen
Frensh pressure cell	G. Heinemann, Schwäbisch Gmünd
Fiberlite F9 / F40 rotors	ThermoFisher, Waltham, USA
GelDoc™ XR+	Bio-Rad, München
Gel electrophoresis device	Waasetec, Göttingen
Hydro tech vacuum pump	Bio-Rad, Munich
Incubator Innova R44	New Brunswick, Neu-Isenburg
Incubator shaker Innova 2300	New Brunswick, Neu-Isenburg
LabCycler	LabCycler SensorQuest, Göttingen
Magnetic stirrer	JAK Werk, Staufen
Microplate reader SynergyMx Mini-Protean	BioTek, Bad Friedrichshall
Mikroprozessor pH-Meter 766 Calimatic	Knick, Berlin
Mini-Protean III System	Bio-Rad, Munich
Nanodrop ND-1000	ThermoFisher, Waltham, USA
Nitrocellulose membrane	Bio-Rad, Munich
Open air shaker Innova 2300	New Brunswick, Neu-Isenburg
Refrigerated centrifuge PrimoR	Heraeus Chris, Osterode
Scale Sartorius universal	Sartorius, Göttingen
SDS-PAGE glass plates	Bio-Rad, Munich
Special accuracy weighing machine	Sartorius, Göttingen
Spectral photometer Ultraspec 2000	Amersham, Freiburg

Stereo Lumar V12 stereo microscope	Carl Zeiss, Göttingen
Sterile bench Hera Safe	ThermoFisher, Waltham, USA
Thermocycler	Biometra, Göttingen
TS Sorvall WX ultraseries centrifuge	Beckmann Coulter, Krefeld
Ultra centrifuge, Sorvall Ultra Pro 80	ThermoFisher, Waltham, USA
UV Transilluminator 2000	Bio-Rad, Munich
Vortex	Bender and Hobein, Buchsal
Water desalination plant	Millipore, Schwalbach

### 6.2.5 Materials

96-well plates	Sarstedt, Nümbrecht
Centrifuge cups	Beckmann, Munich
Cuvettes (microliter, plastic)	Sarstedt, Nümbrecht
Dialysis tubes	Serva, Heidelberg
Falcon tubes (15 ml, 50 ml)	Sarstedt, Nümbrecht
Gene Amp Reaction tube (PCR)	Perkin Elmer, Weiterstadt
Glass pipettes	Brandt, Wertheim
Microlitre pipettes (2 $\mu$ l, 20 $\mu$ l, 200 $\mu$ l, 1 ml, 5 ml)	Eppendorf, Hamburg
Petri dishes	Greiner, Nürtingen
Pipette tips	Sarstedt, Nümbrecht
Polyvinylidendifluoride membrane (PVDF)	Bio-Rad, Munich
Reaction tubes	Greiner, Nürtingen
Single-use syringes	Becton Dickson, Drogheda, Ireland

### 6.2.6 Software and webpages

Program	Provider	Application
AlphaFold	Jumper <i>et al.</i> , 2021	Prediction of protein structures
AlphaFold Multimer	Evans <i>et al.</i> , 2022	Structural prediction of protein complexes
AxioVision	Zeiss	Microscopy imaging
BLAST NCBI	National institute of Health, USA	BLAST searches
ChemoStar Imager	Intas	Western blot imaging
Gen5™ Data Analysis Software	BioTek®	Plate reader analysis
Geneious Primer 2021.0.3	Biomatters	DNA analysis
ImageLab™ Software	BioRad	Geldoc imaging
Mendeley Desktop	PDFTron™ Systems Inc.	Reference manager
Microsoft Office 365	Microsoft Inc.	Data processing and writing
Pymol 2.0	Schrödinger LLC	Protein structure visualization
SubtiWiki 4.0	Pedreira <i>et al.</i> , 2022	B. subtilis database

## 6.3 Bacterial strains

### 6.3.1 *E. coli* strains

Name	Genotype	Reference / Construction
<b>DH5α</b>	<i>recA1 endA1 gyrA96 thi hsdR17rk- mk<sup>+</sup>relA1 supE44</i> <i>Φ80ΔlacZΔM15 Δ(lacZYA-argF)U169</i>	Sambrook <i>et al.</i> , 1989
<b>Rosetta (DE3)</b>	<i>F<sup>-</sup> ompT hsdS<sub>B</sub>(r<sub>B</sub><sup>-</sup> m<sub>B</sub><sup>-</sup>) gal dcm (DE3) pRARE (cat)</i>	Novagen
<b>BTH101</b>	<i>F<sup>-</sup> cya99 araD139 galE15 galK16 rpsL1 (Str<sup>R</sup>) hsdR2</i> <i>mcrA1 mcrB1</i>	Karimova <i>et al.</i> , 1998

6.3.2 *B. subtilis* strains

Name	Genotype	Construction / Reference
168	<i>trpC2</i>	Laboratory collection
GP879	<i>trpC2</i> $\Delta$ <i>fur::mls</i>	Eilers, 2010
GP3597	<i>trpC2</i> $\Delta$ <i>yugl::cat</i>	LFH $\rightarrow$ 168 (J. Meißner)
GP3598	<i>trpC2</i> $\Delta$ <i>yabR::aphA3</i>	LFH $\rightarrow$ 168 (J. Meißner)
GP3930	<i>trpC2</i> <i>rocF</i> 3x FLAG <i>phleo</i>	LFH $\rightarrow$ 168 (R. Warneke)

## 6.2.3 Strains constructed in this work

Name	Genotype	Construction
GP3694	<i>trpC2</i> $\Delta$ <i>yugl::cat</i> $\Delta$ <i>yabR::aphA3</i>	GP3598 $\rightarrow$ GP3597
GP3700	<i>trpC</i> <i>yugl-FLAG</i> 3x <i>spc</i>	pGP3527 $\rightarrow$ 168
GP3307	<i>trpC2</i> <i>rsbP</i> <sub>D393G</sub> <i>yabR::aphA3</i>	Selection of suppressors on MSSM KCl 0,1
GP3308	<i>trpC2</i> $\Delta$ <i>yugl::tet</i>	LFH $\rightarrow$ 168
GP3309	<i>trpC2</i> $\Delta$ <i>yugl::tet</i> $\Delta$ <i>yabR::aphA3</i>	GP3308 $\rightarrow$ GP3598
GP3310	<i>trpC2</i> <i>amyE::(yugl spec)</i>	LFH $\rightarrow$ 168
GP3311	<i>trpC2</i> <i>amyE::(yugl spec)</i> $\Delta$ <i>yugl::cat</i>	GP3311 $\rightarrow$ GP3597
GP3312	<i>trpC2</i> <i>amyE::(yabR spec)</i>	LFH $\rightarrow$ 168
GP3313	<i>trpC2</i> <i>amyE::(yugl spec)</i> $\Delta$ <i>yabR::aphA3</i>	GP3312 $\rightarrow$ GP3598
GP3314	<i>trpC2</i> <i>yabR</i> 3xFLAG <i>spec</i>	LFH $\rightarrow$ 168
GP3315	<i>trpC2</i> <i>yabR</i> His <i>spec</i>	LFH $\rightarrow$ 168
GP3316	<i>trpC2</i> $\Delta$ <i>kimA::cat</i> $\Delta$ <i>ktrAB::spc</i> $\Delta$ <i>yabR::aphA3</i>	GP3598 $\rightarrow$ GP2498
GP3317	<i>trpC2</i> $\Delta$ <i>yneR::cat</i>	LFH $\rightarrow$ 168
GP3318	<i>trpC2</i> $\Delta$ <i>ydcl::phleo</i>	LFH $\rightarrow$ 168

Name	Genotype	Construction
GP3319	<i>trpC2 ΔydcI::phleo ΔyugI::cat</i>	GP3597 → GP3318
GP3320	<i>trpC2 ΔydcI::phleo ΔyabR::aphA3</i>	GP3598 → GP3318
GP3321	<i>trpC2 Δfur::mIs ΔylnA::cat</i>	LFH → GP879
GP3322	<i>trpC2 yugI-His::spec</i>	LFH → 168
GP3323	<i>trpC2 ΔrsbP::phleo</i>	LFH → 168
GP3324	<i>trpC2 ΔylnA::cat</i>	LFH → 168
GP3325	<i>trpC2 ΔylnA::cat fur<sub>Y44C</sub></i>	Suppressor of GP3324
GP3326	<i>trpC2 ΔylnA::cat fur<sub>R23C</sub></i>	Suppressor of GP3325
GP3327	<i>trpC amyE::(yabR-lacZ cat)</i>	pGP3596 → 168
GP3328	<i>trpC amyE::(rsbP-lacZ cat)</i>	pGP3597 → 168
GP3329	<i>trpC amyE::(fur-lacZ aphA3)</i>	pGP3592 → 168
GP3330	<i>trpC amyE::(ylnA-lacZ aphA3)</i>	pGP3593 → 168
GP3331	<i>trpC amyE::(dhbA-lacZ aphA3)</i>	pGP3594 → 168
GP3332	<i>trpC2 ΔrsbP::phleo yabR::aphA3</i>	GP3323 → GP3598
GP3333	<i>trpC amyE::(yabR-lacZ cat) ΔrsbP::phleo</i>	GP3323 → GP3327
GP3334	<i>trpC amyE::(rsbP-lacZ cat) yabR::aphA3</i>	GP3598 → GP3328

## 6.4 Plasmids

### 6.4.1 Plasmids used in this work

Name	Description	Construction / Reference
P25-N	Fusion of the target protein to the N-terminus of the T25 domain	Karimova <i>et al.</i> , 1998
pAC5	Construction of translational <i>lacZ</i> fusions in <i>B. subtilis</i> , integrates into the <i>amyE</i> site	Martin-Verstraete <i>et al.</i> , 1992

Name	Description	Construction / Reference
<b>pAC5</b>	Construction of translational <i>lacZ</i> fusions in <i>B. subtilis</i> , integrates into the <i>amyE</i> site	Martin-Verstraete <i>et al.</i> , 1992
<b>pAC7</b>	Construction of translational <i>lacZ</i> fusions in <i>B. subtilis</i> , integrates into the <i>amyE</i> site	Weinrauch <i>et al.</i> , 1991
<b>pBQ200</b>	Constitutive overexpression of proteins in <i>B. subtilis</i>	Martin-Verstraete <i>et al.</i> , 1992
<b>pDG1726</b>	Plasmid for the amplification of the spec cassette for LFH-PCR	Guérout-Fleury <i>et al.</i> , 1995
<b>pDG780</b>	Plasmid for the amplification of the kan cassette for LFH-PCR	Guérout-Fleury <i>et al.</i> , 1995
<b>pET SUMO</b>	Fusion of SUMO protein and a His(6) tag at the N-terminus of a protein for inducible overexpression via IPTG in <i>E. coli</i>	Hanington <i>et al.</i> , 2006
<b>pGEM-cm</b>	Plasmid for the amplification of the cat cassette for LFH-PCR	Guérout-Fleury <i>et al.</i> , 1995
<b>pGP1331</b>	fusion of 3x FLAG tag to the C-terminus of a protein in the natural locus of the protein in <i>B. subtilis</i>	Lehnik-Habrink <i>et al.</i> , 2010
<b>pGP380</b>	Expression of proteins in <i>B. subtilis</i> allows fusion to a Strep-tag at the N-terminus of the protein	Herzberg <i>et al.</i> , 2007
<b>pGP382</b>	Expression of proteins in <i>B. subtilis</i> allows fusion to a Strep-tag at the C-terminus of the protein	Herzberg <i>et al.</i> , 2007
<b>pGP2583</b>	IPTG induced overexpression of His-YlaN in <i>E. coli</i>	Mehne, 2014
<b>pKT25</b>	Fusion of the target protein to the C-terminus of the T25 domain	Karimova <i>et al.</i> , 1998
<b>pKT25zip</b>	Control plasmid, expressing leucine zipper fused to T25 fragment of adenylate cyclase	Karimova <i>et al.</i> , 1998
<b>pUT18</b>	Fusion of the target protein to the N-terminus of the T18 domain	Karimova <i>et al.</i> , 1998
<b>pUT18C</b>	Fusion of the target protein to the C-terminus of the T18 domain	Karimova <i>et al.</i> , 1998



Name	Description	Construction / Reference
pUT18Czip	Control plasmid, expressing leucine zipper fused to T18 fragment of adenylate cyclase	Karimova <i>et al.</i> , 1998
pWH844	IPTG-inducible overexpression of N-terminally His-tagged proteins in <i>E. coli</i>	Schirmer <i>et al.</i> , 1997

#### 6.4.2 Plasmids constructed in this work

Plasmid	Vector	Construction
pGP3510	pET SUMO/ <i>XhoI</i> + <i>BsaI</i>	PCR-product <i>fabF</i> , RB57/58 ( <i>XhoI</i> + <i>BsaI</i> )
pGP3522	pGP380/ <i>Bam</i> HI+ <i>Pst</i> I	PCR-product <i>yabR</i> , RB109/RB110 ( <i>Bam</i> HI+ <i>Pst</i> I)
pGP3523	pGP380/ <i>Bam</i> HI+ <i>Pst</i> I	PCR-product <i>yugI</i> , RB113/RB114 ( <i>Bam</i> HI+ <i>Pst</i> I)
pGP3524	pGP382/ <i>Bam</i> HI+ <i>Pst</i> I	PCR-product <i>yugI</i> , RB115/RB116 ( <i>Bam</i> HI+ <i>Pst</i> I)
pGP3525	pWH844/ <i>Bam</i> HI+ <i>Pst</i> I	PCR-product <i>yabR</i> , RB109/RB110 ( <i>Bam</i> HI + <i>Pst</i> I)
pGP3526	pWH844/ <i>Bam</i> HI+ <i>Pst</i> I	PCR-product <i>yugI</i> , RB113/RB114 ( <i>Bam</i> HI+ <i>Pst</i> I)
pGP3527	pGP1331/ <i>Eco</i> RI+ <i>Pst</i> I	PCR-product <i>yugI</i> RB118/RB116 ( <i>Eco</i> RI+ <i>Pst</i> I)
pGP3528	pUT18/ <i>Kpn</i> I+ <i>Xba</i> I	PCR-product <i>nusA</i> RB119/RB120 ( <i>Kpn</i> I+ <i>Xba</i> I)
pGP3529	pUT18/ <i>Kpn</i> I+ <i>Xba</i> I	PCR-product <i>rpsC</i> RB121/RB122 ( <i>Kpn</i> I+ <i>Xba</i> I)
pGP3530	pUT18/ <i>Kpn</i> I+ <i>Xba</i> I	PCR-product <i>rpsF</i> RB123/RB124 ( <i>Kpn</i> I+ <i>Xba</i> I)
pGP3531	pUT18/ <i>Kpn</i> I+ <i>Xba</i> I	PCR-product <i>rpsJ</i> RB125/RB126 ( <i>Kpn</i> I+ <i>Xba</i> I)
pGP3532	pUT18/ <i>Kpn</i> I+ <i>Xba</i> I	PCR-product <i>rpsR</i> RB127/RB128 ( <i>Kpn</i> I+ <i>Xba</i> I)
pGP3533	pUT18/ <i>Kpn</i> I+ <i>Xba</i> I	PCR-product <i>yabR</i> RB129/RB130 ( <i>Kpn</i> I+ <i>Xba</i> I)
pGP3534	pUT18/ <i>Kpn</i> I+ <i>Xba</i> I	PCR-product <i>ykuJ</i> RB131/RB132 ( <i>Kpn</i> I+ <i>Xba</i> I)
pGP3535	pUT18/ <i>Kpn</i> I+ <i>Xba</i> I	PCR-product <i>yugI</i> RB133/RB134 ( <i>Kpn</i> I+ <i>Xba</i> I)
pGP3536	pUT18C/ <i>Kpn</i> I+ <i>Xba</i> I	PCR-product <i>nusA</i> RB119/RB120 ( <i>Kpn</i> I+ <i>Xba</i> I)
pGP3537	pUT18C/ <i>Kpn</i> I+ <i>Xba</i> I	PCR-product <i>rpsC</i> RB121/RB122 ( <i>Kpn</i> I+ <i>Xba</i> I)
pGP3538	pUT18C/ <i>Kpn</i> I+ <i>Xba</i> I	PCR-product, <i>rpsF</i> RB123/RB124 ( <i>Kpn</i> I+ <i>Xba</i> I)

## 6. Appendix

Plasmid	Vector	Construction
pGP3539	pUT18C/ <i>KpnI</i> + <i>XbaI</i>	PCR-product <i>rpsJ</i> RB125/RB126 ( <i>KpnI</i> + <i>XbaI</i> )
pGP3540	pUT18C/ <i>KpnI</i> + <i>XbaI</i>	PCR-product <i>rpsR</i> RB127/RB128 ( <i>KpnI</i> + <i>XbaI</i> )
pGP3541	pUT18C/ <i>KpnI</i> + <i>XbaI</i>	PCR-product <i>yabR</i> RB129/RB130 ( <i>KpnI</i> + <i>XbaI</i> )
pGP3542	pUT18C/ <i>KpnI</i> + <i>XbaI</i>	PCR-product <i>ykuJ</i> RB131/RB132 ( <i>KpnI</i> + <i>XbaI</i> )
pGP3543	pUT18C/ <i>KpnI</i> + <i>XbaI</i>	PCR-product <i>yugI</i> RB133/RB134 ( <i>KpnI</i> + <i>XbaI</i> )
pGP3544	pKT25/ <i>KpnI</i> + <i>XbaI</i>	PCR-product <i>nusA</i> RB119/RB120 ( <i>KpnI</i> + <i>XbaI</i> )
pGP3545	pKT25/ <i>KpnI</i> + <i>XbaI</i>	PCR-product <i>rpsC</i> RB121/RB122 ( <i>KpnI</i> + <i>XbaI</i> )
pGP3546	pKT25/ <i>KpnI</i> + <i>XbaI</i>	PCR-product <i>rpsF</i> RB123/RB124 ( <i>KpnI</i> + <i>XbaI</i> )
pGP3547	pKT25/ <i>KpnI</i> + <i>XbaI</i>	PCR-product <i>rpsJ</i> RB125/RB126 ( <i>KpnI</i> + <i>XbaI</i> )
pGP3548	pKT25/ <i>KpnI</i> + <i>XbaI</i>	PCR-product <i>rpsR</i> RB127/RB128 ( <i>KpnI</i> + <i>XbaI</i> )
pGP3549	pKT25/ <i>KpnI</i> + <i>XbaI</i>	PCR-product <i>yabR</i> RB129/RB130 ( <i>KpnI</i> + <i>XbaI</i> )
pGP3550	pKT25/ <i>KpnI</i> + <i>XbaI</i>	PCR-product <i>ykuJ</i> RB131/RB132 ( <i>KpnI</i> + <i>XbaI</i> )
pGP3551	pKT25/ <i>KpnI</i> + <i>XbaI</i>	PCR-product <i>yugI</i> RB133/RB134 ( <i>KpnI</i> + <i>XbaI</i> )
pGP3552	p25-N/ <i>KpnI</i> + <i>XbaI</i>	PCR-Prod <i>nusA</i> RB119/RB120 ( <i>KpnI</i> + <i>XbaI</i> )
pGP3553	p25-N/ <i>KpnI</i> + <i>XbaI</i>	PCR-product <i>rpsC</i> RB121/RB122 ( <i>KpnI</i> + <i>XbaI</i> )
pGP3554	p25-N/ <i>KpnI</i> + <i>XbaI</i>	PCR-product <i>rpsF</i> RB123/RB124 ( <i>KpnI</i> + <i>XbaI</i> )
pGP3555	p25-N/ <i>KpnI</i> + <i>XbaI</i>	PCR-product <i>rpsJ</i> RB125/RB126 ( <i>KpnI</i> + <i>XbaI</i> )
pGP3556	p25-N/ <i>KpnI</i> + <i>XbaI</i>	PCR-product <i>rpsR</i> RB127/RB128 ( <i>KpnI</i> + <i>XbaI</i> )
pGP3557	p25-N/ <i>KpnI</i> + <i>XbaI</i>	PCR-product <i>yabR</i> RB129/RB130 ( <i>KpnI</i> + <i>XbaI</i> )
pGP3558	p25-N/ <i>KpnI</i> + <i>XbaI</i>	PCR-product <i>ykuJ</i> RB131/RB132 ( <i>KpnI</i> + <i>XbaI</i> )
pGP3559	p25-N/ <i>KpnI</i> + <i>XbaI</i>	PCR-product <i>yugI</i> RB133/RB134 ( <i>KpnI</i> + <i>XbaI</i> )
pGP3560	pGP1331/ <i>EcoRI</i> + <i>PstI</i>	PCR-Prod <i>yabR</i> RB112/RB117 ( <i>EcoRI</i> + <i>PstI</i> )
pGP3561	pET SUMO/ <i>XhoI</i> + <i>BamHI</i>	PCR-product <i>yabR</i> RB174/RB175 ( <i>XhoI</i> + <i>BamHI</i> )
pGP3562	pET SUMO/ <i>XhoI</i> + <i>BsaI</i>	PCR-product <i>yugI</i> RB176/RB177 ( <i>XhoI</i> + <i>BsaI</i> )
pGP3563	pET SUMO/ <i>XhoI</i> + <i>BsaI</i>	PCR-product <i>ydjO</i> , RB178/RB179 ( <i>XhoI</i> + <i>BsaI</i> )

## 6. Appendix

Plasmid	Vector	Construction
pGP3564	pUT18/ <i>KpnI</i> + <i>XbaI</i>	PCR-product <i>dhaS</i> RB224/225 ( <i>KpnI</i> + <i>XbaI</i> )
pGP3565	pUT18C/ <i>KpnI</i> + <i>XbaI</i>	PCR-product <i>dhaS</i> RB224/225 ( <i>KpnI</i> + <i>XbaI</i> )
pGP3566	pKT25/ <i>KpnI</i> + <i>XbaI</i>	PCR-product <i>dhaS</i> RB224/225 ( <i>KpnI</i> + <i>XbaI</i> )
pGP3567	p25-N/ <i>KpnI</i> + <i>XbaI</i>	PCR-product <i>dhaS</i> RB224/225 ( <i>KpnI</i> + <i>XbaI</i> )
pGP3568	pUT18/ <i>KpnI</i> + <i>Bam</i> HI	PCR-product <i>gabD</i> RB226/227 ( <i>KpnI</i> + <i>Bam</i> HI)
pGP3569	pUT18C/ <i>KpnI</i> + <i>Bam</i> HI	PCR-product <i>gabD</i> RB226/227 ( <i>KpnI</i> + <i>Bam</i> HI)
pGP3570	pKT25/ <i>KpnI</i> + <i>Bam</i> HI	PCR-product <i>gabD</i> RB226/227 ( <i>KpnI</i> + <i>Bam</i> HI)
pGP3571	p25-N/ <i>KpnI</i> + <i>Bam</i> HI	PCR-product <i>gabD</i> RB226/227 ( <i>KpnI</i> + <i>Bam</i> HI)
pGP3572	pUT18/ <i>KpnI</i> + <i>XbaI</i>	PCR-product <i>ycgL</i> RB228/229 ( <i>KpnI</i> + <i>XbaI</i> )
pGP3573	pUT18C/ <i>KpnI</i> + <i>XbaI</i>	PCR-product <i>ycgL</i> RB228/229 ( <i>KpnI</i> + <i>XbaI</i> )
pGP3574	pKT25/ <i>KpnI</i> + <i>XbaI</i>	PCR-product <i>ycgL</i> RB228/229 ( <i>KpnI</i> + <i>XbaI</i> )
pGP3575	p25-N/ <i>KpnI</i> + <i>XbaI</i>	PCR-product <i>ycgL</i> RB228/229 ( <i>KpnI</i> + <i>XbaI</i> )
pGP3576	pUT18/ <i>XbaI</i> + <i>Bam</i> HI	PCR-product <i>yurR</i> RB230/231 ( <i>Bam</i> HI+ <i>XbaI</i> )
pGP3577	pUT18C/ <i>XbaI</i> + <i>Bam</i> HI	PCR-product <i>yurR</i> RB230/231 ( <i>Bam</i> HI+ <i>XbaI</i> )
pGP3578	pKT25/ <i>XbaI</i> + <i>Bam</i> HI	PCR-product <i>yurR</i> RB230/231 ( <i>Bam</i> HI+ <i>XbaI</i> )
pGP3579	p25-N/ <i>XbaI</i> + <i>Bam</i> HI	PCR-product <i>yurR</i> RB230/231 ( <i>Bam</i> HI+ <i>XbaI</i> )
pGP3581	pUT18C/ <i>KpnI</i> + <i>XbaI</i>	PCR-product <i>alaS</i> RB232/233 ( <i>KpnI</i> + <i>XbaI</i> )
pGP3582	pKT25/ <i>KpnI</i> + <i>XbaI</i>	PCR-product <i>alaS</i> RB232/233 ( <i>KpnI</i> + <i>XbaI</i> )
pGP3583	p25-N/ <i>KpnI</i> + <i>XbaI</i>	PCR-product <i>alaS</i> RB232/233 ( <i>KpnI</i> + <i>XbaI</i> )
pGP3584	pUT18/ <i>KpnI</i> + <i>XbaI</i>	PCR-product <i>yoZC</i> RB234/235 ( <i>KpnI</i> + <i>XbaI</i> )
pGP3585	pUT18C/ <i>KpnI</i> + <i>XbaI</i>	PCR-product <i>yoZC</i> RB234/235 ( <i>KpnI</i> + <i>XbaI</i> )
pGP3586	pKT25/ <i>KpnI</i> + <i>XbaI</i>	PCR-product <i>yoZC</i> RB234/235 ( <i>KpnI</i> + <i>XbaI</i> )
pGP3587	p25-N/ <i>KpnI</i> + <i>XbaI</i>	PCR-product <i>yoZC</i> RB234/235 ( <i>KpnI</i> + <i>XbaI</i> )
pGP3588	pBQ200/ <i>Bam</i> HI+ <i>XbaI</i>	PCR-product <i>yneR</i> RB239/240 ( <i>Bam</i> HI+ <i>XbaI</i> )
pGP3589	pET SUMO/ <i>Bam</i> HI+ <i>Xho</i> I	PCR-product <i>fur</i> RB222/RB223 ( <i>Bam</i> HI+ <i>Xho</i> I)

Plasmid	Vector	Construction
pGP3590	pET SUMO/ <i>Bam</i> HI+ <i>Xho</i> I	PCR-product <i>fur</i> Y44C RB222/RB223 ( <i>Bam</i> HI+ <i>Xho</i> I)
pGP3591	pET SUMO/ <i>Bam</i> HI+ <i>Xho</i> I	PCR-product <i>fur</i> R23C RB222/RB223 ( <i>Bam</i> HI+ <i>Xho</i> I)
pGP3592	pAC7/ <i>Eco</i> RI+ <i>Bam</i> HI	PCR-product P <sub>fur</sub> , LD5/6 ( <i>Eco</i> RI+ <i>Bam</i> HI)
pGP3593	pAC7/ <i>Eco</i> RI+ <i>Bam</i> HI	PCR-product P <sub>ylaN</sub> , LD9/10 ( <i>Eco</i> RI+ <i>Bam</i> HI)
pGP3594	pAC7/ <i>Eco</i> RI+ <i>Bam</i> HI	PCR-product P <sub>dhbA</sub> , LD1/2 ( <i>Eco</i> RI+ <i>Bam</i> HI)
pGP3595	pAC7/ <i>Eco</i> RI+ <i>Bam</i> HI	PCR-product P <sub>yvmC</sub> RB249/250 ( <i>Eco</i> RI+ <i>Bam</i> HI)
pGP3596	pAC5/ <i>Eco</i> RI+ <i>Bam</i> HI	PCR-product P <sub>yabR</sub> RB241/242 ( <i>Eco</i> RI+ <i>Bam</i> HI)
pGP3597	pAC5/ <i>Eco</i> RI+ <i>Bam</i> HI	PCR-product P <sub>rsbP</sub> RB243/244 ( <i>Eco</i> RI+ <i>Bam</i> HI)
pGP3598	pBQ200/ <i>Bam</i> HI+ <i>Pst</i> I	PCR-product <i>yabR</i> RB110/111 ( <i>Bam</i> HI+ <i>Pst</i> I)
pGP3599	pBQ200/ <i>Xba</i> I+ <i>Sal</i> I	PCR-product <i>rsbP</i> RB245/246 ( <i>Xba</i> I+ <i>Sal</i> I)

## 6.5 Oligonucleotides

### 6.5.1 Oligonucleotides designed for this work

Name	Sequence 5'→3', restriction sites are underlined, extra bp are in bold	Purpose
RB109	AAAGGATCCATGTCGATTGAAGTTGGC AGCAAG	fwd. primer for amplification of <i>yabR</i>
RB110	TTTCTGCAGTTATCCTCTTCTTGCTCCGC G	rev. primer for amplification of <i>yabR</i>
RB111	AAAGGATCCAAAGGAGGAAACAATCAT GTCGATTGAAGTTGGCAGCAAG	fwd. primer for amplification of <i>yabR</i> incl. SD
RB112	TTTCTGCAGTCCTCTTCTTGCTCCGCGC	rev. primer for amplification of <i>yabR</i> w/o stop codon
RB113	AAAGGATCCATGGCAGCAAATTTGAA GTGGGC	fwd. primer for amplification of <i>yugI</i>
RB114	TTTCTGCAGTTATTTTTGATAAGGTCTT TGCGGTTGG	rev. primer for amplification of <i>yugI</i>

Name	Sequence 5'→3', restriction sites are underlined, extra bp are in bold	Purpose
RB115	AAAGGATCCAAAGGAGGAAACAATCAT GGCAGCAAAATTTGAAGTGGGC	fwd. primer for amplification of <i>yugI</i> incl. SD
RB116	TTTCTGCAGTTTTTTGATAAGGTCTTTGC GGTTGGA	rev. primer for amplification of <i>yugI</i> w/o stop codon
RB117	AAAGAATTCTGAAAAGTTTAAAGACAAA ACAAACGGATTTAAAA	fwd. primer for amplification of <i>yabR</i>
RB118	AAAGAATTCTTCCTGCACAAAACAACAT AAAAAAGATAC	fwd. primer for amplification of <i>yugI</i>
RB119	AAATCTAGAGATGAGCAGTGAATTATTA GATGCTCTCA	fwd. primer for amplification of <i>nusA</i> for bacterial two-hybrid
RB120	TTTGGTACCGCTTCATCCGATTCAGCAG TTTCAGG	rev. primer for amplification of <i>nusA</i> for bacterial two-hybrid
RB121	AAATCTAGAGGTGGGTCAAAGGTAAA TCCAGTC	fwd. primer for amplification of <i>rpsC</i> for bacterial two-hybrid
RB122	TTTGGTACCGCTTTTCCTCCTTCCTCATT TTCTTCTTAG	rev. primer for amplification of <i>rpsC</i> for bacterial two-hybrid
RB123	AAATCTAGAGATGAGAAAGTACGAAGT TATGTACATTATC	fwd. primer for amplification of <i>rpsF</i> for bacterial two-hybrid
RB124	TTTGGTACCGCTTCTTCTTTAACAAC AATGTGGCGA	rev. primer for amplification of <i>rpsF</i> for bacterial two-hybrid
RB125	AAATCTAGAGATGGCAAACAAAAAAT TCGTATTCGTTTG	fwd. primer for amplification of <i>rpsJ</i> for bacterial two-hybrid
RB126	TTTGGTACCGCAAGTTTAATTCGATATC GACACCAGATG	rev. primer for amplification of <i>rpsJ</i> for bacterial two-hybrid
RB127	AAATCTAGAGATGGCAGGAGGACGCAG AG	fwd. primer for amplification of <i>rpsR</i> for bacterial two-hybrid
RB128	TTTGGTACCGCCTCACCGCTTACGTATG GAAGT	rev. primer for amplification of <i>rpsR</i> for bacterial two-hybrid
RB129	AAATCTAGAGATGTCGATTGAAGTTGGC AGCAAG	fwd. primer for amplification of <i>yabR</i> for bacterial two-hybrid

Name	Sequence 5'→3', restriction sites are underlined, extra bp are in bold	Purpose
RB130	TTT <u>GGTACCG</u> CTCCTCTTCTTGCTCCGCG C	rev. primer for amplification of <i>yabR</i> for bacterial two-hybrid
RB131	AAATCTAGAGATGTCACAATTAATGGGT ATCATCACAC	fwd. primer for amplification of <i>ykuJ</i> for bacterial two-hybrid
RB132	TTT <u>GGTACCG</u> CCTGAAGAAGTTCAAAGA TTTCGATGGAA	rev. primer for amplification of <i>ykuJ</i> for bacterial two-hybrid
RB133	AAATCTAGAGATGGCAGCAAATTTGA AGTGGGC	fwd. primer for amplification of <i>yugI</i> for bacterial two-hybrid
RB134	TTT <u>GGTACCG</u> CTTTTTTGATAAGGTCTTT GCGGTTGGA	rev. primer for amplification of <i>yugI</i> for bacterial two-hybrid
RB135	CTAATACGACTCACTATAGGGAGA TTTGGTGGCGATAGCGAAGAG	fwd. primer for amplification of 5S rRNA for <i>in vitro</i> transcription incl. T7 promotor
RB136	TGCTTGGCGGCGTCCTAC	rev. primer for amplification of 5S rRNA for <i>in vitro</i> transcription
RB137	<b>CTAATACGACTCACTATAGGGAGA</b> ATTTATCGGAGAGTTTGATCCTGGC	fwd. primer for amplification of 16S rRNA for <i>in vitro</i> transcription incl. T7 promotor
RB138	TAGAAAGGAGGTGATCCAGCC	rev. primer for amplification of 16S rRNA for <i>in vitro</i> transcription
RB139	CTAATACGACTCACTATAGGGAGA GGTTAAGTTAGAAAGGGCGCAC	fwd. primer for amplification of 23S rRNA for <i>in vitro</i> transcription incl. T7 promotor
RB140	TGGTTAAGTCCTCGATCGATTAGTAT	rev. primer for amplification of 23S rRNA for <i>in vitro</i> transcription
RB141	CCGAGCGCCTACGAGGAATTTGTATCG GCTGTTTCTTGCACTTTGCAG	rev. upstream LFH for deletion of <i>ykuJ</i> incl. kan flank
RB142	ACAGATTGCAGCTTCAGGATTACA	fwd. primer upstream LFH for deletion of <i>ykuJ</i>
RB143	<b>CCTATCACCTCAAATGGTTGCTG</b> CATATCCGTTTGATAATATCGACATGGT T	rev. primer downstream LFH for deletion of <i>ykuJ</i> incl. kan flank
RB144	CAATAATATAAACTTTATCAGTATTTGTC GAAAAGTT	fwd. primer downstream LFH for deletion of <i>ykuJ</i>

Name	Sequence 5'→3', restriction sites are underlined, extra bp are in bold	Purpose
RB145	GGAGACCGTCTATGAGCACTC	fwd. sequencing primer LFH for deletion of <i>ykuJ</i>
RB146	CTAATACGACTCACTATAGGGAGA AACTGGGGAACCTTGAGTGCAGA	fwd. primer for amplification of 16S-RNA (650 bp-751 bp) for <i>in vitro</i> transcription incl. T7 promotor
RB147	CAGAGAGTCGCCTTCGCC	rev. primer for amplification of 16S-RNA (650 bp-751 bp) for <i>in vitro</i> transcription
RB148	CTAATACGACTCACTATAGGGAGA AACAGGATTAGATACCCTGGTAGT	fwd. primer for amplification of 16S-RNA (790 bp-891 bp) for <i>in vitro</i> transcription incl. T7 promotor
RB149	GGAGTGCTTAATGCGTTAGCTG	rev. primer for amplification of 16S-RNA (790 bp-891 bp) for <i>in vitro</i> transcription
RB150	<b>CTAATACGACTCACTATAGGGAGA</b> CGGTGGAGCATGTGGTTTAATTC	fwd. primer for amplification of 16S-RNA (950 bp-1071 bp) for <i>in vitro</i> transcription incl. T7 promotor
RB151	AACCATGCACCACCTGTCCT	rev. primer for amplification of 16S-RNA (950 bp-1071 bp) for <i>in vitro</i> transcription
RB152	CTAATACGACTCACTATAGGGAGA AGATGTTGGGTTAAGTCCCGCA	fwd. primer for amplification of 16S-RNA (1090 bp-1181 bp) for <i>in vitro</i> transcription incl. T7 promotor
RB153	TTGTCACCGGCAGTCACCTT	rev. primer for amplification of 16S-RNA (1090 bp-1181 bp) for <i>in vitro</i> transcription
RB154	AAATTTTATTTAGGTATAATTAAGCAA ACGATCTTTTT	fwd. primer for amplification of <i>yabR</i> -FLAG from pGP3560
RB155	<b>CCGAGCGCCTACGAGGAATTTGTATCG</b> TTATCACTTGTCGTCATCGTCTTTGT	rev. primer for amplification of <i>yabR</i> -FLAG from pGP3560
RB156	AAAAAGATCGTTTGCTTAATTATACCTA AATAAAAATTT	fwd. primer upstream LFH to fuse of a His tag to <i>yabR</i>
RB157	AAAAAACTCATTACGACACGTGTTATTTTC	rev. primer upstream LFH to fuse of a His tag to <i>yabR</i>

Name	Sequence 5'→3', restriction sites are underlined, extra bp are in bold	Purpose
RB158	<b>CCTATCACCTCAAATGGTTCGCTG</b> CTTGCTGCTTTCTATAAAATAAATGAAG CA	fwd. primer to fuse of a His tag to <i>yabR</i> incl. kan flag
RB159	CCGAGCGCCTACGAGGAATTTGTATCGC TA GTGATGGTGTGATGGTGTGATG TCCTCTTCTTGCTCCGCGC	primer to fuse of a His tag to <i>yabR</i> incl. His tag, stop codon kan flag
RB160	ATGGCAGCAAATTTGAAGTGGGC	fwd. primer to fuse of a His tag to <i>yugI</i> incl.
RB161	CCGAGCGCCTACGAGGAATTTGTATCG CTA GTGATGGTGTGATGGTGTGATGTTTTTGTATA AGGTCTTTCGGTTGGACATTTT	primer to fuse of a His tag to <i>yugI</i> incl. His tag, stop codon kan flag
RB162	GCCCACTCAAATTTTGCTGCCAT	rev. primer upstream LFH to fuse of a His tag to <i>yugI</i>
RB163	GCTGAATGAGATTGCTGAGTTTGC	fwd. primer upstream LFH to fuse of a His tag to <i>yugI</i>
RB164	CCTATCACCTCAAATGGTTCGCTG GCATGAAAAAAGCACCGGACAG	fwd. primer downstream LFH to fuse of a His tag to <i>yugI</i> incl. kan flag
RB165	AGTTTGTAAATAACAGATCCTGAGTTCAT T	rev. primer downstream LFH to fuse of a His tag to <i>yugI</i>
RB166	TACAACGGCAGACAAAGGATTTAAAG	fwd. sequencing primer for <i>yugI</i> -His LFH
RB167	GCGCTGTTTCAATGACTGTACG	fwd. sequencing primer for <i>yugI</i> -His LFH
RB168	<b>AAAGGAGGAAACAATC</b> ATGTCGATTGAAGTTGGCAGCAAG	fwd. primer for amplification of <i>yabR</i> incl. SD
RB169	<b>GGCTAGCTGTCGACTAAGCTT</b> TTATCCTCTTCTTGCTCCGCG	rev. primer for amplification of <i>yabR</i> incl. pDR110 overhang
RB170	AAGCTTAGTCGACAGCTAGCC	rev. <i>amyE</i> up region for integration of <i>goi</i> in <i>amyE</i> locus
RB171	<b>GATTGTTTCCTCCTTT</b> AATTGTTATCCGCTCACAATTCCACA	fwd. <i>amyE</i> down region for integration of <i>goi</i> in <i>amyE</i> locus
RB172	<b>AAAGGAGGAAACAATC</b> ATGGCAGCAAATTTGAAGTGGGC	fwd. primer for amplification of <i>yugI</i> incl. SD



Name	Sequence 5'→3', restriction sites are underlined, extra bp are in bold	Purpose
RB173	<b>GGCTAGCTGTCGACTAAGCTT</b> TTATTTTTGATAAGGCTTTGCGGTTGG	rev. primer for amplification of <i>yugI</i> incl. pDR110 overhang
RB174	AAAGGATCCGCATGTCGATTGAAGTTG GCAGCAAG	fwd. primer for amplification of <i>yabR</i>
RB175	TTTCTCGAGTTATCCTCTTCTTGCTCCGC G	rev. primer for amplification of <i>yabR</i>
RB176	AAAGGTCTCATGGTATGGCAGCAAAT TTGAAGTGGGC	fwd. primer for amplification of <i>yugI</i>
RB177	TTTCTCGAGTTATTTTTGATAAGGCTTT TGCAGTTGG	rev. primer for amplification of <i>yugI</i>
RB178	TTTGGTCTCATGGTATGTCTTACTATAAC AAACGAAATCAAGAAC	fwd. primer for amplification of <i>ydjO</i>
RB179	AAACTCGAGCTAGCTTGTTTTCGTTTGG CTGTT	rev. primer for amplification of <i>ydjO</i>
RB180	CCTATCACCTCAAATGGTTCGCTG TCA AGATGACAAGCGATCTTCGCTGT	rev. primer for deletion of <i>yabR</i> C-term. (54 bp) incl. stop codon and kan flag
RB181	<b>CCGAGCGCCTACGAGGAATTTGTATCG</b> CTTGCTGCTTTCTATAAAATAAATGAAG CAT	fwd. primer for deletion of <i>yabR</i> C-term. (54 bp) incl. kan flag
RB182	<b>CCTATCACCTCAAATGGTTCGCTG TCA</b> ATCTTTAATGTGTTGAAACCTTGTTGGT G	rev. primer for deletion of <i>yugI</i> C-term. (54 bp) incl. stop codon and kan flag
RB183	CCGAGCGCCTACGAGGAATTTGTATCG GCATGAAAAAAGCACCGGACAG	fwd. primer for deletion of <i>yugI</i> C-term. (54 bp) incl. kan flag
RB184	<b>CCTATCACCTCAAATGGTTCGCTG</b> GCGG TTCTTGATTTGTTTGTATAGT	rev. upstream LFH for deletion of <i>ydjO</i> incl. kan flank
RB185	CAGGACTATACACCGCTATCGAAA	fwd. primer upstream LFH for deletion of <i>ydjO</i>
RB186	<b>CCGAGCGCCTACGAGGAATTTGTATCG</b> AATCTCCAAAACAACAGCCAAACGA	rev. primer downstream LFH for deletion of <i>ydjO</i> incl. kan flank

## 6. Appendix

Name	Sequence 5'→3', restriction sites are underlined, extra bp are in bold	Purpose
RB187	CTTAGGAAAAGCGGACGAAAGC	fwd. primer downstream LFH for deletion of <i>ydjO</i>
RB188	ACCGTTTTGTGCATCACTGACG	fwd. sequencing primer LFH for deletion of <i>ydjO</i>
RB189	TGAAATGAGGCTTTTTAAATTGGATCTG AA	rev. sequencing primer LFH for deletion of <i>ydjO</i>
RB190	AAATCTAGAGATGTCTTACTATAACAAA CGAAATCAAGAAC	fwd. primer for amplification of <i>ydjO</i> for bacterial two-hybrid
RB191	TTTGGTACC <b>CG</b> GCTTGTTCGTTGGCT GTTGTTTT	rev. primer for amplification of <i>ydjO</i> for bacterial two-hybrid
RB192	AAAGGATCCATGGAAACGTCAGCCCTT TAAAACA	fwd. primer for amplification for <i>ydcl</i>
RB193	TTTTCTAGATTATTTTACCATAGACAGCG ATACTCTG	rev. primer for amplification for <i>ydcl</i>
RB194	<b>CCTATCACCTCAAATGGTTCGCTG</b> CGTGTTCGATAAACCTATTTCTTTC G	rev. upstream LFH for deletion of <i>ydcl</i> incl. kan flank
RB195	CTGGATCGGCGTTGTGTCAGA	fwd. primer upstream LFH for deletion of <i>ydcl</i>
RB196	CCGAGCGCCTACGAGGAATTTGTATCG TTTGGGTTGACGGCGTAGATG	rev. primer downstream LFH for deletion of <i>ydcl</i> incl. kan flank
RB197	GGCGCCTCTTCAGCCACTT	fwd. primer downstream LFH for deletion of <i>ydcl</i>
RB198	TCATTGGGACTGAACTGTCTAAAGA	fwd. sequencing primer LFH for deletion of <i>ydcl</i>
RB199	GCTTGACCAACGGGCCGAT	rev. sequencing primer LFH for deletion of <i>ydcl</i>
RB200	<b>CCGAGCGCCTACGAGGAATTTGTATCG</b> CTTCTTTATACCAGTTCAATGCGTCT	rev. upstream LFH for deletion of <i>yneR</i> incl. kan flank
RB201	TTGTAGGGTTCACAGGGATAATTTCA	fwd. primer upstream LFH for deletion of <i>yneR</i>

Name	Sequence 5'→3', restriction sites are underlined, extra bp are in bold	Purpose
RB202	<b>CCTATCACCTCAAATGGTTCGCTG</b> GACGCTGATGAACCGTTTTTGAAT	rev. primer downstream LFH for deletion of <i>yneR</i> incl. kan flank
RB203	ATGTGGAAAAATTGCAGGATATGGTTC	fwd. primer downstream LFH for deletion of <i>yneR</i>
RB204	AAACTCTCCGCCACTCCAGG	fwd. sequencing primer LFH for deletion of <i>yneR</i>
RB205	GGAGGTACATCCGAATGACAAAG	rev. sequencing primer LFH for deletion of <i>yneR</i>
RB206	CTTTTCTGAGAGCTCTTCTGA	sequencing primer for <i>ycl</i>
RB207	TCAGGAAAGAGCTCTCAGAAAAG	sequencing primer for <i>ycl</i>
RB208	GATAGAACAGGCATCCACCC	sequencing primer for <i>ycl</i>
RB209	CCGAGCGCCTACGAGGAATTTGTATCG CCGCATGGTGCATCATTCAATTG	rev. upstream LFH for deletion of <i>rsbP</i> incl. kan flank
RB210	TCCTCCTCTGCATCTTCCAAT	fwd. primer upstream LFH for deletion of <i>rsbP</i>
RB211	<b>CCTATCACCTCAAATGGTTCGCTG</b> CATAAGAGTGATGACGAATGTTTTATAT TAGT	rev. primer downstream LFH for deletion of <i>rsbP</i> incl. kan flank
RB212	AGCGAACGGAATGAAGGTGCT	fwd. primer downstream LFH for deletion of <i>rsbP</i>
RB213	ACATGAGCACCTCCTGATCGTT	fwd. sequencing primer LFH for deletion of <i>rsbP</i>
RB214	TCCGCATCTGGAATCACCCG	rev. sequencing primer LFH for deletion of <i>rsbP</i>
RB215	AAAGGTACCATGGACAAACAATTGAAT GATGCACC	fwd. primer for amplification of <i>rsbP</i>
RB216	TTTGAATTCCTATTTTACATCAACTAATA TAAAACATTCGTCATC	rev. primer for amplification of <i>rsbP</i>
RB217	AAAGAATTCGTGAAAATCTTTTCCTTG AGAGTCATC	fwd. primer for amplification of <i>ykvP</i>

Name	Sequence 5'→3', restriction sites are underlined, extra bp are in bold	Purpose
RB218	TTT <u>AAGCTT</u> TTTAGAATAATTTGTTATTAA TATTTCTAAACAGTTTCTC	rev. primer for amplification of <i>ykvP</i>
RB219	AAAGGATCCATGTTTTCAAAGATAAGC TTCCCATTAT	fwd. primer for amplification of <i>exuT</i>
RB220	TTTCTGCAGTTAATAAGACACAGGATTC TCAGCTTCT	rev. primer for amplification of <i>exuT</i>
RB221	CTTTTATTGCCGGTGCTTCCTTG	sequencing primer for <i>exuT</i>
RB222	AAAGGATCC <b>GC</b> ATGGAAAACCGTATTG ATCGTATTAAGAAA	fwd. primer for amplification of <i>fur</i>
RB223	TTTCTCGAGCTATTCAGTTTCTTTCCGT TACAGC	rev. primer for amplification of <i>fur</i>
RB224	AAATCTAGAGATGAGTTCTTTAACGATG CAAGTGAC	fwd. primer for amplification of <i>dhaS</i> for bacterial two-hybrid
RB225	TTTGGTACCCGGTCTTCAAGTTTACCC ATACACTTTT	rev. primer for amplification of <i>dhaS</i> for bacterial two-hybrid
RB226	AAAGGATCC <b>GC</b> ATGCCAGATCAATTAAC GGTCTACAA	fwd. primer for amplification of <i>gabD</i> for bacterial two-hybrid
RB227	TTTGGTACCC <b>GC</b> TAAACCGATGGACAAAT ATTTTGTTTCAAG	rev. primer for amplification of <i>gabD</i> for bacterial two-hybrid
RB228	AAATCTAGAGATGAAACAAAGAATCATT GATGAATTAACCGG	fwd. primer for amplification of <i>ycgL</i> for bacterial two-hybrid
RB229	TTTGGTACCCGGCTTCCTCCATCCTTCCA CAC	rev. primer for amplification of <i>ycgL</i> for bacterial two-hybrid
RB230	AAATCTAGAGATGAAATCGTACATCATC GTCGGC	fwd. primer for amplification of <i>yurR</i> for bacterial two-hybrid
RB231	TTTGGATCC <b>CG</b> TGCAAGTGCTCCGGCTG G	rev. primer for amplification of <i>yurR</i> for bacterial two-hybrid
RB232	AAATCTAGAGATGAAACACTTAACTTCT GCGGAAGT	fwd. primer for amplification of <i>alaS</i> for bacterial two-hybrid
RB233	TTTGGTACCC <b>CG</b> TAAAACGGATTTACCC AATCTTCTACA	rev. primer for amplification of <i>alaS</i> for bacterial two-hybrid

Name	Sequence 5'→3', restriction sites are underlined, extra bp are in bold	Purpose
RB234	AAATCTAGAGATGATTCATAAAAATTGG CTTGAAAAAGAAACC	fwd. primer for amplification of <i>yozc</i> for bacterial two-hybrid
RB235	TTTGGTACCCGCATCTCTCGAAGTATTC TTTATAATAGCC	rev. primer for amplification of <i>yozc</i> for bacterial two-hybrid
RB236	TTTGCCTTCACCCTGACGG	fwd. primer for amplification of Fur box in promoter region of <i>dhbA</i>
RB237	CAGCCCCTGTTATAAAAGCAATTTTTC	rev. primer for amplification of Fur box in promoter region of <i>dhbA</i>
RB238	AATGCGTTGCCGTGTGGTTTTTAAT	sequencing primer for <i>alaS</i>
RB239	AAAGGATCC <b>AAAGGAGGAAACAATC</b> ATGAATATGACAATTAACGAAGACGCAT TG	fwd. primer for amplification of <i>yneR</i> incl. SD
RB240	TTTTCTAGATTATTGGTATTCAAAACCG GTTTCATCAG	rev. primer for amplification of <i>yneR</i>
RB241	AAAGAATTCGGAGCGATCATCTGGCTG G	fwd. primer for amplification of P <sub>yabR</sub>
RB242	TTTGGATCCGTCAGGAATACTAGGGCGC C	rev. primer for amplification of P <sub>yabR</sub>
RB243	AAAGAATTCATGAGCACCTCTGATCG TTT	fwd. primer for amplification of P <sub>rsbP</sub>
RB244	TTTGGATCCATAGATGCTTTGCCGCTGC CT	rev. primer for amplification of P <sub>rsbP</sub>
RB245	AAATCTAG <b>AAAAGGAGGAAACAATC</b> ATGGACAAACAATTGAATGATGCACC	fwd. primer for amplification of <i>rsbP</i> incl. SD
RB246	TTT <u>TCGACT</u> TATTTTACATCAACTAATA TAAAACATTCGTCATC	rev. primer for amplification of <i>rsbP</i>

## 6.5.2 Additional oligonucleotides used in this work

Name	Sequence 5'→3', restriction sites are underlined, extra bp are in bold	Purpose
<b>cat check fwd</b>	CTAATGTCACTAACCTGCCC	sequencing out of <i>cat</i> resistance cassette
<b>cat check rev</b>	GTCTGCTTCTTCATTAGAATCAATCC	sequencing out of <i>cat</i> resistance cassette
<b>cat fwd (kan)</b>	CGGCAATAGTTACCCTTATTATCAAG	amplification of <i>cat</i> resistance cassette
<b>cat rev (kan)</b>	CCAGCGTGGACCGGCGAGGCTAGTTAC CC	amplification of <i>cat</i> resistance cassette
<b>CZ126</b>	CAGCGAACCATTTGAGGTGATAGGGAA CGATGACC TCTAATAATTG	sequencing out of <i>phleo</i> resistance cassette
<b>CZ127</b>	CGATACAAATTCCTCGTAGGGCGCTCGGG TAGTATTT TTTGAGAAGATCAC	sequencing out of <i>phleo</i> resistance cassette
<b>CZ128</b>	CCAAAGTGAAACCTAGTTTATC	amplification of <i>phleo</i> resistance cassette
<b>CZ129</b>	CGAGACTTTGCAGTAATTGATC	amplification of <i>phleo</i> resistance cassette
<b>DW67</b>	CAAAATTGGGTGCGCAAAAGAAC	amplification of RAT sequence for <i>in vitro</i> transcription
<b>DW70</b>	CTAATACGACTCACTATAGGGAGAACGT GTTACTGATTCGATCAGGC	amplification of RAT sequence for <i>in vitro</i> transcription incl. T7 promoter
<b>FM46</b>	AAATCTAGAGATGTTTCAAATAGTATG AAACAACGAATGAATTGGGAAG	amplification of <i>odhA</i>
<b>FM47</b>	TTTGGTACCCGGTTTTTTCGAGTCAAGC TATCAGATACAATACG	amplification of <i>odhA</i>
<b>FM48</b>	GAGCGCGAGTGGCTGACAAGAAAG	sequencing of <i>odhA</i>
<b>FM49</b>	GGAGACGCTGCATTCCCTGGG	sequencing of <i>odhA</i>
<b>FM50</b>	GTGCTCCGCAAGCTGAATGGCG	sequencing of <i>odhA</i>
<b>JM201</b>	<b>CCTATCACCTCAAATGGTTCGCTG</b> CAAA TTTTGCTGCCATTATAACAACCT	rev. upstream LFH for deletion of <i>yugI</i> incl. kan flank

## 6. Appendix

Name	Sequence 5'→3', restriction sites are underlined, extra bp are in bold	Purpose
JM202	CATT <u>CCTGAGCCGTGTTTTGTT</u>	fwd. primer upstream LFH for deletion of <i>yugI</i>
JM203	CCGAGCGCCTACGAGGAATTTGTATCGC CAACCGCAAAGACCTTATCAAAA	rev. primer downstream LFH for deletion of <i>yugI</i> incl. kan flank
JM204	TATTTTTCTTTTGTTCCTCCAGTTTGTAAATA ACA	fwd. primer downstream LFH for deletion of <i>yugI</i>
JM205	TCAGCCGTTATTTGAGCAACAG	fwd. sequencing primer LFH for deletion of <i>yugI</i>
JM206	GTGGCTCATCATGTCAACCATC	rev. sequencing primer LFH for deletion of <i>yugI</i>
JM207	CCTATCACCTCAAATGGTTCGCTG TTGCTGCCAACTTCAATCGAC	rev. upstream LFH for deletion of <i>yabR</i> incl. kan flank
JM208	TCATTCGTGCCAAAACAGCC	fwd. primer upstream LFH for deletion of <i>yabR</i>
JM209	CCGAGCGCCTACGAGGAATTTGTATCG CAAACGTGGAGGGCGC	rev. primer downstream LFH for deletion of <i>yabR</i> incl. kan flank
JM210	AGCCATGGAGAAGAACACGAC	fwd. primer downstream LFH for deletion of <i>yabR</i>
JM211	CGAACAACAAGGGGATAAAGCTAAAG	fwd. sequencing primer LFH for deletion of <i>yabR</i>
JM212	TATTTTTAATGATTGTTTCACTTTTTTTCAC AGTAAA	rev. sequencing primer LFH for deletion of <i>yabR</i>
kan check fwd	CATCCGCAACTGTCCATACTCTG	sequencing out of <i>kan</i> resistance cassette
kan check rev	CTGCCTCCTCATCCTCTTCATCC	sequencing out of <i>kan</i> resistance cassette
kan fwd	CAGCGAACCATTTGAGGTGATAGG	amplification of <i>kan</i> resistance cassette
kan rev	CGATACAAATTCCTCGTAGGCGCTCGG	amplification of <i>kan</i> resistance cassette
LD01	AAAGAATTCGAGTTTTCAGGAGAAGGA CATATTC	amplification of <i>dhbA</i> promotor region

Name	Sequence 5'→3', restriction sites are underlined, extra bp are in bold	Purpose
LD02	TTT <u>GGATCC</u> CAGCTTTTCAGGATTATAATC AACTGCC	amplification of <i>dhbA</i> promotor region
LD05	AAAGGATCCTCTGCGCTTAAATGGTCTT CTTCG	amplification of <i>fur</i> promotor region
LD06	AAAGAATT <u>C</u> CTGTTTTTAGCGCTGATTC ATCTCT	amplification of <i>fur</i> promotor region
LD09	AAAGAATTCTCGGGATCGGCATATTCGG	amplification of <i>ylaN</i> promotor region
LD10	AAAGGATCCTTCAAATCTTCTCAGCGT CCACT	amplification of <i>ylaN</i> promotor region
M13_puc_ fwd	GTAAAACGACGGCCAGTG	sequencing of various plasmids
M13_puc_ rev	GGAAACAGCTATGACCATG	sequencing of various plasmids
ML84	CTAATGGGTGCTTTAGTTGAAGA	<i>cat</i> check up-fragment
ML85	CTCTATTCAGGAATTGTCAGATAG	<i>cat</i> check down-fragment
ML107	GCTTCATAGAGTAATTCTGTAAAGG	sequencing of various plasmids
ML108	GACATCTAATCTTTTCTGAAGTACATCC	sequencing of various plasmids
RW210	AAAAGATCTATGTTTGCAAACGATTCA AAACCTCTTTAC	LFH primer upstream region for integration into <i>amyE</i> gene
RW213	TTT <u>CTCGAG</u> TCAATGGGGAAGAGAACC GCTTA	LFH primer downstream region for integration into <i>amyE</i> gene
spec check fwd	GTTATCTTGAGAGAATATTGAATGGAC	sequencing out of <i>spec</i> resistance cassette
spec check rev	CGTATGTATTCAAATATATCCTCCTCAC	sequencing out of <i>spec</i> resistance cassette
spec fwd (kan)	CAGCGAACCATTTGAGGTGATAGGGAC TGGCTCGCTAATAACGTAACGTGACTGG CAAGAG	amplification of <i>spec</i> resistance cassette



Name	Sequence 5'→3', restriction sites are underlined, extra bp are in bold	Purpose
<b>spec (kan)</b>	<b>CGATACAAATTCCTCGTAGGGCGCTCGGC</b> GTAGCGAGGGCAAGGGTTTATTGTTTC TAAAATCTG	amplification of <i>spec</i> resistance cassette
<b>T7-prom.</b>	TAATACGACTCACTATAGGG	sequencing of various plasmids
<b>T7-term</b>	GCTAGTTATTGCTCAGCGG	sequencing of various plasmids
<b>tc check rev</b>	CATCGGTCATAAAATCCGTAATGC	sequencing out of <i>tet</i> resistance cassette
<b>Tc-fwd2 (kan)</b>	GCTTATCAACGTAGTAAGCGTGG	amplification of <i>tet</i> resistance cassette
<b>tc-rev (kan)</b>	GAACTCTCTCCCAAAGTTGATCCC	amplification of <i>tet</i> resistance cassette

## 6.6 Curriculum vitae

### Personal information

Rica Bremenkamp

Date of birth 24.05.1995, Uslar

Contact ricabre@t-online.de

Nationality German

### Education

**11/1019-12/2022**

**PhD student at the GGNB program Microbiology and Biochemistry,**  
Georg-August-University Göttingen  
Dept. of General Microbiology, workgroup of Prof. Dr. Stülke  
*Project: " Validation of novel protein-protein interactions in *Bacillus subtilis*"*

**10/2017-10/2019**

**MSc in Molecular Life Science: Microbiology, Biotechnology and Biochemistry**  
Georg-August-University Göttingen  
Dept. of General Microbiology, workgroup of Dr. Commichau  
*Project: "Control of the essential diadenylate cyclase CdaA by the phosphoglucosamine mutase GlmM in *Listeria monocytogenes*"*

**10/2014-09/2017**

**BSc in Biology**  
**Martin-Luther-Universität Halle-Wittenberg**  
Dept. of General Microbiology, workgroup of Prof. Dr. Sawers  
*Project: Einfluss verschiedener Aminosäureaustausche in den Reifungsproteinen HybG und HypC und deren Auswirkung auf die Hydrogenaseaktivität"*